CR-152194

STI Technical Report No. 1126-1

A STUDY OF KEY FEATURES OF THE
RAE ATMOSPHERIC TURBULENCE MODEL

Contract NAS2-9942

October 1978

1. Report No. NASA CR-152194	2. Government Accession No.	3. Recipient's Catalog No.
4. Title and Subtitle A STUDY OF KEY FEATURES OF THE RAE ATMOSPHERIC TURBULENCE MODEL		5. Report Date October 1978
		6. Performing Organization Code
7. Author(s) Wayne F. Jewell and Robert K. Heffley		8. Performing Organization Report No. STI TR-1126-1
		10. Work Unit No.
9. Performing Organization Name and Address Systems Technology, Inc. 2672 Bayshore-Frontage Road, Suite 505 Mountain View, California 94043		11. Contract or Grant No. NAS2-9942
		13. Type of Report and Period Covered Informal
12. Sponsoring Agency Name and Address National Aeronautics and Space Administration Ames Research Center, Moffett Field, CA 94035		14. Sponsoring Agency Code

15. Supplementary Notes

16. Abstract

A complex atmospheric turbulence model developed by the RAE for use in aircraft simulation is analyzed in terms of its temporal, spectral, and statistical characteristics. First, a direct comparison is made between cases of the RAE model and the more conventional Dryden turbulence model. Next the control parameters of the RAE model are systematically varied and the effects noted. The RAE model is found to possess a high degree of flexibility in its characteristics, but the individual control parameters are cross-coupled in terms of their effect on various measures of intensity, bandwidth, and probability distribution. While a guide is given to the setting of model control parameters, the resulting effect on pilot opinion is not known.

17. Key Words (Suggested by Author(s)) Atmospheric Turbulence Gusts Wind Shear Aircraft Simulation	18. Distribution Statement		
19. Security Classif. (of this report)	20. Security Classif. (of this page)	21. No. of Pages 84	22. Price*

SYSTEMS TECHNOLOGY, INC.

2072 BAYSHORE FRONTAGE ROAD • MOUNTAIN VIEW, CALIFORNIA 94043• PHONE (415) 961-4674

Technical Report No. 1126-1

A STUDY OF KEY FEATURES OF THE RAE ATMOSPHERIC TURBULENCE MODEL

Wayne F. Jewell
Robert K. Heffley

October 1978

ABSTRACT

A complex atmospheric turbulence model developed by the RAE for use in aircraft simulation is analyzed in terms of its temporal, spectral, and statistical characteristics. First, a direct comparison is made between cases of the RAE model and the more conventional Dryden turbulence model. Next the control parameters of the RAE model are systematically varied and the effects noted. The RAE model is found to possess a high degree of flexibility in its characteristics, but the individual control parameters are cross-coupled in terms of their effect on various measures of intensity, bandwidth, and probability distribution. While a guide is given to the setting of model control parameters, the resulting effect on pilot opinion is not known.

TABLE OF CONTENTS

LIST OF FIGURES

LIST OF FIGURES (Concluded)

LIST OF TABLES

SYMBOLS

DT   Frametime

F   Probability distribution control for the RAE model

g   Gravitational specific force constant

HCG   Altitude

h   Altitude perturbation

L_u u-Gust scale length

L_w w-Gust scale length

NGUSTS   Bandwidth control for the RAE model

$P(u/\sigma_u)$ u-Gust probability distribution function

$P(w/\sigma_w)$ w-Gust probability distribution function

R   Decay ratio control for the RAE model

SIGMA   Intensity control for the RAE model

T   Duration of a specified time window

T_{run} Total duration of a given turbulence sample

t   Time

u   Longitudinal (x-axis) gust component, i.e., u-gust

V   True airspeed

w   Vertical (z-axis) gust component, i.e., w-gust

$\bar{x}$ Mean value of x, i.e., $\Sigma x_i/N$ for N samples

Z_u Gust derivative for z-force due to u-gust

$1/T_{\theta_1}$ Low frequency root of pitch attitude numerator for elevator control

$1/T_{\theta_2}$ High frequency root of pitch-attitude numerator for elevator control

α_4 Kurtosis, μ_4/μ_2^2

SYMBOLS (Concluded)

μ_k k^{th} central moment, $\Sigma(\bar{x} - x_i)^k/N$

ρ_Λ^2 Overall coherence

ρ_{uw}^2 Coherence between u and w

$\rho_{u^2w^2}^2$ Coherence between u^2 and w^2

σ_u u-Gust standard deviation

$\bar{\sigma}_u$ Average u-gust standard deviation over a limited time window

$\sigma_{\Delta u_1}$ Standard deviation of average u-gust velocity change over a specified time window

$\sigma_{\Delta u_2}$ Standard deviation of net u-gust velocity change over a specified time window

σ_{σ_u} RMS dispersion of u-gust standard deviation over a limited time window

σ_w w-Gust standard deviation

$\bar{\sigma}_w$ Average w-gust standard deviation over a limited time window

σ_{σ_w} RMS dispersion of w-gust standard deviation over a limited time window

Φ_{uu} u-Gust power spectral density, $\sigma_u^2 = \int_0^\infty \Phi_{uu}\, dw$

Φ_{ww} w-Gust power spectral density, $\sigma_w^2 = \int_0^\infty \Phi_{ww}\, dw$

ω Frequency

SECTION I

INTRODUCTION

A complex atmospheric turbulence model has been developed by the Royal Aeronautical Establishment (RAE) for use in manned and unmanned aircraft simulation. This model, which is described in Ref. 1, has been used to some extent in this country and in Europe (e.g., Refs. 2 and 3). Unfortunately, using the RAE model involves setting several parameters, the effects of which are not well understood.

The purpose of the study reported here, therefore, was to improve our understanding of the characteristics of atmospheric turbulence represented by the RAE model and its parameters. This was accomplished by considering the model in terms of its temporal, spectral, and statistical characteristics. A variety of metrics was applied. In addition, a direct comparison was made between one particular RAE model formulation and the widely used Dryden turbulence model (Ref. 4).

The comparison between the RAE and Dryden turbulence models is presented in Section II with the RAE model parameters set to yield Gaussian-like characteristics of the turbulence. In addition to considering the two models, per se, this section also contains a discussion of the spectral and statistical parameters used to quantify the characteristics of the turbulence models.

Section III describes in great detail the effects of perturbing each of the RAE model input parameters in terms of temporal, spectral, and statistical parameters used to quantify the characteristics of the turbulence models. The perturbations of each of the RAE model input parameters are made with respect to the baseline settings used in Section II. The reader who is primarily interested in an overview of the effects of the RAE model inputs may omit Section III and proceed directly to Section IV.

Section IV gives a summary of the analyses reported and recommendations of how the RAE model should be used in a real-time simulation environment. Recommendations for future analyses of atmospheric turbulence models are also presented.

SECTION II

COMPARISON OF RAE AND DRYDEN MODEL BASELINE CASES

Baseline cases for the RAE and Dryden models are compared in this section. The main objective is to call attention to major features of the RAE model and to present the various means of quantifying those features. The Dryden model is used as a point of comparison because it is a familiar standard and is relatively simple to quantify.

The numerical values of model parameters were chosen to make the temporal, spectral, and statistical characteristics of both model baseline cases approximately equivalent. Since the RAE model is fundamentally different from the Dryden model in its mathematical form and involves more parameters, true equivalence among all the above mentioned characteristics is difficult to achieve. The following specific conditions were chosen:

> Airspeed, 250 ft/sec
>
> Altitude, 800 ft
>
> u-Gust intensity, 1 ft/sec rms

These numerical values were then used to pick the model parameters given in Tables 1 and 2.

The baseline cases are analyzed in terms of their temporal, spectral, and statistical characteristics. The results are presented in the following subsections.

A. TEMPORAL DESCRIPTION

Two sets of time histories are given for each of the two baseline cases. First, a complete time history of u- and w-gusts is given for the RAE and Dryden models. This is followed by a plot which illustrates the effect of one of the gust components on a simplified pilot-aircraft model.

TABLE 1

RAE MODEL BASELINE PARAMETERS*

Bandwidth control, NGUSTS[†] = 5 gusts/sec

Probability distribution control[‡], F = 0.0

Decay ratio control, R = 0.7

Altitude, HCG = 800 ft

Frame time, DT = 0.1 sec

Intensity control, SIGMA = 1.0

---

* The model parameters given in this table are the subject of Section III and are explained fully therein.

† A rule of thumb for setting NGUSTS is: $NGUSTS = \dfrac{\cdot V \, (ft/sec)}{50 \, (ft/sec)}$

‡ The term "global intermittency" is applied to this parameter in Ref. 1, but, based on our analysis, we consider "probability distribution control" to be more descriptive.

TABLE 2

DRYDEN MODEL BASELINE PARAMETERS

Scale lengths, $L_u = \sqrt[3]{1750^2 \cdot 800} = 1348.1 \text{ ft}$

and $L_w = 800 \text{ ft}$

Intensities, $\sigma_u = 1 \text{ ft/sec}$ and $\sigma_w = \sqrt{\dfrac{L_w}{L_u}} \cdot \sigma_u = 0.770 \text{ ft/sec}$

Spectral forms:

$$\frac{\Phi_{uu}}{\sigma_u^2} = \frac{2}{\pi} \frac{V}{L_u} \frac{1}{\omega^2 + \left(\frac{V}{L_u}\right)^2}$$

$$\frac{\Phi_{ww}}{\sigma_w^2} = \frac{3}{\pi} \frac{V}{L_w} \frac{\omega^2 + \frac{1}{3}\left(\frac{V}{L_u}\right)^2}{\left[\omega^2 + \left(\frac{V}{L_w}\right)^2\right]^2}$$

Complete time histories of the two baseline cases are shown in Fig. 1. There is no clear distinction to be made between the baseline RAE and Dryden models in this figure. Magnitudes and apparent frequency content of u- and w-gusts are comparable within each of the models as well as one model against the other. That is to say, it would be difficult to distinguish specific gust components or distinguish the models themselves from the time histories. (Naturally this applies only to the baseline cases chosen here — it is not a general observation.) The spectral and statistical descriptions to follow will better distill the distinguishing features which do indeed exist.

In order to obtain a first order approximation of the effect of u-gusts on an aircraft, the following procedure was applied. The closed loop pilot-aircraft combination was represented by a pitch-attitude-constrained transfer function of the altitude response to a u-gust, i.e.,

$$\frac{h}{u} = \frac{X_u}{\left(s + \frac{1}{T_{\theta_1}}\right)\left(s + \frac{1}{T_{\theta_2}}\right)}$$

Where X_u is the partial derivative of x-force due to a u-gust (approximately $-C_x/V$)

$\frac{1}{T_{\theta_1}}$ is the low frequency attitude numerator zero (approximately equal to speed damping)

$\frac{1}{T_{\theta_2}}$ is the high frequency attitude numerator zero (approximately equal to heave damping)

For the cases presented here,

$$X_u = -0.3/sec$$

$$\frac{1}{T_{\theta_1}} = 0.1 \text{ rad/sec}$$

$$\frac{1}{T_{\theta_2}} = 0.5 \text{ rad/sec}$$

Figure 2 shows a time history of u-gust and the corresponding altitude excursion based on the above method. Any differences between the models are not discernible from these time histories.
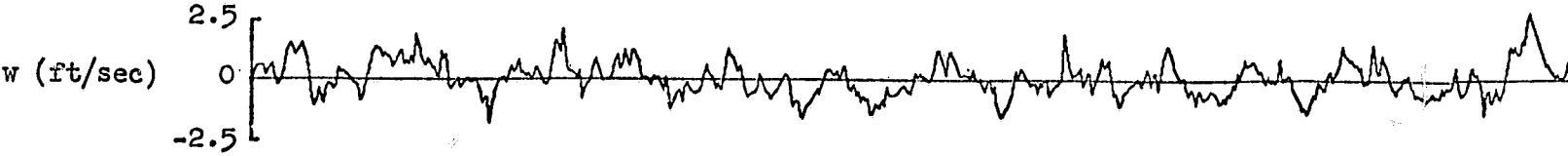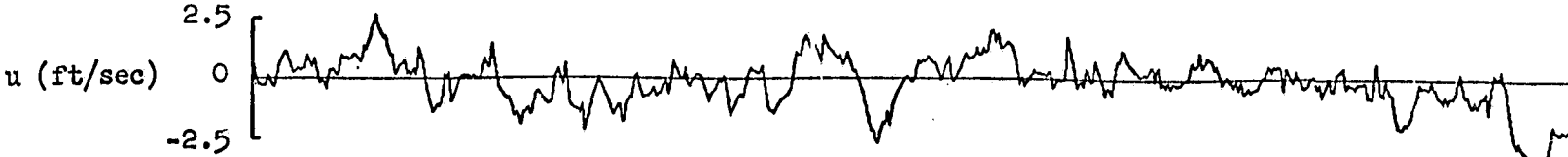
RAE BASELINE CASE

DRYDEN BASELINE CASE
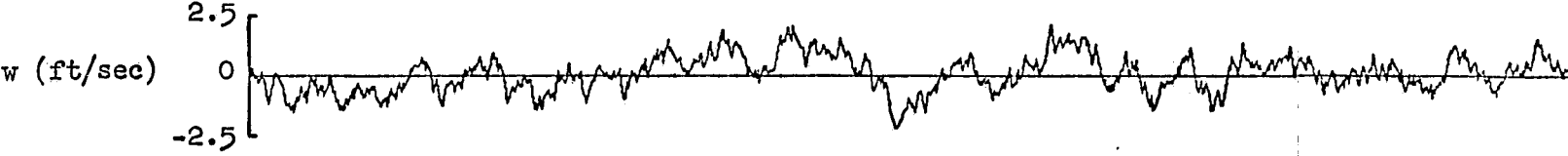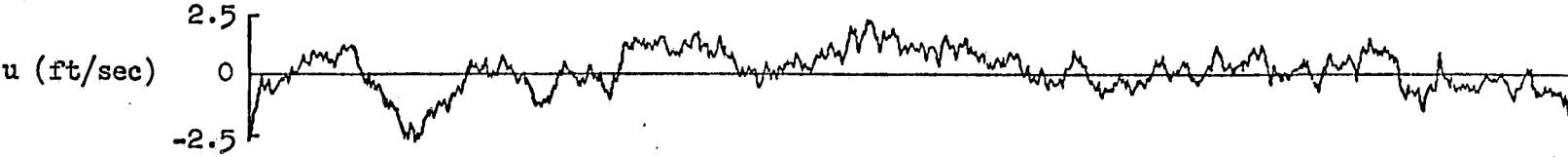
80   90   100   110   120   130   140   150   160   170   180   190   200   204.8

time (sec)
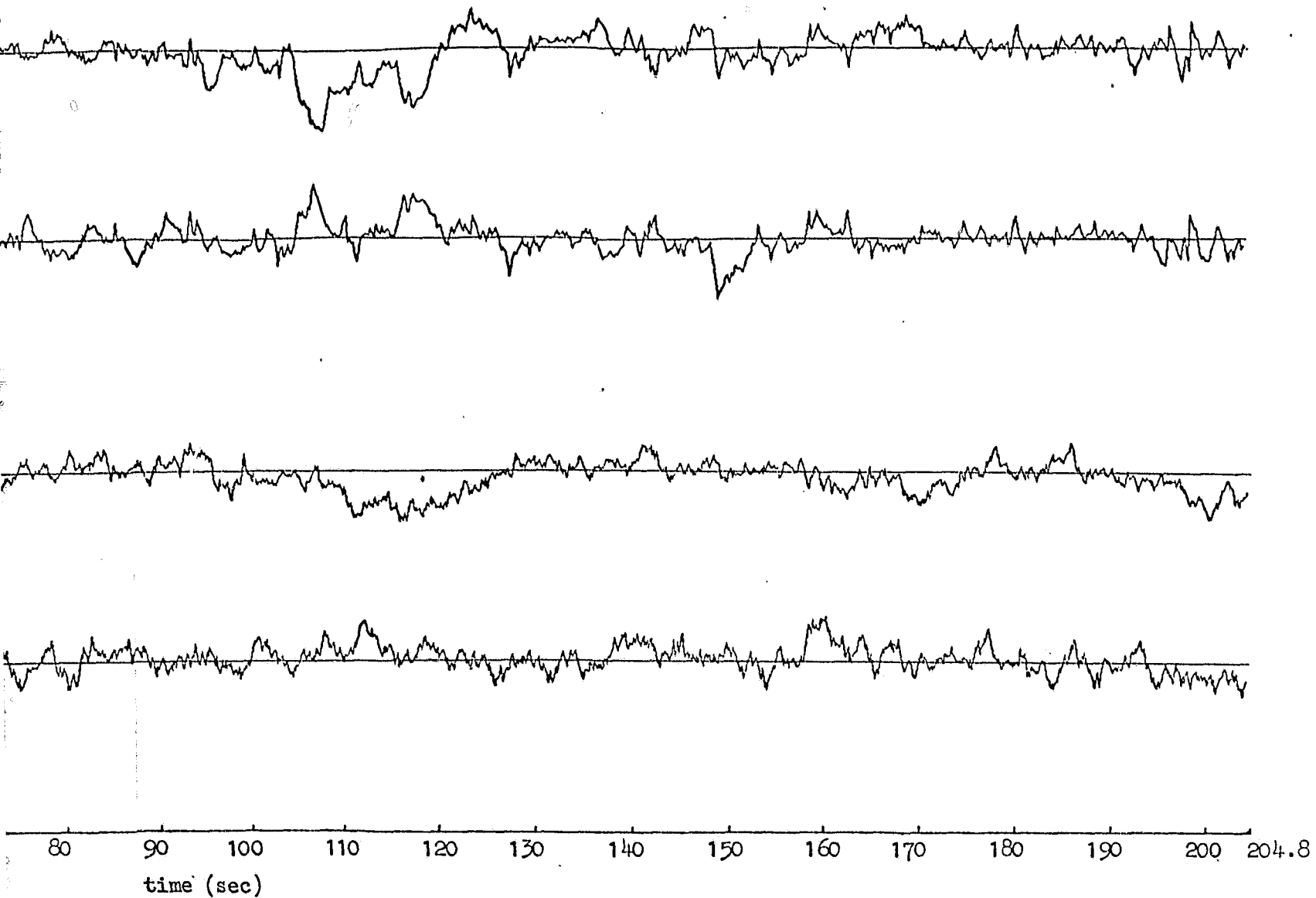
Figure 1. Comparative Time
Histories of u- and w-Gusts
for RAE and Dryden Model
Baseline Cases

5
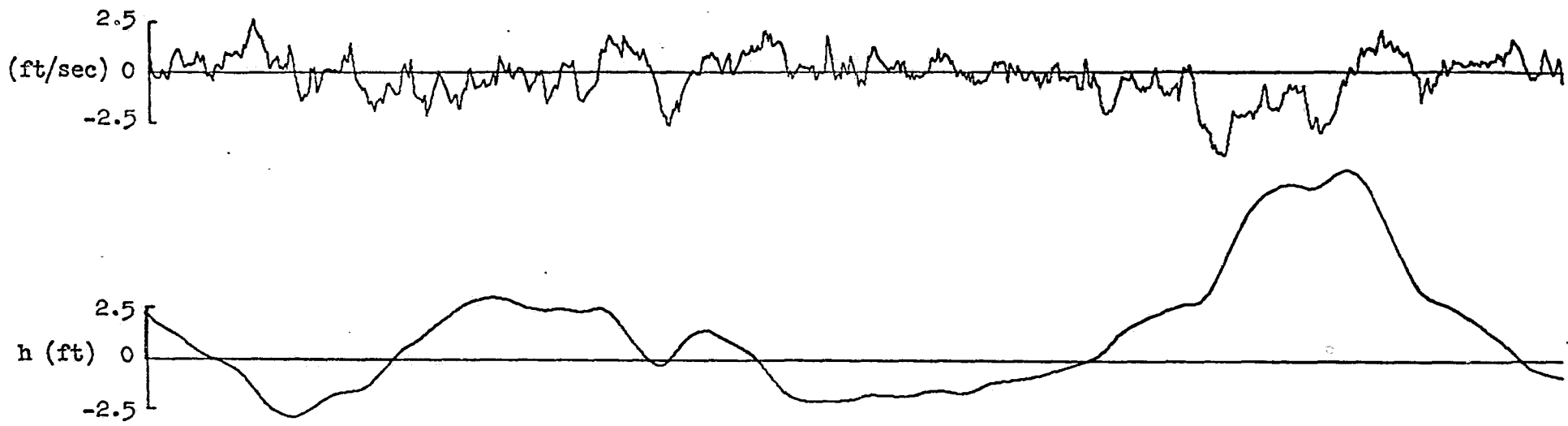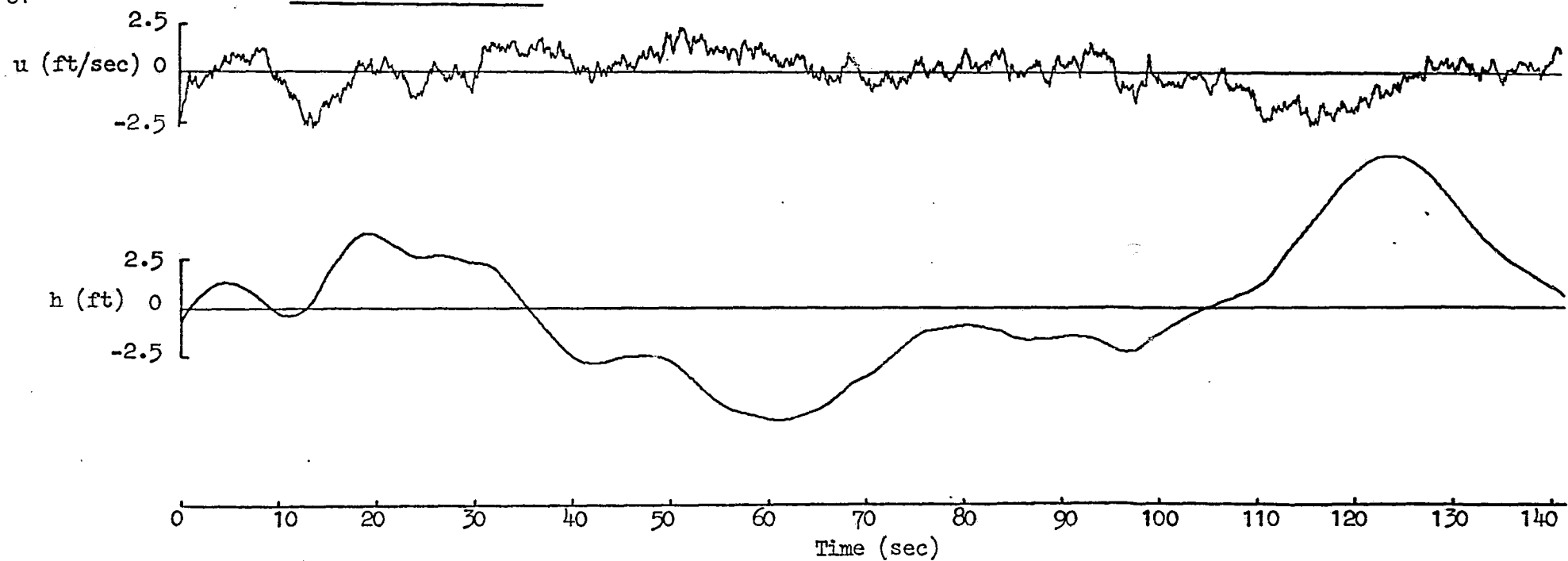
Figure 2. Comparative Time Histories for u-Gust and Altitude Excursion Due to u-Gust for RAE and Dryden Model Baseline Cases

B. SPECTRAL DESCRIPTION

The turbulence resulting from the two models were spectrally analyzed using a fast Fourier transform routine and the results presented in a variety of ways. From past experience (Ref. 5) we had found that plotting linear $\omega \cdot \phi(\omega)$ versus $\log \omega$ provided better insights to the spectral distribution than did the usual plot of $\log \phi(\omega)$ versus $\log \omega$. This was because the former way of plotting showed the true proportion of spectral power versus frequency while, at the same time, utilizing a log scale for frequency. Finally, a third way of presenting spectral information is presented here: a plot of cumulative power fraction (i.e., the fraction of the total power) versus frequency as defined below. Cumulative power fraction, PF:

$$PF \triangleq \frac{\displaystyle\int_0^{\omega(PF)} \phi(\omega) \, dw}{\displaystyle\int_0^{\infty} \phi(\omega) \, dw}$$

This is perhaps the most precise way of describing spectral power distribution.

Figure 3 shows comparative power spectral density plots of $\log \phi_{uu}(\omega)/\sigma_u^2$ versus $\log \omega$ for the baseline RAE and Dryden cases. Both cases exhibit the features of a typical first order low-pass filter, as shown by the solid line representing ideal Dryden model power spectra. From this figure it is difficult to observe any significant difference in amplitude or break frequency between the two baseline cases. Some disparity appears in the randomness of the estimated power spectra for u-gust.

The same observations apply to the w-gust and the coherence between u- and w-gusts (Fig. 3). There is no apparent difference between the two models — only the normal amount of randomness in the low frequency spectral measurements.

A better distinction in spectral characteristics is shown by the plots of $\omega \cdot \phi(\omega)$ versus frequency shown in Fig. 4. Although the dispersion in spectral measurements is prominent, it is possible to see more spectral power in the vicinity of 1 rad/sec in the RAE u-gust baseline case. For w-gusts,

□ RAE Baseline
△ Dryden Baseline
— Theoretical Dryden
Open: u-gust
Closed: w-gust
Half-Open: Coherence

ORIGINAL PAGE IS
OF POOR QUALITY

Figure 3.   Power Spectral Density and Coherence of u- and w-Gusts
Resulting From the RAE and Dryden Turbulence Models
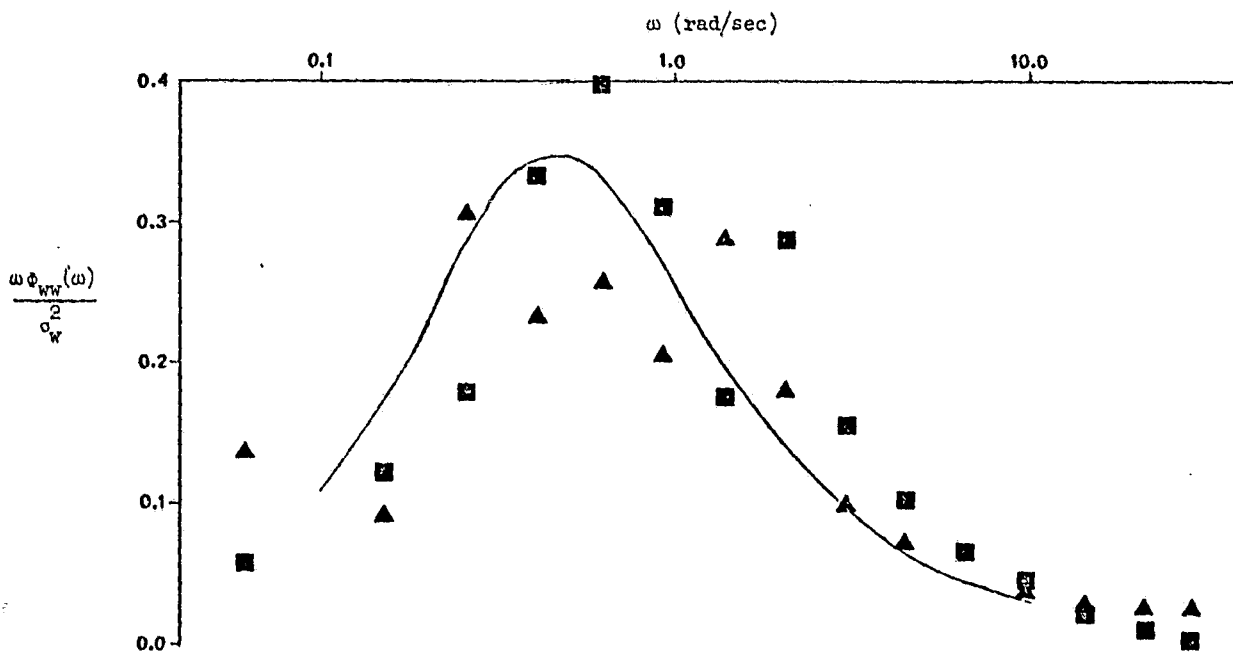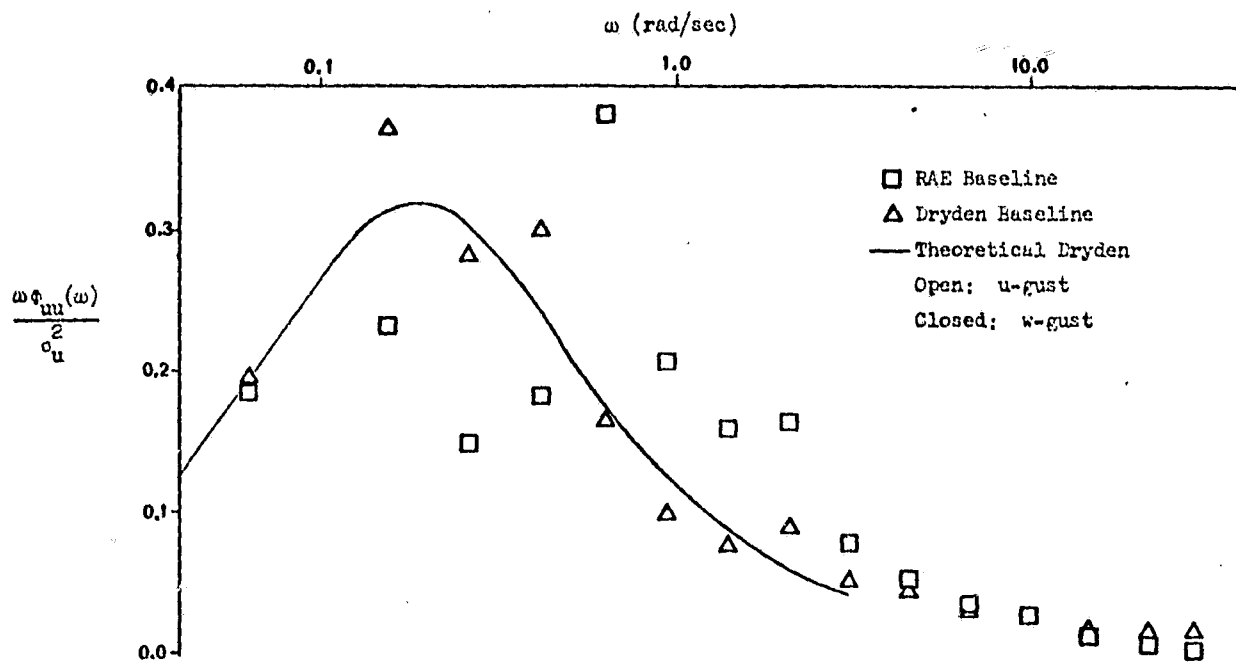
Figure 4. Weighted Power Spectral Density of u- and w-Gusts Resulting From the RAE and Dryden Turbulence Models

the same difference in power spectral density between the two models appears with one exception at 1.69 rad/sec.
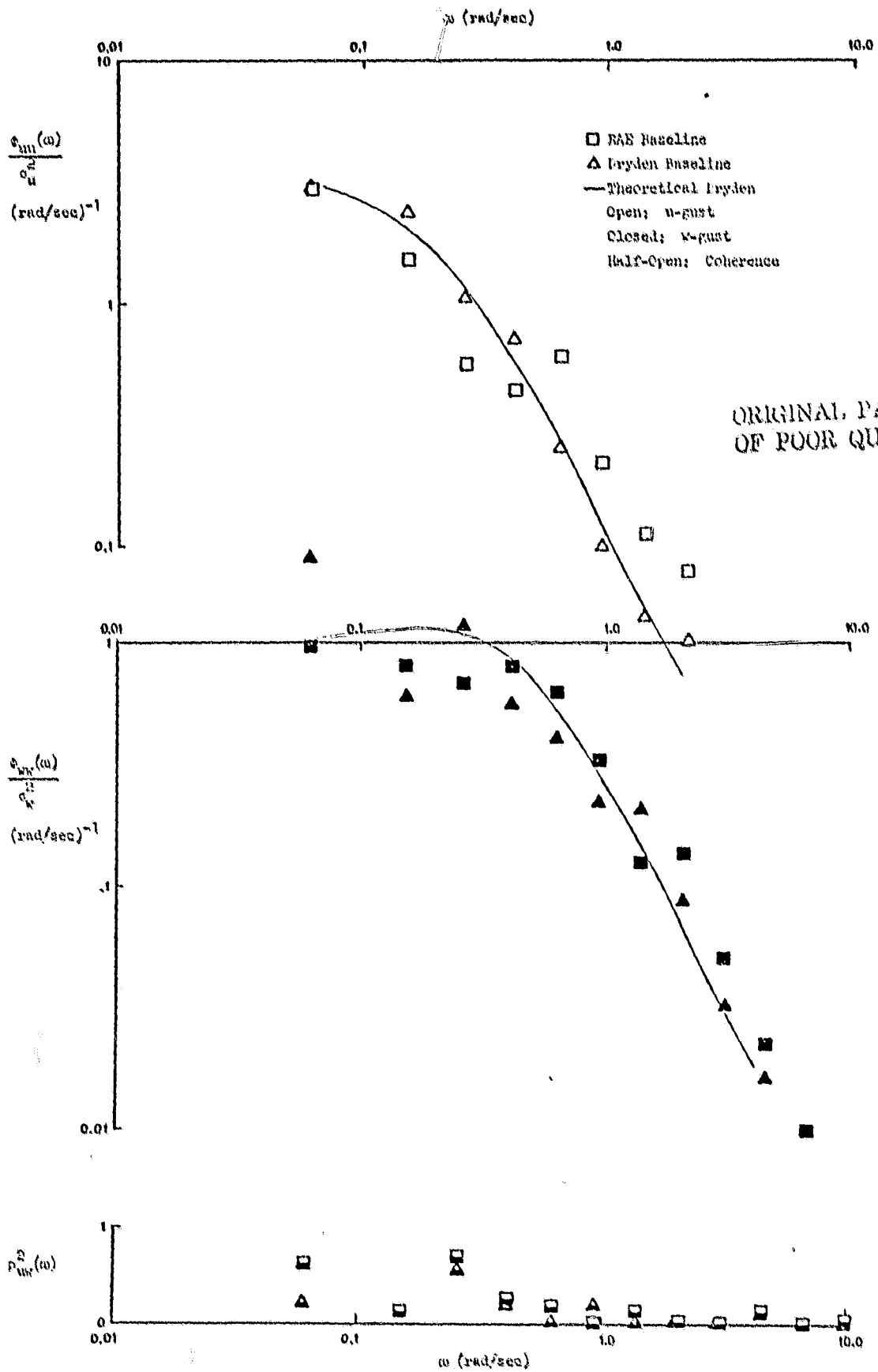
Our best resolution of measured spectral power distribution came about from consideration of cumulative power fraction versus frequency (see previous definition). The three fractions of the total power to be considered were 0.10, 0.50, and 0.90*. The resulting power fraction plots are presented in Fig. 5 for u- and w-gusts. Idealized Dryden model characteristics are shown by a solid line.

The spectral power in the RAE model clearly is centered about a higher frequency for both gust components. The implication is that a rule of thumb for setting the bandwidth control, NGUSTS, i.e., NGUSTS $= \frac{V}{50}$, does not provide a half-power point equivalent to the Dryden model under the same conditions. In fact, the rule of thumb yields a half-power frequency for u-gust which was higher than that for the Dryden model by a factor of two in this case. Most important, this is not clearly visible in the traditional plot of log Φ versus log ω (Fig. 3).

C. STATISTICAL DESCRIPTION

The most interesting comparisons between the RAE and Dryden models were found in the various statistical descriptions which were considered.

1. Probability Distribution Function

The basic u- and w-gust probability distributions for both models are shown in Fig. 6. The scale of the probability axis was chosen such that a normal distribution would plot as a straight line. It is seen from Fig. 6 that the Dryden model used here is not perfectly Gaussian, although it should be. The RAE model deviates further from a Gaussian distribution, but not dramatically. We shall see a greater deviation from a Gaussian probability distribution for other RAE model parameters considered in Section III.

---

* Due to the courseness of the spectral estimates, it was not always possible to obtain the frequency exactly at these values of the power fractions (e.g., the frequency at a power fraction of 0.15 instead of 0.10 would be obtained).

Figure 5. Power Fraction of the u and w Variance Versus
Frequency for the Dryden and RAE Models
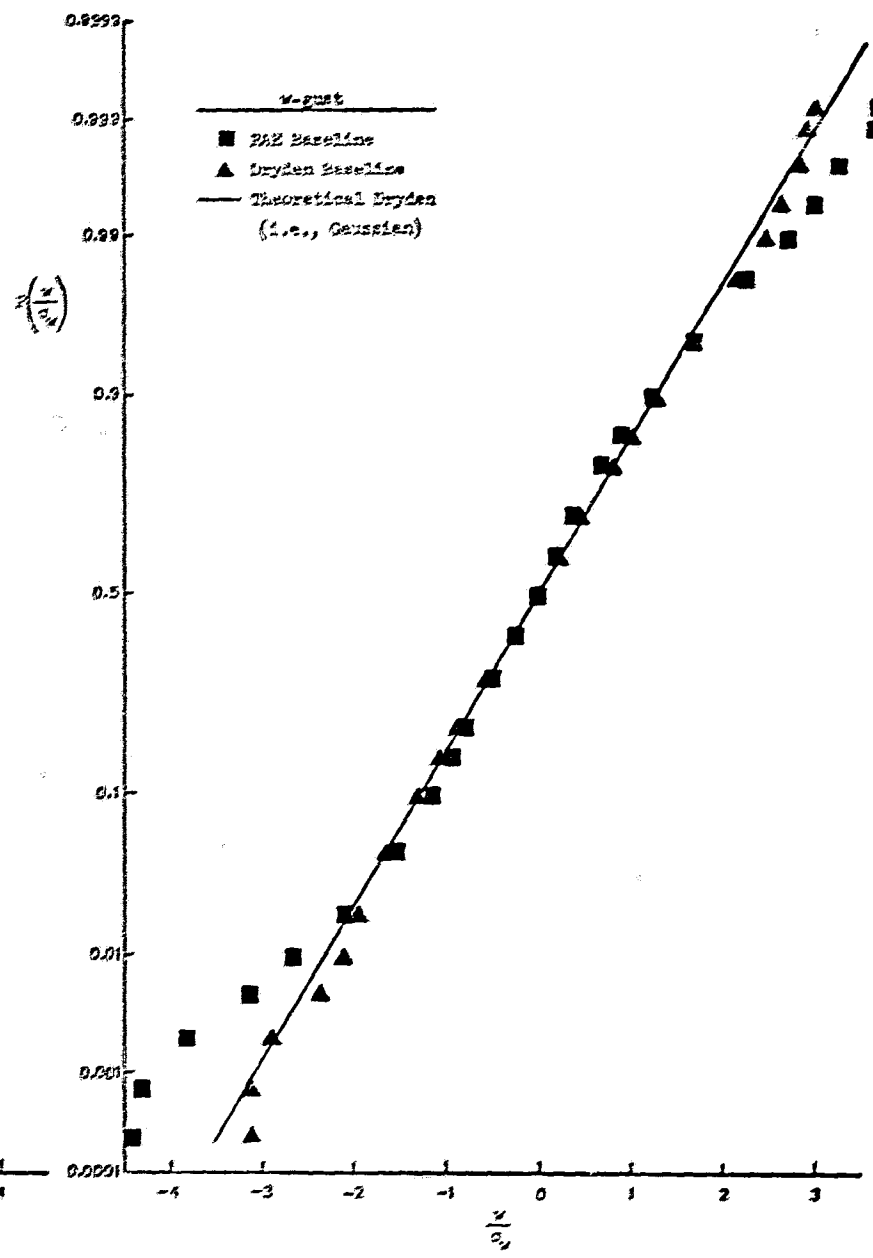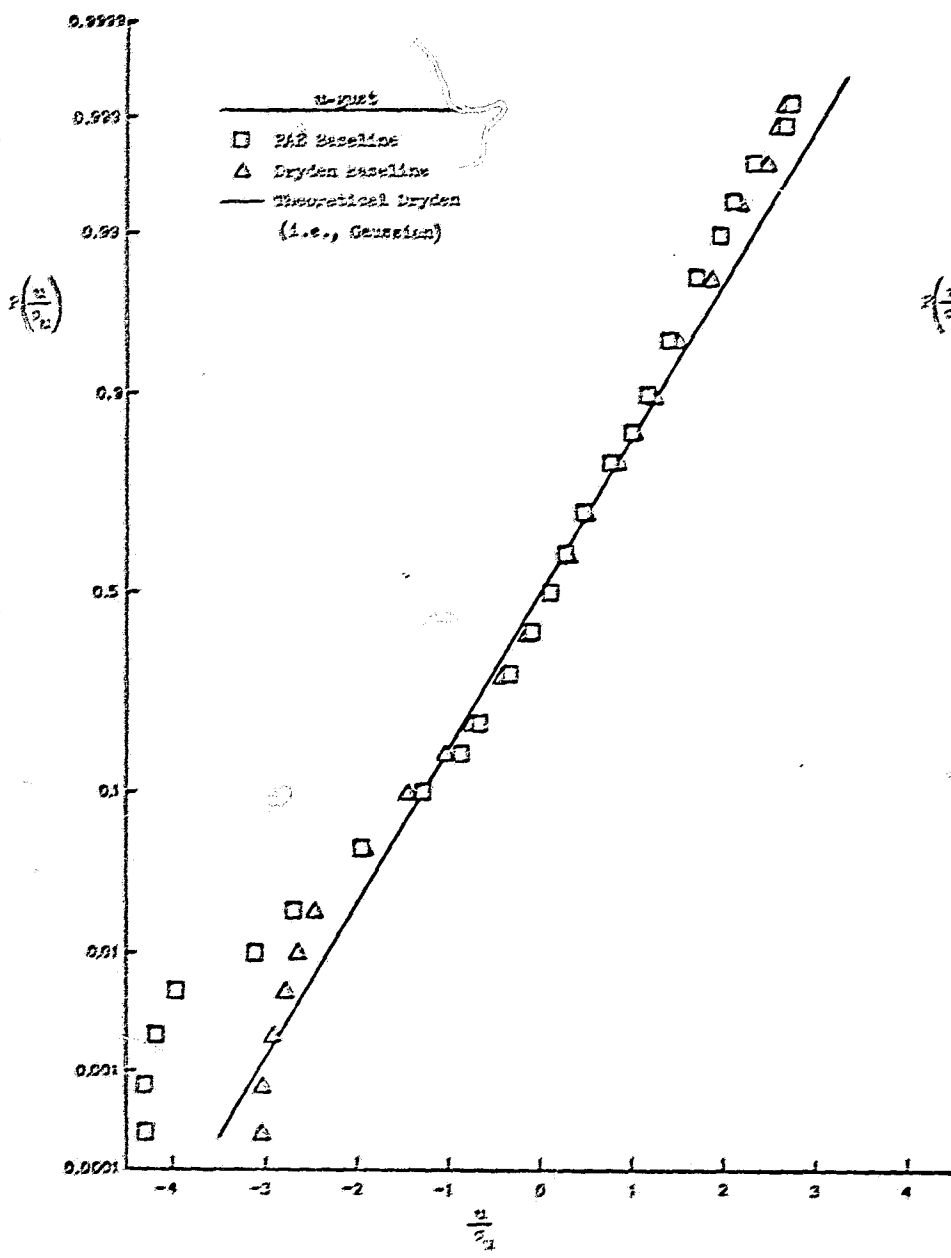
Figure 6. Probability Distribution Functions of u- and w-Gust
for Baseline PAB and Dryden Cases

2. Time-Stationarity

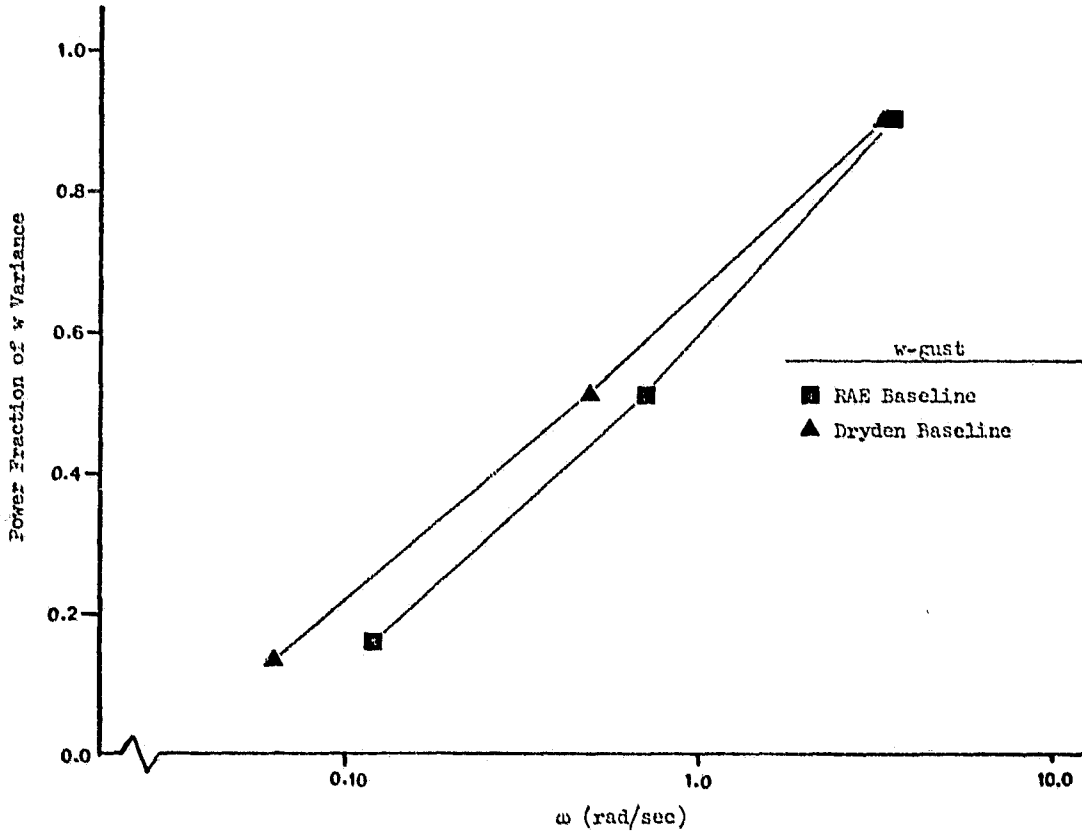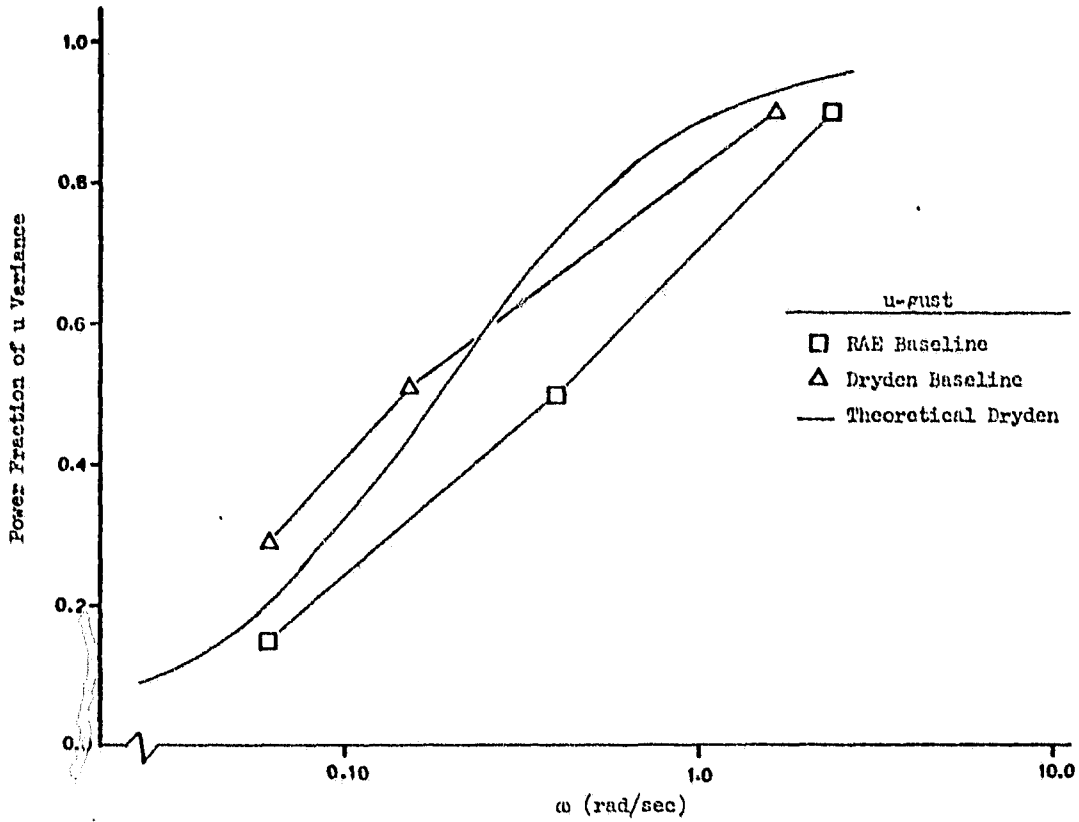One method used to examine statistical characteristics was to apply a "sliding temporal window" to the turbulence samples considered. Thus over a window having a duration of T seconds, various statistical relationships were measured and expressed as functions of T.

The sliding window was considered to be one device for measuring the essential features connected with wind shear. Windows much shorter or much longer than predominant pilot-vehicle response time constants should be of lesser consequence than windows which are approximately equal to those time constants. Naturally, the precise range of important pilot-vehicle response time constants (or frequencies) depends upon the specific aircraft, its configuration and flight condition, and, most importantly, upon the pilot's closed loop structure and degree of tightness. If normal landing approach flight path and airspeed regulation is involved, the respective crossover frequencies will be about 0.1 rad/sec and 0.3 rad/sec. The corresponding significant window length, therefore, would presumably be about 3 to 10 sec in duration.

Another way of interpreting window duration is its relationship to the average duration of an approach. Suppose a landing approach normally takes one to two minutes. We could therefore concern ourselves with statistical properties over that period. The above concepts are illustrated in Fig. 7.

We shall see that such properties can vary appreciably from "steady-state" values. Furthermore, measures of stationarity are provided by the mean and dispersion of various statistical measurements (e.g., the variance, kurtosis, etc.) due to sampling the turbulence via different window durations. Convergence of the mean of the statistical measurements to a limit is one indication of stationarity. In addition, a low dispersion of the statistical measurements is another indication of stationarity. Reference 6 contains a more detailed discussion of conditions for stationarity of stochastic processes.

a. <u>Standard Deviation</u>. Standard deviation was the most elementary statistical property measured as a function of window duration. Figure 8

Statistical
Feature

Time response
of pilot-vehicle

Duration
of approach

Mean plus one standard deviation

Mean of statistical feature

Mean minus one standard deviation

1   10   100   1000

Window Duration, T (sec)
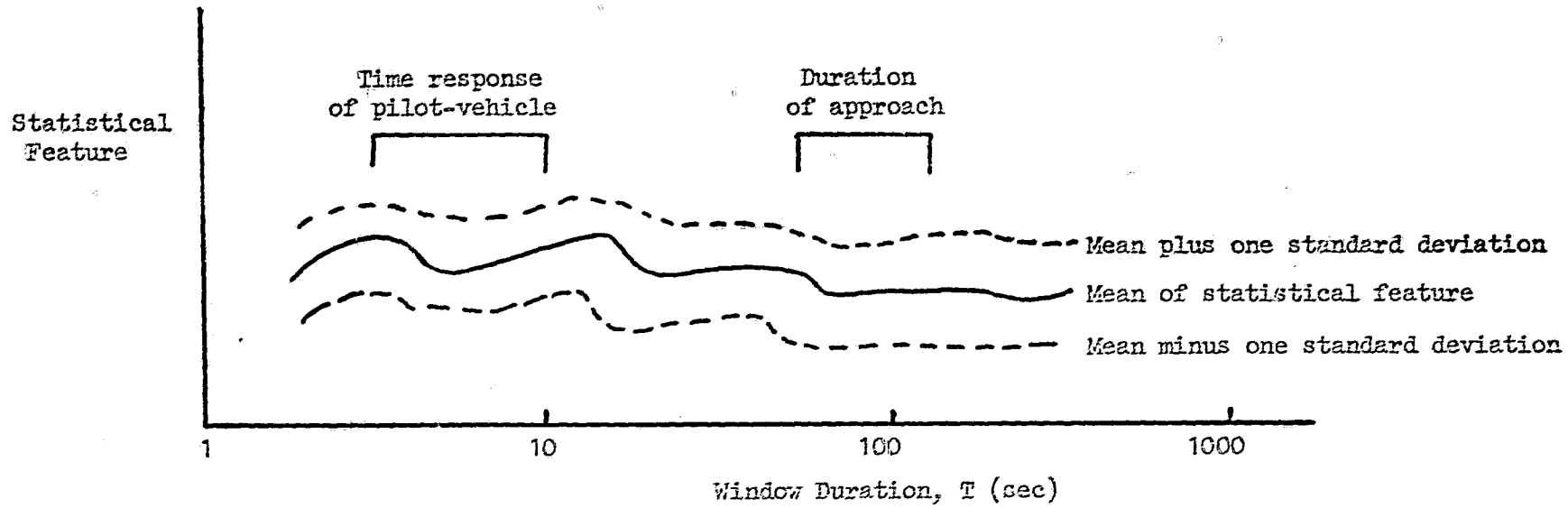
Figure 7. Generic Example of Sliding Window Concept
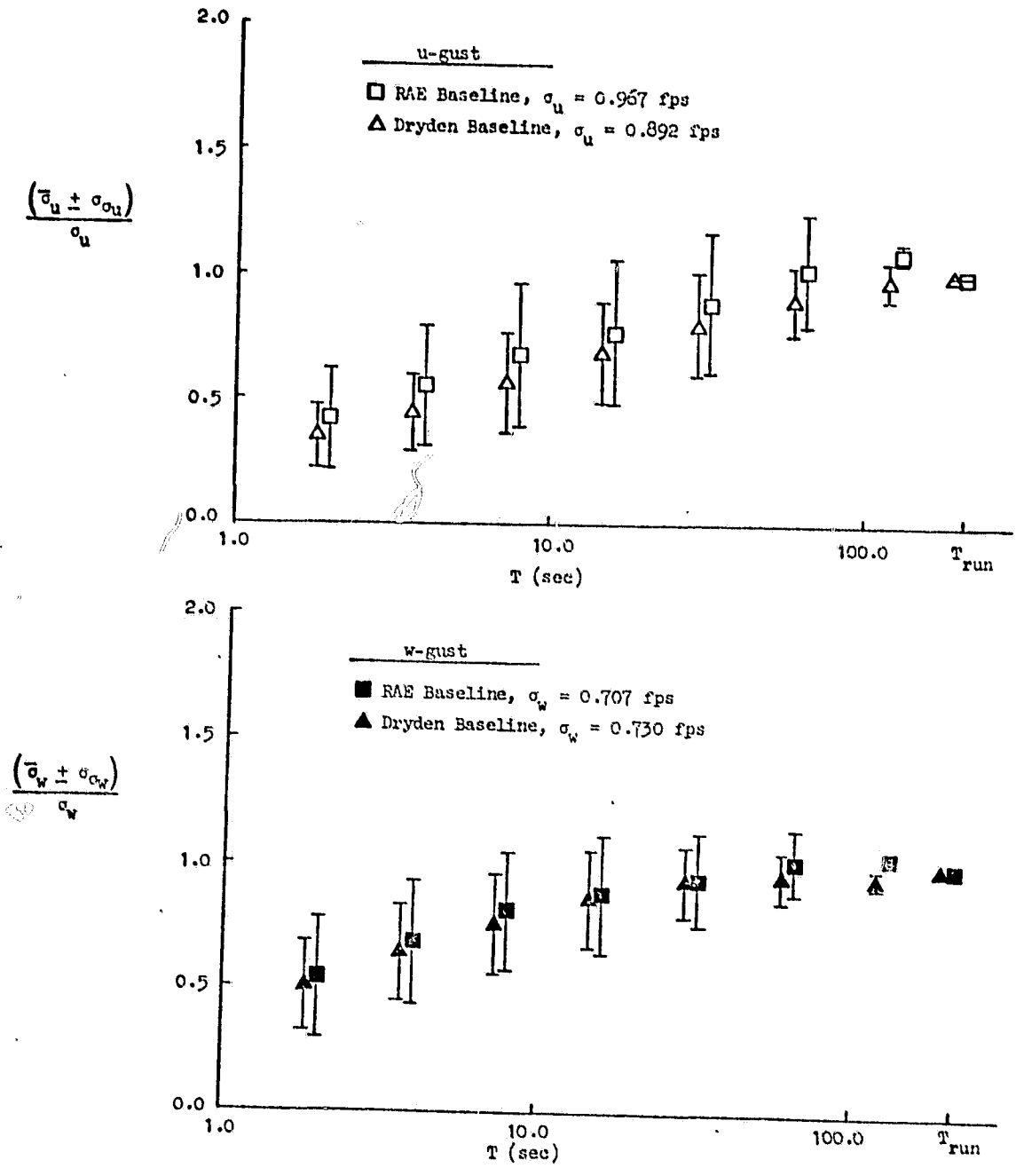
Figure 8.   RMS u- and w-Gusts for the Dryden and RAE Turbulence Models

shows rms u-gust in terms of its own average $(\overline{\sigma}_u)$ and standard deviation (σ_{σ_u}) relative to the overall rms (σ_u) for varying window duration, T. Note that as T approaches the total sample duration, T_{run} (204.8 sec):

$$\frac{\overline{\sigma}_u}{\sigma_u} \longrightarrow 1$$

$$\text{and} \qquad \frac{\sigma_{\sigma_u}}{\sigma_u} \longrightarrow 0$$

The sample size limitation causes $\sigma_{\sigma_u} \longrightarrow 0$ as $T \longrightarrow T_{run}$ (e.g., the variance of one sample is zero). If T_{run} were doubled then σ_{σ_u} would approach zero as $T \longrightarrow 2\,T_{run}$, but would be non-zero at $T = T_{run}$. On the other hand, for $T \ll T_{run}$ the rms is smaller and the variability is larger. For example:

T	$\dfrac{\overline{\sigma}_u}{\sigma_u}$		$\dfrac{\sigma_{\sigma_u}}{\sigma_u}$	
	RAE	Dryden	RAE	Dryden
8 sec	0.7	0.6	0.25	0.20
64 sec	1.0	0.9	0.20	0.15

We note that the Dryden rms ratio is somewhat smaller (i.e., $\overline{\sigma}_u/\sigma_u$ is smaller) than the RAE rms ratio for any given window length. This is consistent with the difference in half-power points noted earlier. Also, σ_{σ_u} for the RAE u-gust is consistently greater than that for the Dryden u-gust, which indicates that the RAE turbulence is less stationary than the Dryden turbulence.

Figure 8 shows the rms dependence on window length for w-gust, and we can observe less difference between the models than for the u-gust. Again, this is consistent with the spectral differences noted earlier.

b. Kurtosis. Kurtosis, a measure of the fourth order central moment, was calculated in terms of the sliding window and was more sensitive to some model differences than variance. Figure 9 shows comparative kurtosis for
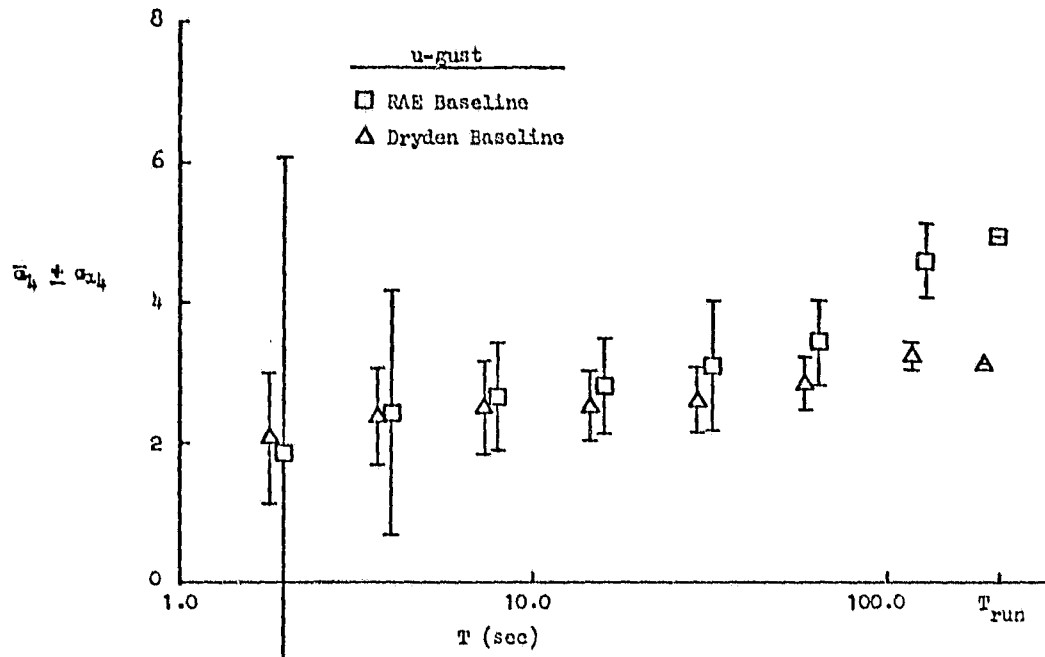
Figure 9. Kurtosis of u- and w-Gusts for the
Dryden and RAE Turbulence Models

u-gust and w-gust. Kurtosis for a normally distributed random variable
should be three, and this is the case for u- and w-gust as T becomes large
for the Dryden turbulence. (Kurtosis for the entire Dryden model samples
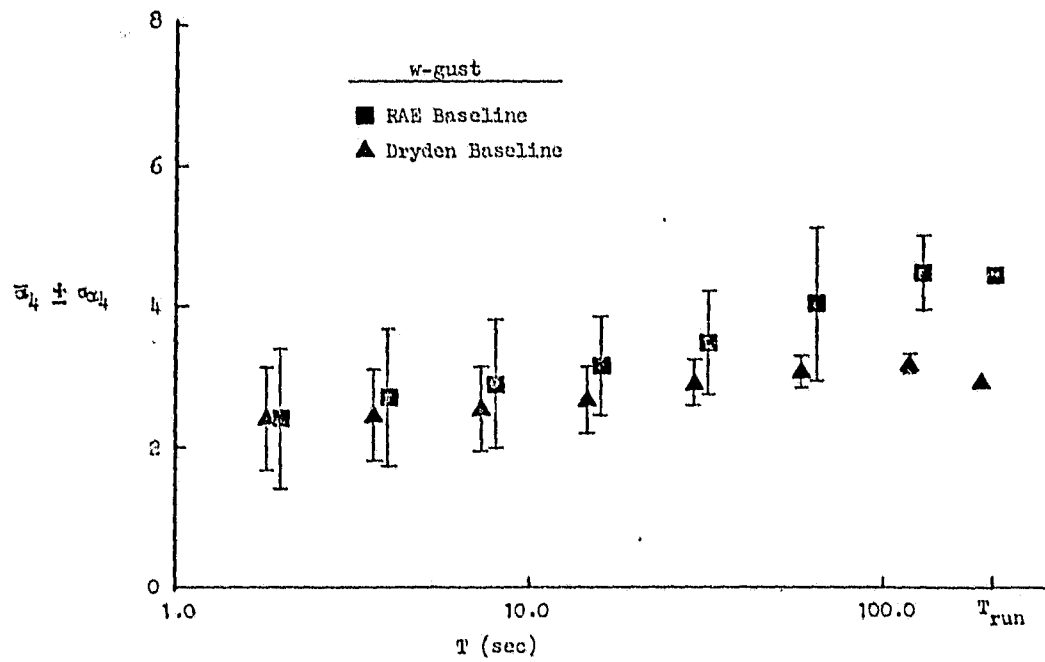were measured as 3.1 and 2.9 for u- and w-gusts, respectively.) The mean
kurtosis of the RAE model was found to be larger than that of the Dryden
model for longer duration windows but not for shorter durations, say, less
than 16 sec. In the latter case, the mean kurtosis was about equal. As a
result we might expect to find little evidence of so-called non-Gaussian
effects in the short term compared to the very long term or steady state.

Another feature plotted in Fig. 9 is the variation of kurtosis as a given
window is moved along the finite duration samples. This feature is shown by
the vertical bars extending from the mean kurtosis. The variation in u-gust
kurtosis becomes very large for short windows in the case of the RAE model.
We find it difficult to relate this statistical feature to a specific time
domain feature but believe that it may reflect the large amplitude rates
of change in u-gust which occur from time to time in the RAE model. It may
also relate to the feature to be discussed next.

3. Effective Wind Shear

Wind shear was one characteristic of particular interest in this study.
In previously unpublished work (Ref. 7) we had derived analytical relation-
ships for the Dryden model to characterize the effective change in gust
amplitude over a given time interval (window). Two ways of expressing this
feature are illustrated in Fig. 10. The first way involves a least squares
fit of $u(t)$ over a given time interval and thus represents an effective rate
of change of u-gust. The second metric takes the simple increment in u over
a given time interval. Both metrics are averaged over a finite duration run

① $\Delta u = \frac{\partial u}{\partial t} \cdot T$

② $\Delta u = u(t+T) - u(t)$

Lease squares
fit of u(t)
from t_1 to t_2

u

① $\Delta u = \frac{\partial u}{\partial t} \cdot (t_2 - t_1)$

② $\Delta u = u(t_2) - u(t_1)$

T

t_1

t_2

t
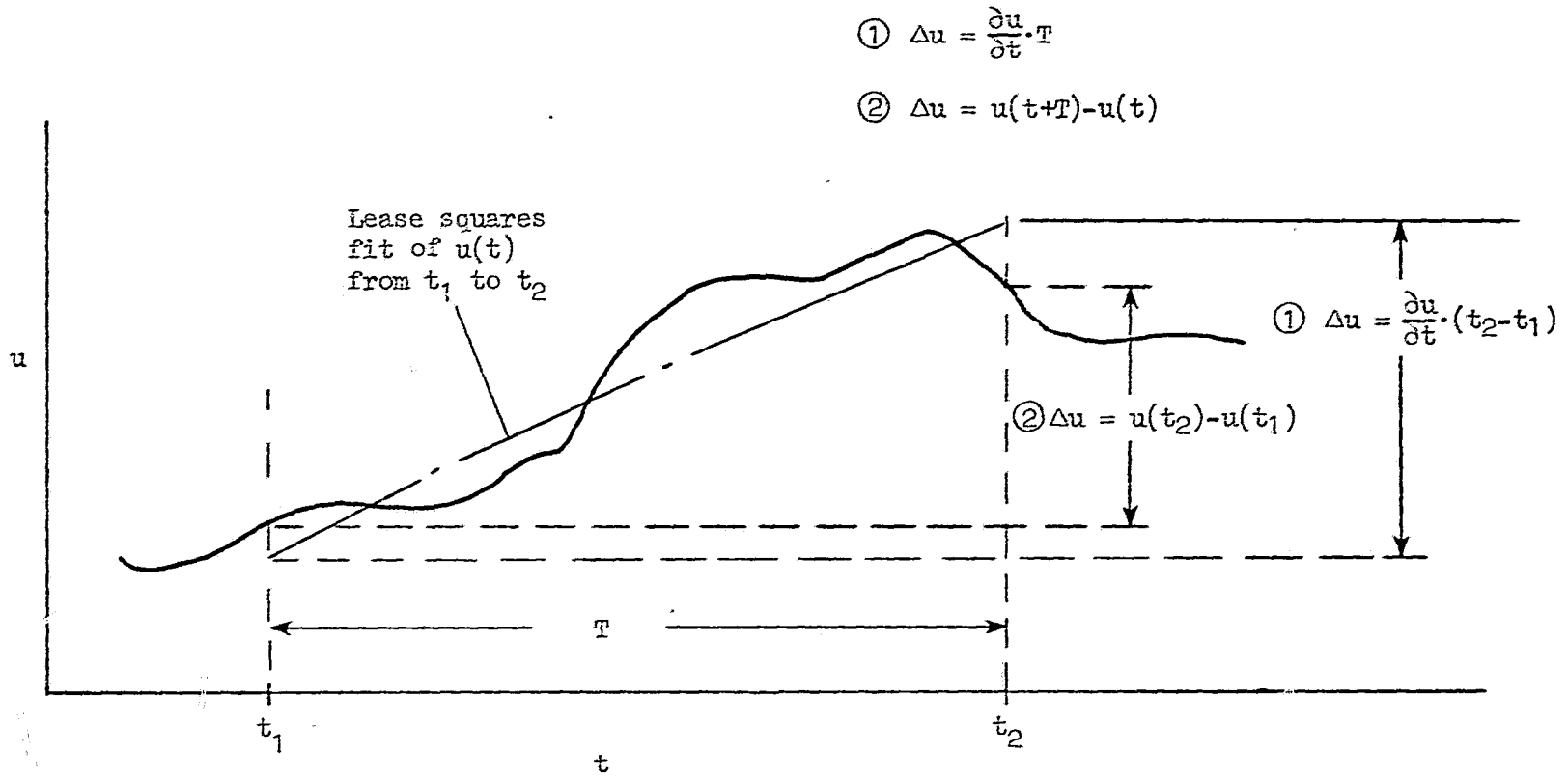
Figure 10.   Two Methods of Expressing Gust Velocity Change Over a Time Window

using the sliding window idea. For an infinitely long sample of a Dryden model u-gust the following relationships can be derived:

1. For $\Delta u_1 \equiv \frac{\partial u}{\partial t} \cdot T$

$$\sigma^2_{\Delta u_1} = \frac{24 \, \sigma_u^2}{\eta^4} \left[\eta^3 + 3 (4 - \eta^2) - 3 (2 + \eta)^2 \, e^{-\eta} \right]$$

$$\text{where} \quad \eta \triangleq \left| \frac{V \cdot T}{L_u} \right|$$

2. For $\Delta u_2 = u(t+T) - u(t)$

$$\sigma^2_{\Delta u_2} = 2\sigma_u^2 (1 - e^{-\eta})$$

Figure 11 shows the first and second parameters plotted as a function of T for the RAE and Dryden turbulence models. Except at small values of T, neither plot shows any consistent differences between the two turbulence models.

This concludes the comparison of the Dryden and RAE turbulence models and the description of the spectral and statistical measures used to quantify the characteristics of the turbulence models. The next section describes the effects of perturbing each of the RAE model input parameters in terms of the spectral and statistical measures already described.
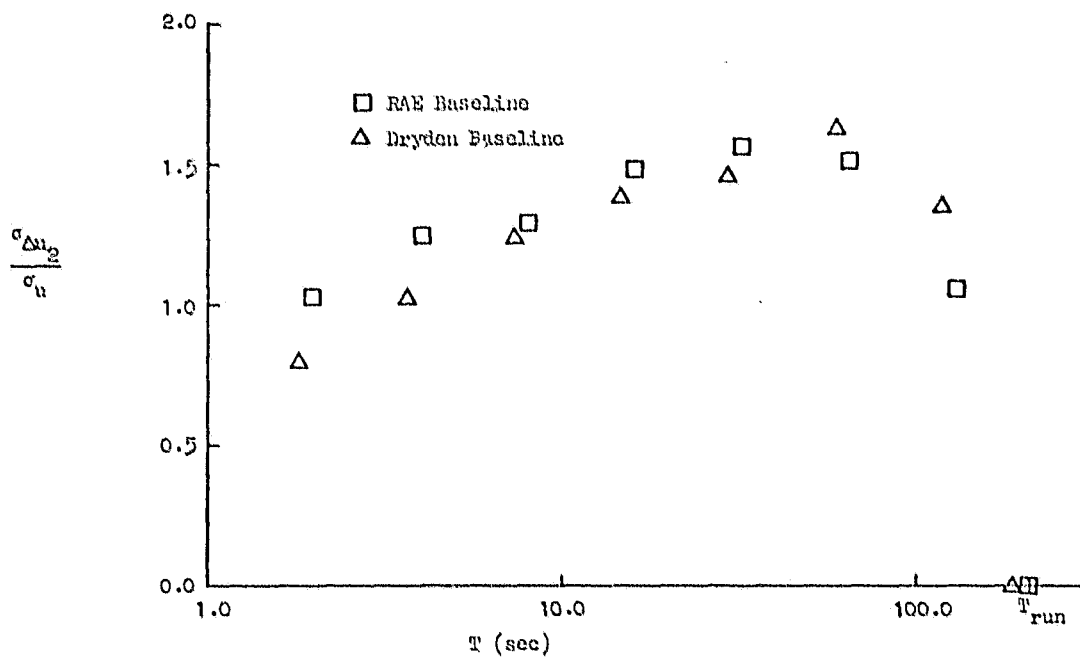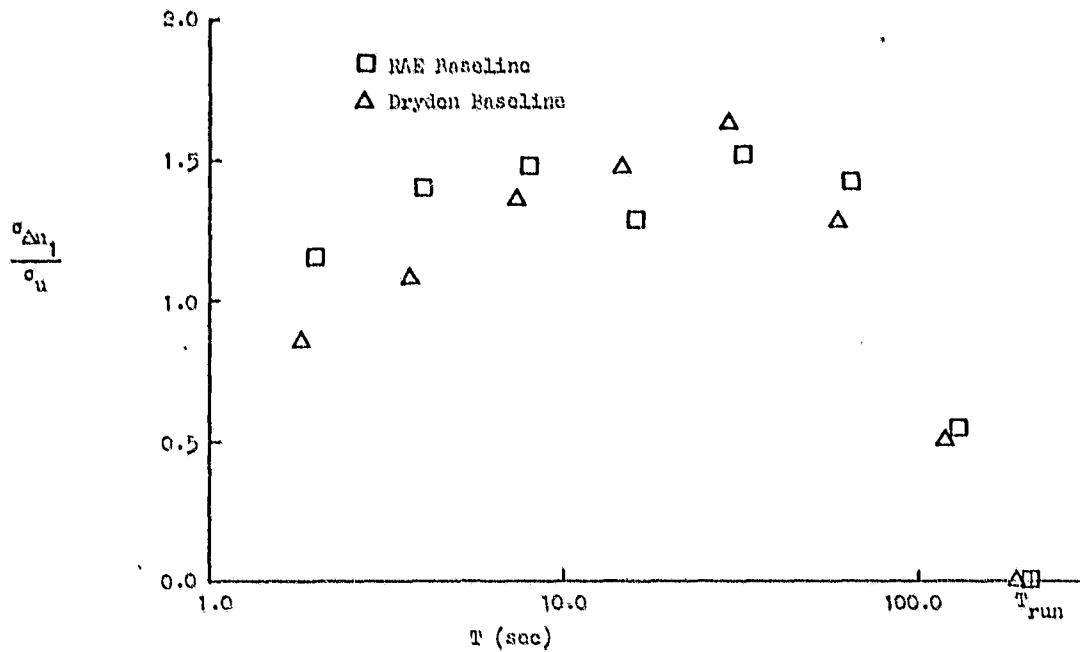
Figure 11. RMS Velocity Increments for the
Dryden and RAE Turbulence Models

SECTION III

EFFECTS OF VARYING THE RAE TURBULENCE MODEL PARAMETERS

The effects of individually perturbing each of the RAE model parameters on the temporal, spectral, and statistical properties of the turbulence are presented and discussed in the following subsections. The perturbations are made with respect to the baseline settings defined in Section II, which were intentionally chosen to yield Gaussian-like characteristics of the RAE turbulence. Thus by perturbing the RAE model parameters with respect to these nominal settings the non-Gaussian characteristics of the RAE turbulence will be demonstrated and quantified. The nominal and perturbed values of the six RAE model parameters are shown in Table 3.

TABLE 3

BASELINE AND PERTURBED VALUES OF THE RAE MODEL PARAMETERS

Parameter	Baseline Value	Perturbed Values
NGUSTS	5 gusts/sec	2, 8 gusts/sec
F	0.0	0.4, 0.8
R	0.7	0.5, 0.9
HCG	800 ft	200, 2500 ft
DT	0.10 sec	0.05, 0.15, 0.20 sec
SIGMA	1.0	——*

---

* The RAE parameter SIGMA is used only to set the variances of the turbulence components. Therefore, perturbations were not analyzed. (See Subsection II.F.)

A brief description of how each parameter is utilized within the RAE model is given at the beginning of each of the following subsections. In addition, whenever it is appropriate, each parameter is quantitatively described in terms of its major impact on the attributes of the RAE turbulence. For example, the parameter NGUSTS primarily affects the frequency content of the turbulence and we have therefore dubbed it the "bandwidth control." NGUSTS does, however, have secondary effects on the statistical characteristics of the turbulence.

Except for the subsection on the effects of altitude, HOG, the spectral and statistical properties of the turbulence are described only for the u-gust component. This is sufficient because above 2500 ft the statistical properties of all three components of the RAE turbulence are equivalent. The only interesting property of the RAE turbulence we discovered by examining the other turbulence components is their unusually high coherence (high with respect to the Dryden model in which the turbulence components are intentionally designed to be independent). This high coherence property is presented and discussed in Subsection III.D.

When generating the RAE turbulence time histories, which were subsequently spectrally and statistically analyzed, the turbulence was always sampled at the same point in time and, even though only 140 sec time histories are shown, the length of the samples was always 204.8 sec (2048 data points with a frame time of 0.10 sec). Slightly different absolute values of the spectral and/or statistical characteristics would be obtained if the run length or the sampling points were changed, but the trends in the turbulence attributes connected with the RAE model parameters reported below should not change.

A. BANDWIDTH CONTROL, NGUSTS

The amount of high frequency power, or "bandwidth," of the RAE turbulence is primarily controlled by the NGUSTS parameter. NGUSTS performs many functions within the RAE turbulence model; however, its primary function is to control the number of new low-, mid-, and high-frequency gusts generated each second. These gusts are inputs to special-purpose filters, and the outputs of the filters are then used to form the three turbulence components: u-gust, v-gust, and w-gust. NGUSTS can take on only integer values and is

limited to

$$1 \leq \text{NGUSTS} \leq 1/\text{DT}$$

where DT is the frame time. The effects of NGUSTS on the temporal, spectral, and statistical properties of the RAE turbulence are presented and discussed below.

u and w-gust time histories for NGUSTS = 2, 5, and 8 gusts/sec are presented in Fig. 12. These show that increasing NGUSTS does indeed increase the bandwidth of the turbulence. This observation is confirmed by examining the plots of power spectra and power fraction plotted versus frequency. An increase in the power at higher frequencies is discernible from the power spectral density plots, $\Phi_{uu}(\omega)/\sigma_u^2$ and $\omega\Phi_{uu}/\sigma_u^2$ versus ω, in Figs. 13 and 14. The effect on spectral power distribution is best depicted by the power fraction plot in Fig. 15. Note that the frequency at a power fraction of 0.90 of the total variance, $\omega(0.90)$, monotonically increases from 1.1 to 4.0 rad/sec as NGUSTS is increased from 2 to 8 gusts/sec. The shift in the power fraction is not as dramatic or consistent at lower frequencies ($\omega(0.15)$ increased from 0.06 to 0.12 rad/sec for NGUSTS = 5 to 8 gusts/sec, but remained at 0.06 rad/sec for NGUSTS = 2 gusts/sec). This indicates that increasing NGUSTS only extends the bandwidth of the turbulence, rather than shifting the entire spectrum to a higher frequency (i.e., the low frequency power remains fairly constant as NGUSTS is increased).

Figure 16 shows that NGUSTS did not affect the probability distribution function (PDF) in a consistent manner. That is, the tails of the PDF were altered by NGUSTS, but the low probability tail was not changed in the same manner as the high probability tail. Also, neither tail was changed monotonically by NGUSTS. Thus it appears that NGUSTS has an effect on the probability distribution functions, and hence will have an effect on the higher order moments.

Figure 17 shows that the mean limited window standard deviation of u-gust, $\bar{\sigma}_u$, monotonically increases with NGUSTS. (The change in $\bar{\sigma}_u$ due to NGUSTS could be compensated for by using the intensity control parameter, SIGMA, as discussed in Subsection III.F.) The dispersion of the limited window standard deviation of u-gust, σ_{σ_u}, increases slightly as NGUSTS is increased
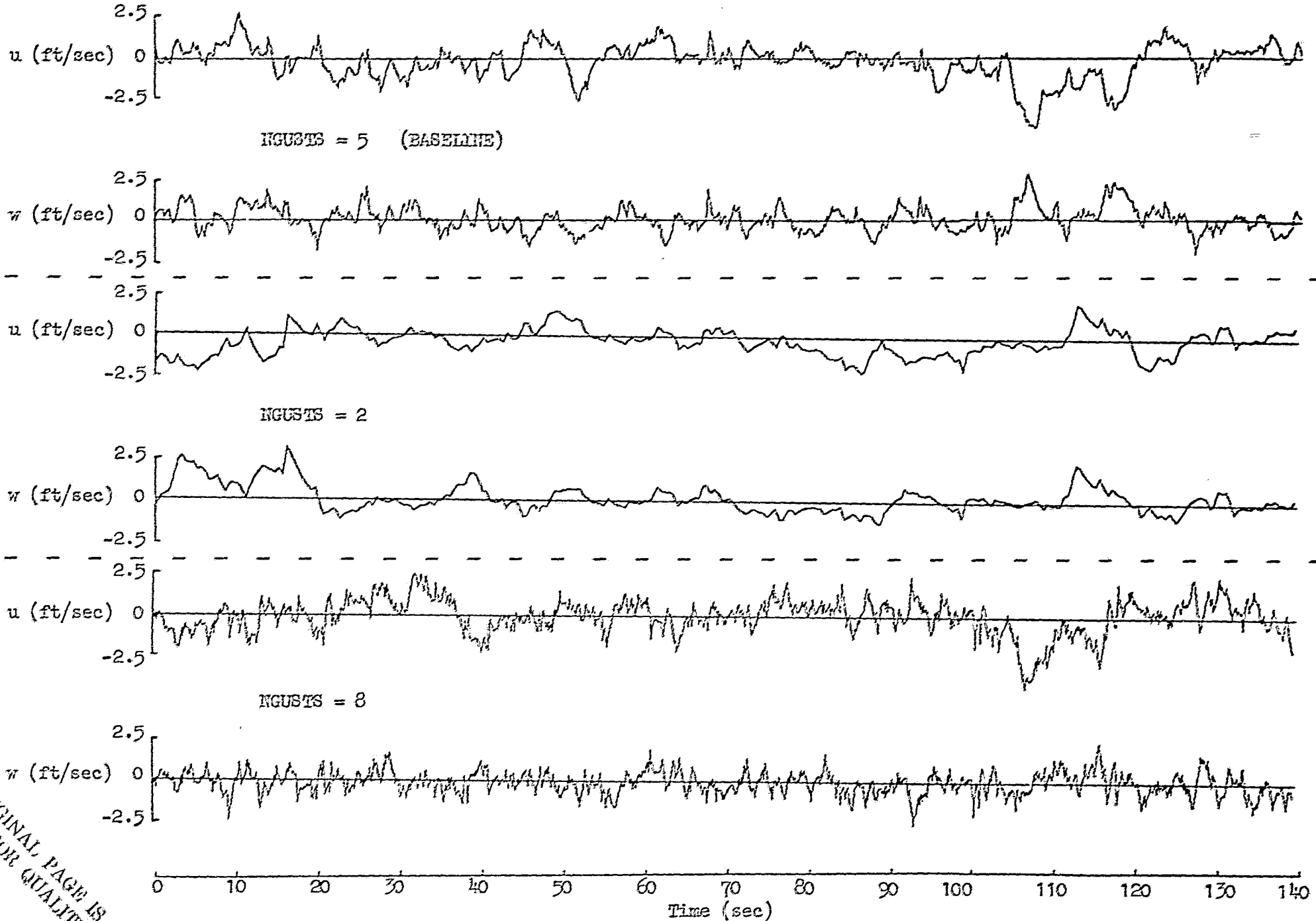
Figure 12. Effects of NGUSTS on Temporal Characteristics of the RAE u- and w-Gust Turbulence
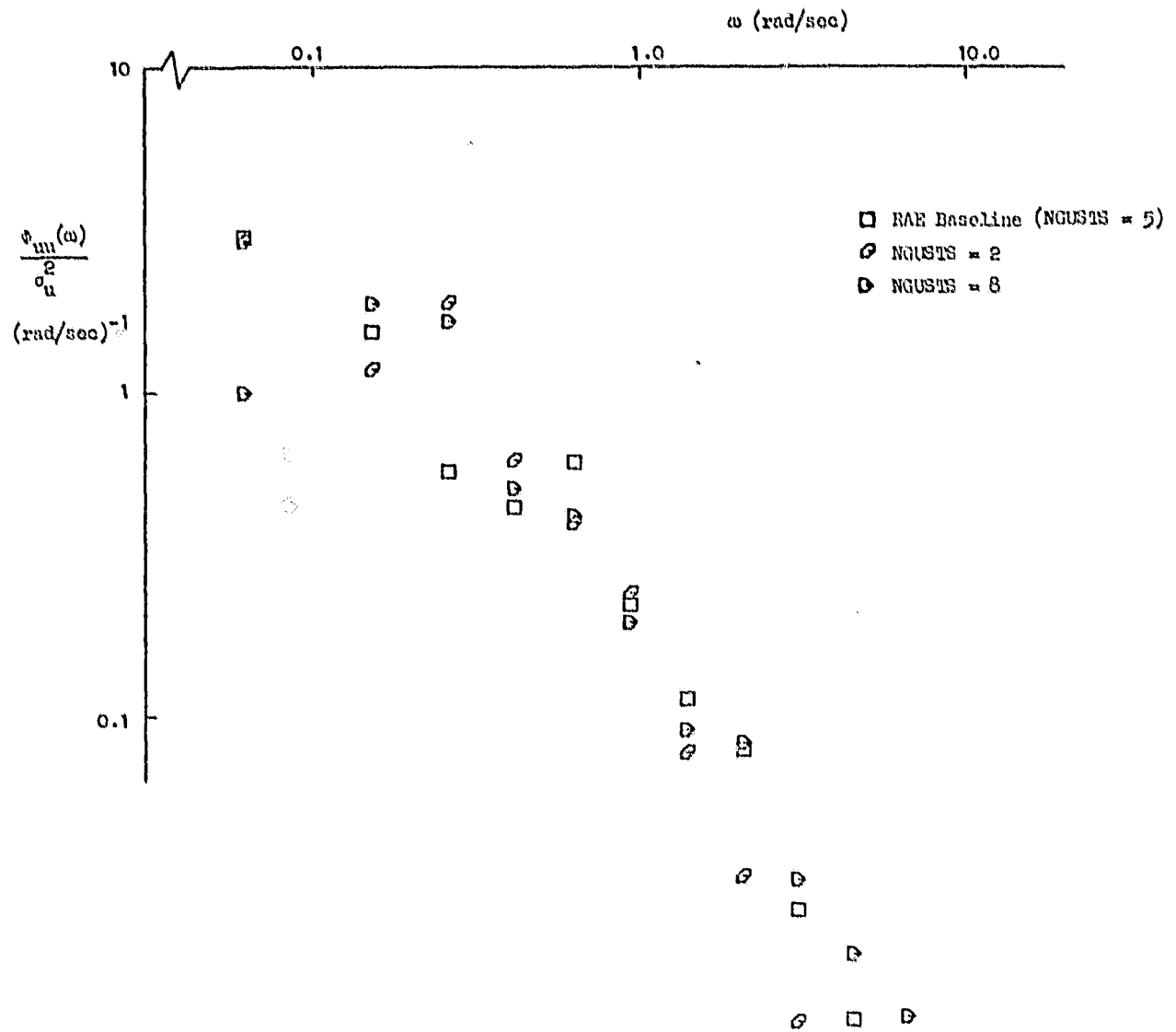
Figure 13. Effects of NGUSTS on $\phi_{uu}(\omega)$ of the RAE Turbulence Model
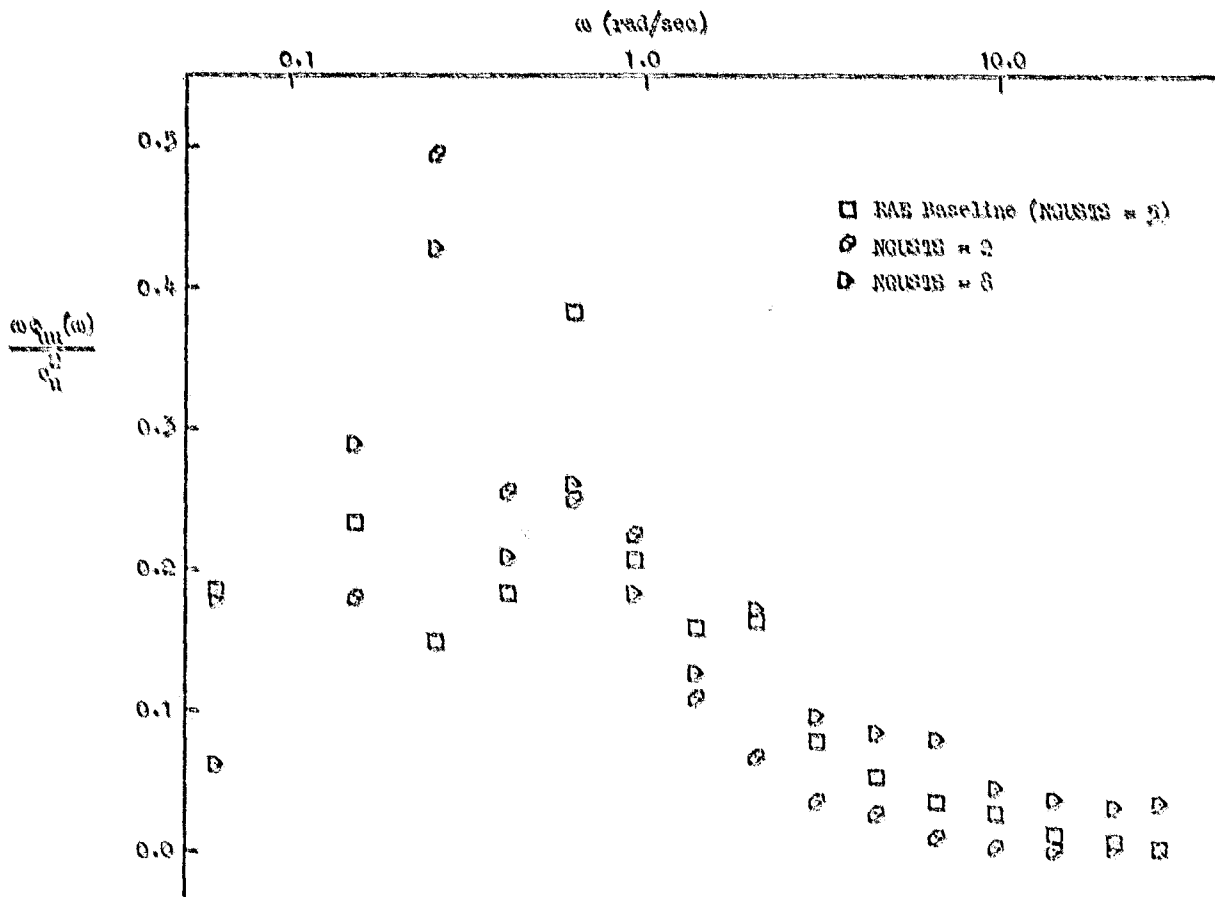
Figure 14. Effects of NGUSIS on $\omega\Phi_{uu}(\omega)$ of the RAE Turbulence Model
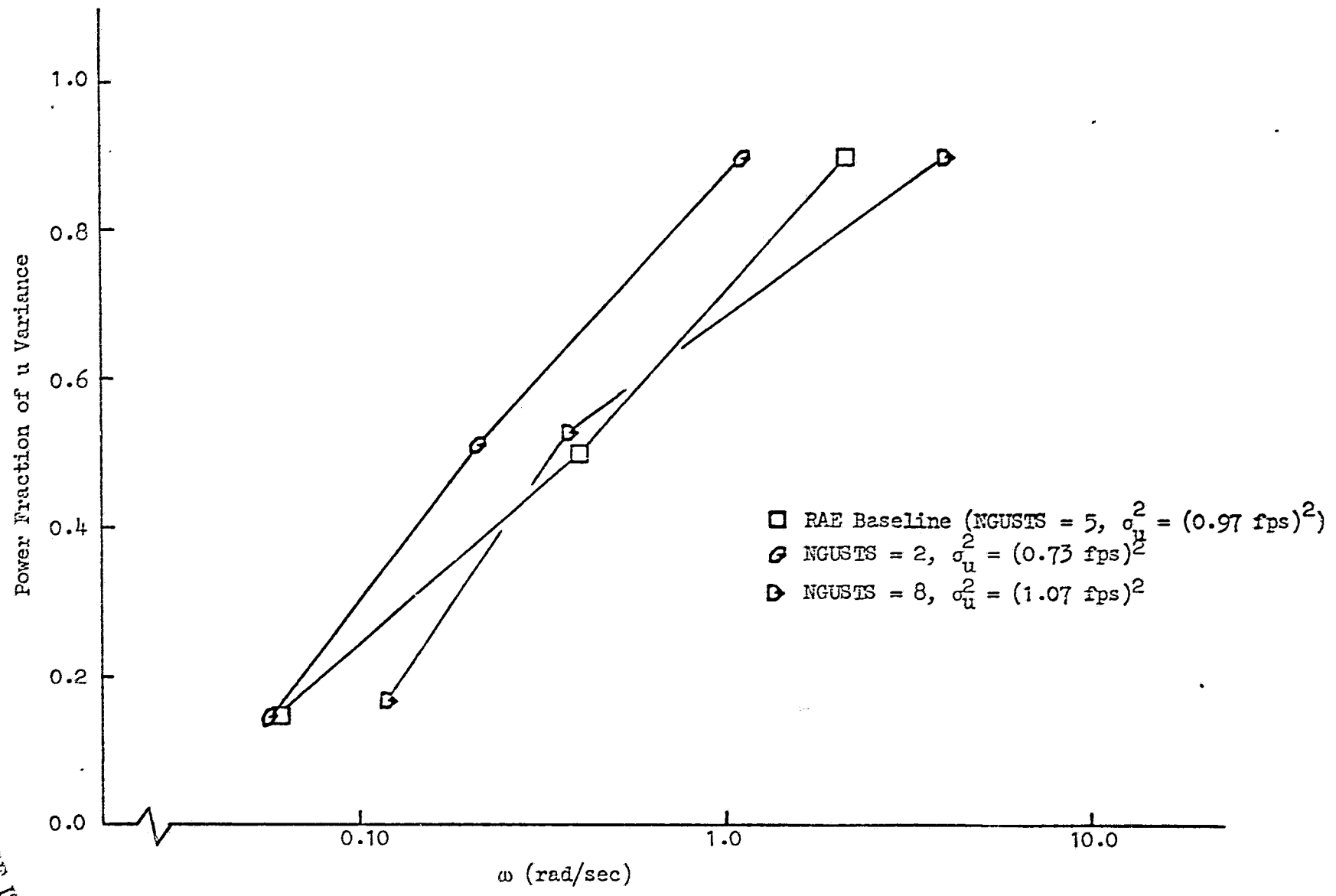
Figure 15. Effects of NGUSTS on the Power Fraction of the u-Gust Variance
Versus Frequency of the RAE Turbulence Model
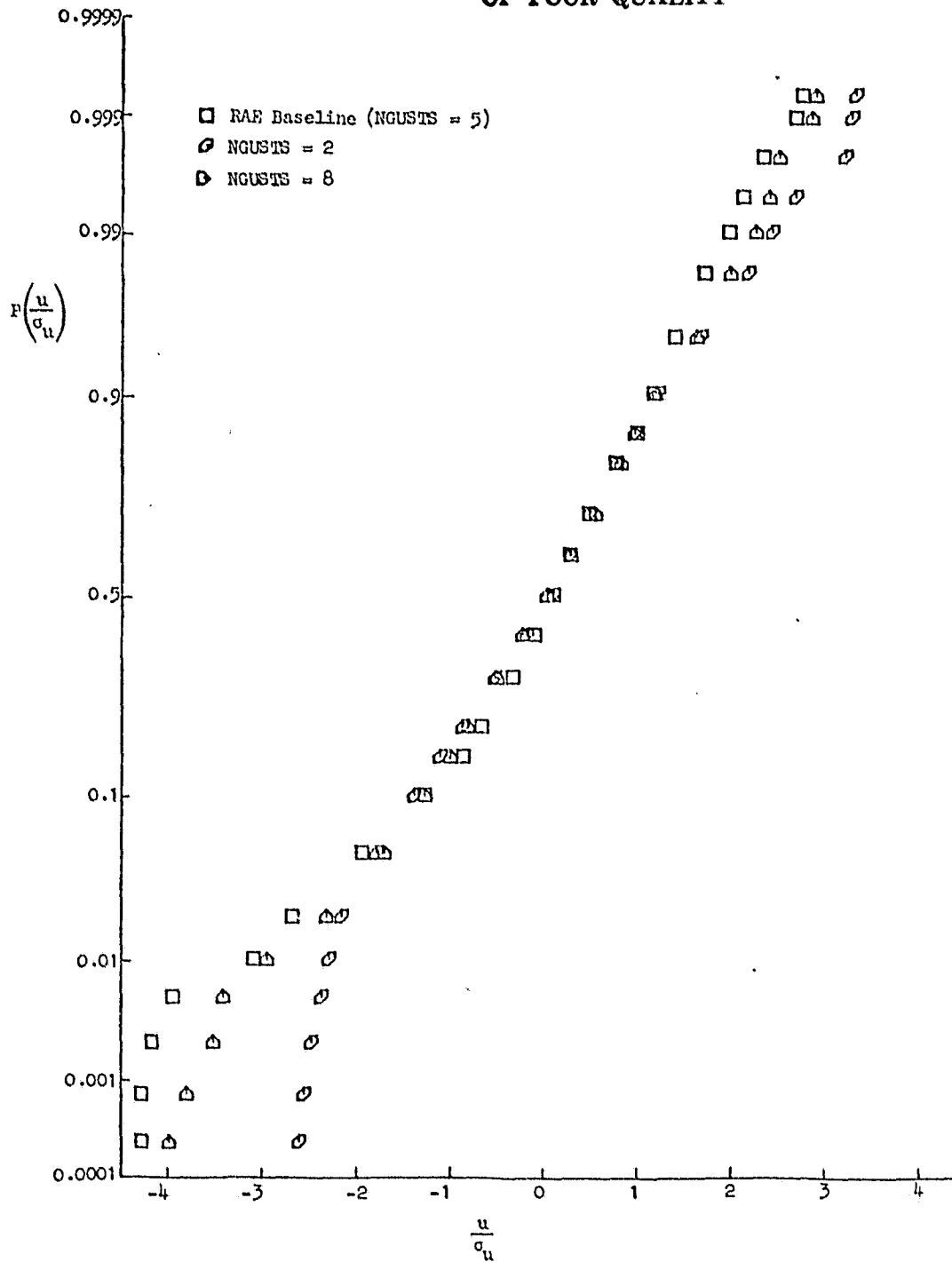
Figure 16. Effects of NGUSTS on the Probability Distribution Function
of u-Gust of the RAE Turbulence Model
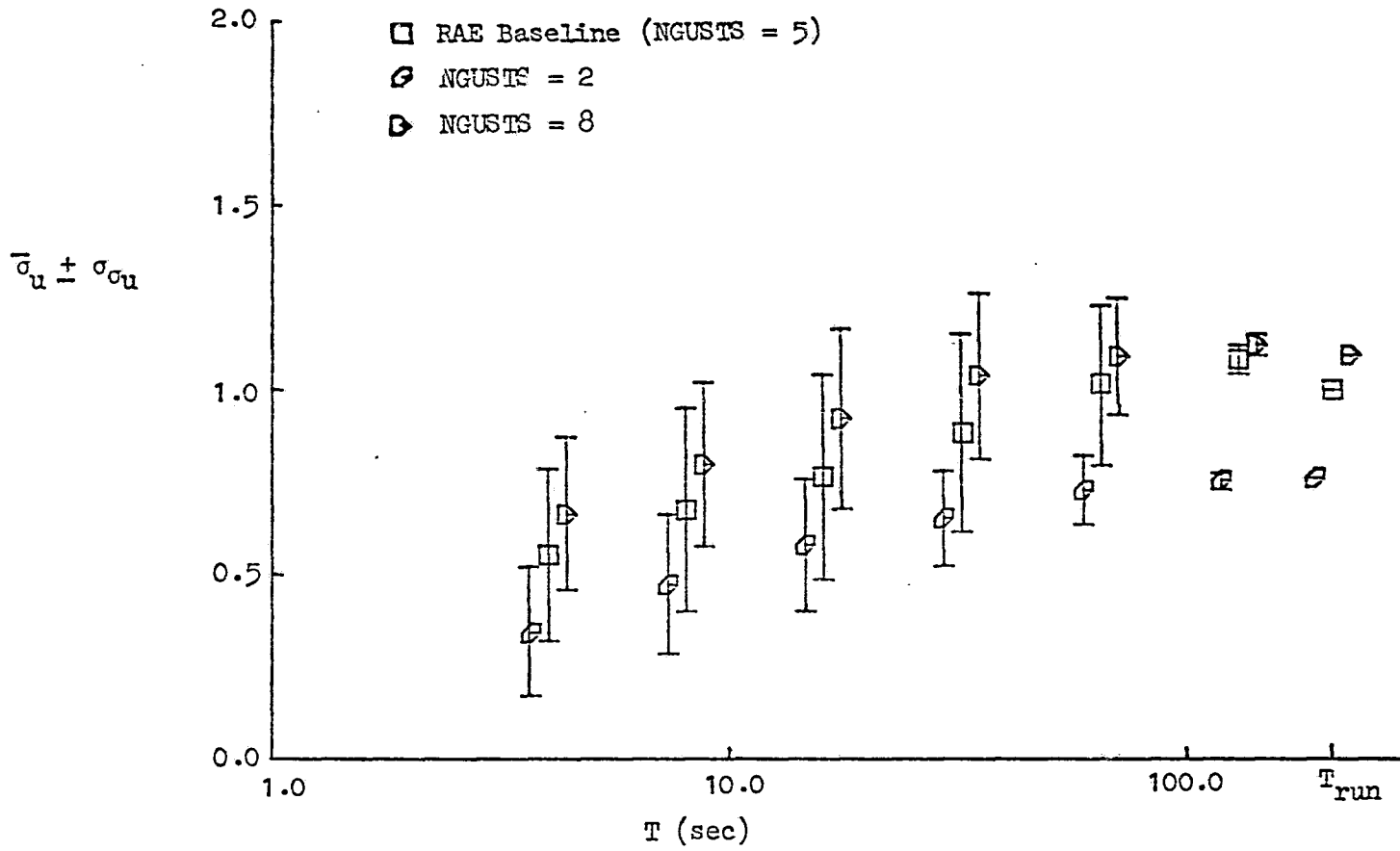
Figure 17. Effects of NGUSTS on the rms u-Gust of the RAE Turbulence Model

from 2 to 5 gusts/sec, but is not noticeably altered as NGUSTS is further increased from 5 to 8 gusts/sec. Thus there appears to be an upper bound on the level of limited sample dispersion in σ_u due to NGUSTS.

The mean and standard deviation of the kurtosis, $\bar{\alpha}_4$ and σ_{α_4}, were not consistently or significantly altered by NGUSTS, as is demonstrated in Fig. 18.

The standard deviation of the effective wind shear, $\sigma_{\Delta u_1}$ is presented in Fig. 19. It is seen that $\sigma_{\Delta u_1}$ was consistently increased as NGUSTS was increased from 2 to 5 gusts/sec, but that $\sigma_{\Delta u_1}$ did not change consistently as NGUSTS was increased from 5 to 8 gusts/sec ($\sigma_{\Delta u_1}$ was increased at some values of T and decreased at others).

B. PROBABILITY DISTRIBUTION FUNCTION CONTROL, F

The purpose of the RAE model parameter F is to alter the shape of the probability distribution function (PDF) (although it is dubbed the "global intermittency parameter" in Ref. 1). As F is increased from its lower limit of 0.0 to its upper limit of 1.0 the shape of the PDF changes from nearly-Gaussian to highly non-Gaussian. The effect is to attenuate the magnitudes of the high probability regions of the PDF and amplify the magnitudes of the low probability regions (i.e., the tails). F also affects, to a certain degree, some of the other characteristics of the turbulence, which are discussed below.

Figure 20 contains time histories of u-gust and w-gust for three different values of F: 0.0, 0.4, and 0.8. The time histories show that the major effect of F is to eliminate many of the low-amplitude gusts and increase the large-amplitude ones, which is the intended purpose of the F parameter.

F appears to have some small and subtle effects on the spectral characteristics as evidenced by the power spectra and power fraction plots presented in Figs. 21, 22, and 23. It is difficult to discern trends from the plots of $\Phi_{uu}(\omega)/\sigma_u^2$ or $\omega\Phi_{uu}(\omega)/\sigma_u^2$ versus ω, however, the power fraction plot of Fig. 23 shows a consistent trend, albeit small, for the low-frequency power to decrease as F is increased. For example, the frequency at a power fraction of 0.50 of the total variance, $\omega(0.50)$, is decreased from 0.4 to 0.25 rad/sec as F is increased from 0.0 to 0.8. The high frequency power, as reflected by $\omega(0.90)$, is unaffected by F.

Figure 18. Effects of NGUSTS on the u-Gust Kurtosis of the RAE Turbulence Model
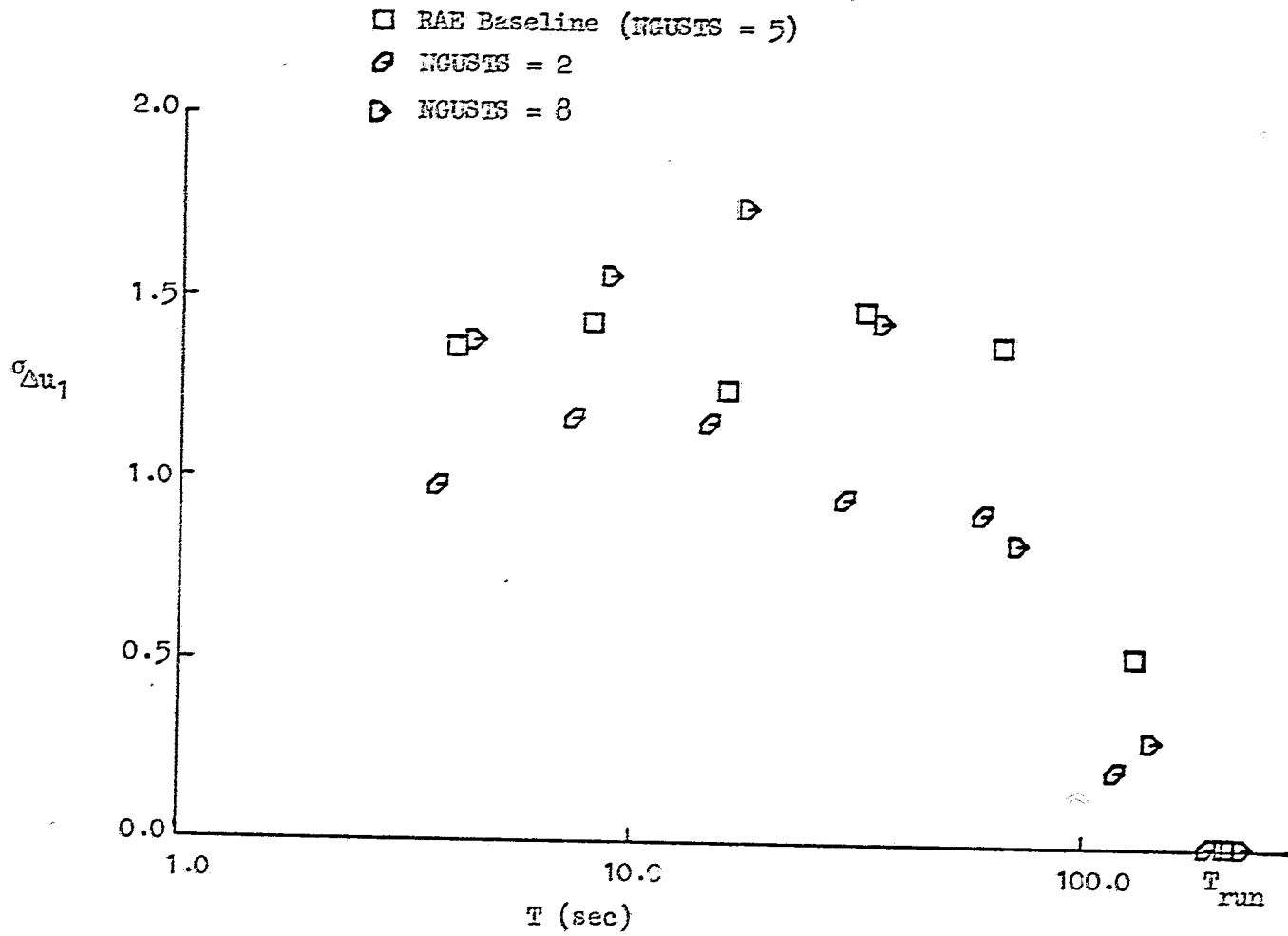
Figure 19. Effects of NGUSTS on the u-Gust Effective Wind Shear Parameter of the RAE Turbulence Model
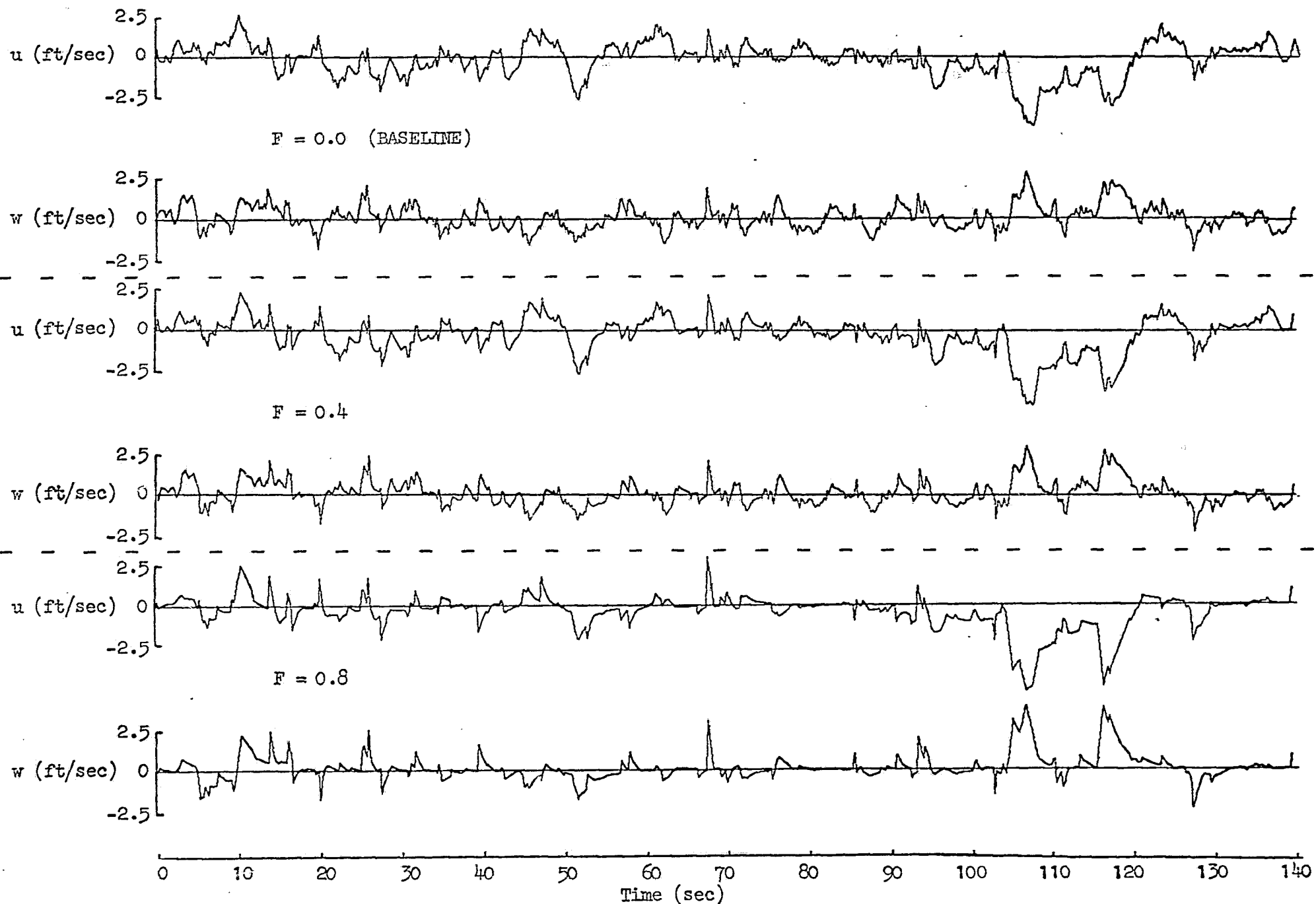
Figure 20. Effects of F on Temporal Characteristics of the RAE u- and w-Gust Turbulence

Figure 21. Effects of F on $\Phi_{uu}(\omega)$ of the RAE Turbulence Model

Figure 22. Effects of F on $\omega\Phi_{uu}(\omega)$ of the RAE Turbulence Model

Figure 23. Effects of F on the Power Fraction of the u-Gust Variance
Versus Frequency of the RAE Turbulence Model

Figure 24 shows that F affects the PDF as expected; that is, increasing F causes the PDF to become less Gaussian-like, as evidenced by comparing the PDFs shown in Fig. 24 to a straight line. The probability distribution functions show that as F is increased the high probability gusts are reduced and the low probability gusts are increased. This is consistent with the observations made of the u-gust time histories shown in Fig. 20. Because of these non-Gaussian characteristics the higher order moments (e.g., the kurtosis) should also be non-Gaussian.

Figure 25 shows that the limited window standard deviation of u-gust, $\bar{\sigma}_u$, is virtually unaffected by F, but that the dispersion of the limited window standard deviation of u-gust, σ_{σ_u}, is monotonically increased as F is increased from 0.0 to 0.8. Furthermore, note that σ_{σ_u} for any one value of F is unchanged for values of T between 4 and 64 sec.

Figure 26 shows that the limited window mean kurtosis of u-gust, $\bar{\alpha}_4$, and the standard deviation of the kurtosis of u-gust, σ_{α_4}, are only slightly increased as F is increased from 0.0 to 0.4, but are dramatically increased as F is increased from 0.4 to 0.8. Thus F is a highly non-linear control with respect to the kurtosis. It is seen that α_4 will vary between about 2.4 and 9.0 for F = 0.8, but only between about 2.2 and 4.4 for F = 0.0 or 0.4 for a window length of 32 sec.

F has virtually no affect on the effective wind shear parameter, $\sigma_{\Delta u_1}$, as shown in Fig. 27.

C. DECAY RATIO CONTROL, R

The decay ratio, R, is a parameter in the filter of the RAE model, and is used recursively to restore the high-, mid-, and low-frequency components of u-gust, v-gust, and w-gust to zero (refer to Ref. 1 for a more detailed discussion). As will be demonstrated below, R affects not only the temporal and spectral characteristics but also the statistical characteristics. Because of its multi-dimensional effects on the turbulence characteristics, it is not recommended that R be varied unless the desired spectral and statistical characteristics cannot be obtained with a combination of NGUSTS and F. R is limited to values greater than 0.0 and less than 1.0.

Figure 24. Effects of F on the Probability Distribution Function
of u-Gust of the RAE Turbulence Model

Figure 25. Effects of F on the rms u-Gust of the RAE Turbulence Model
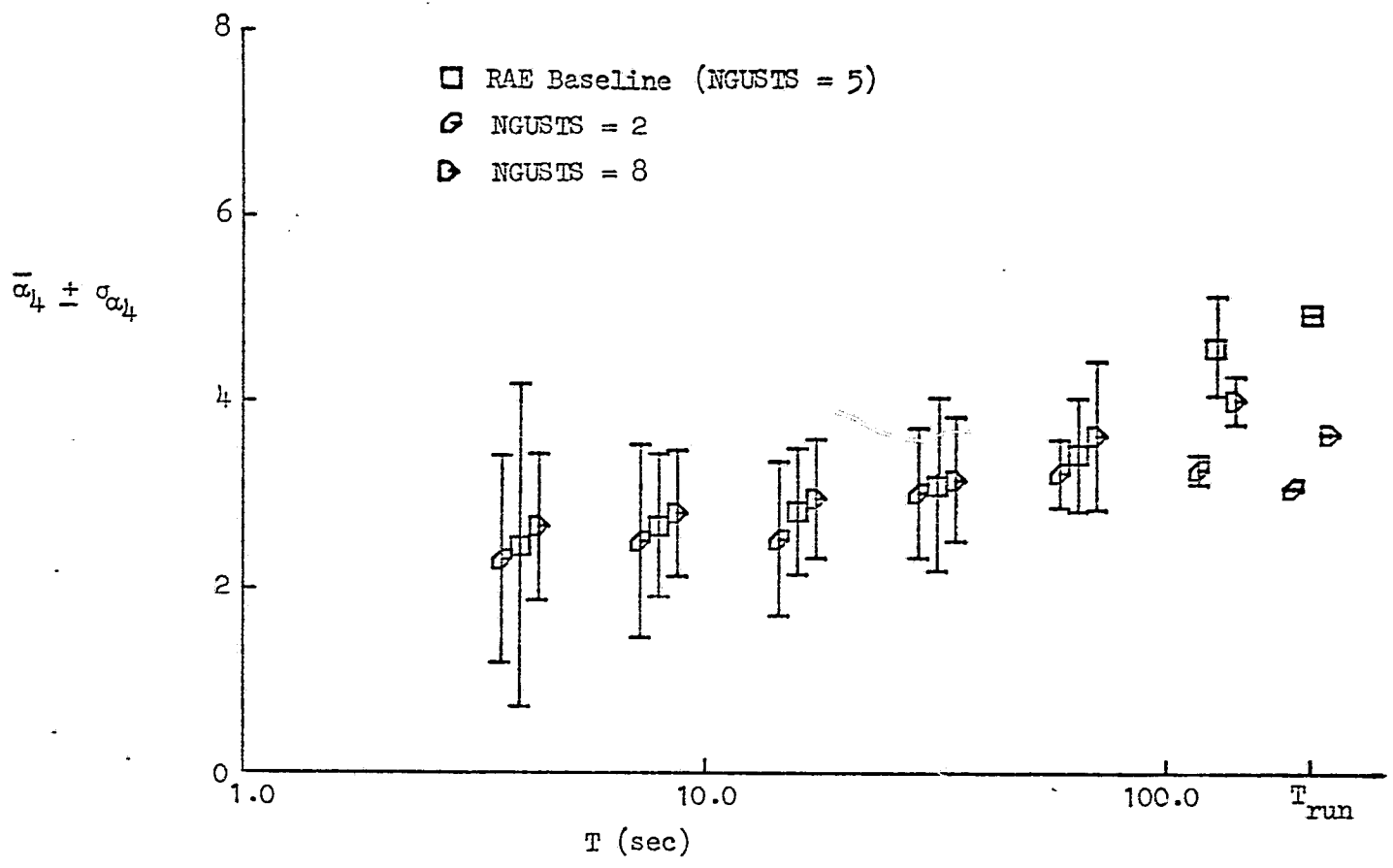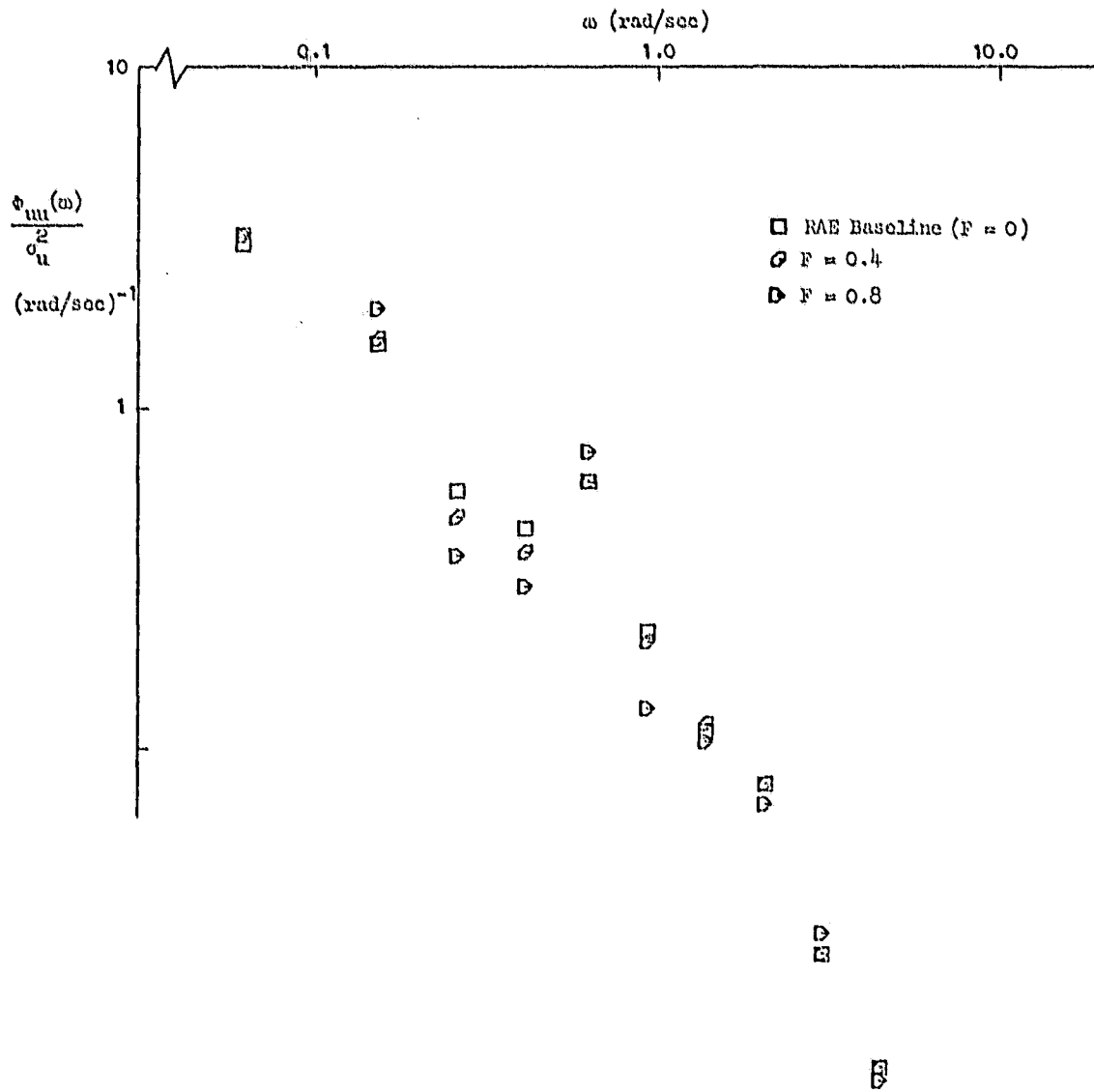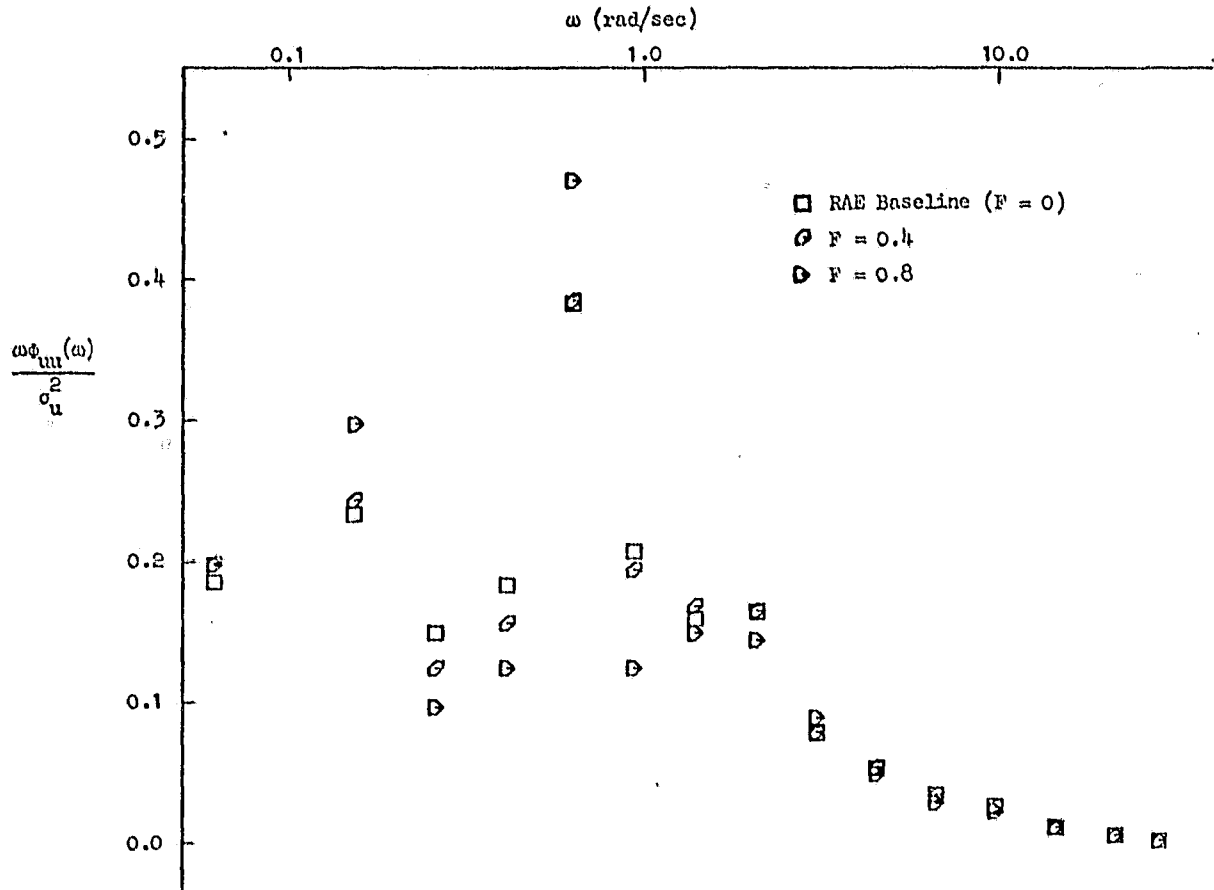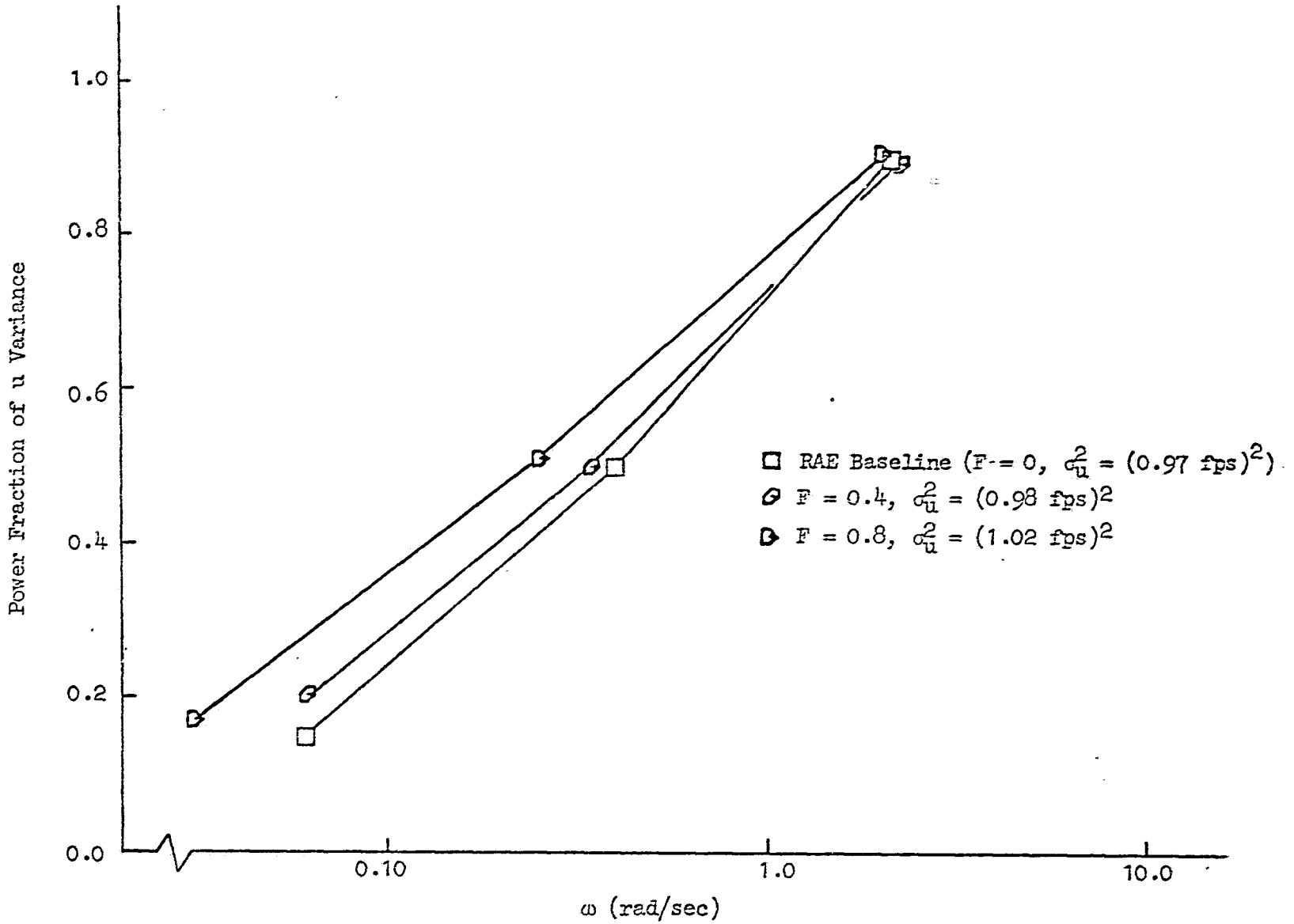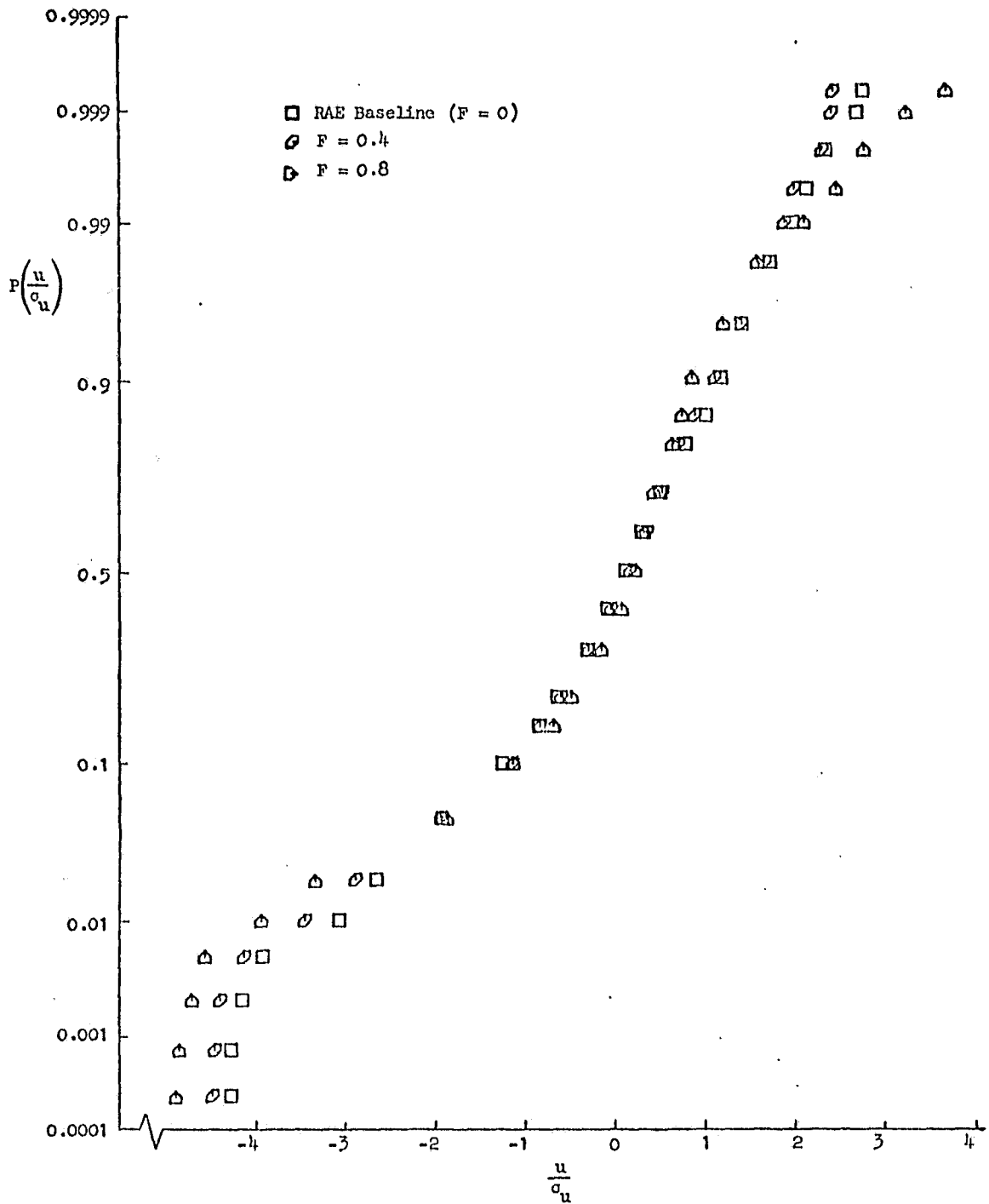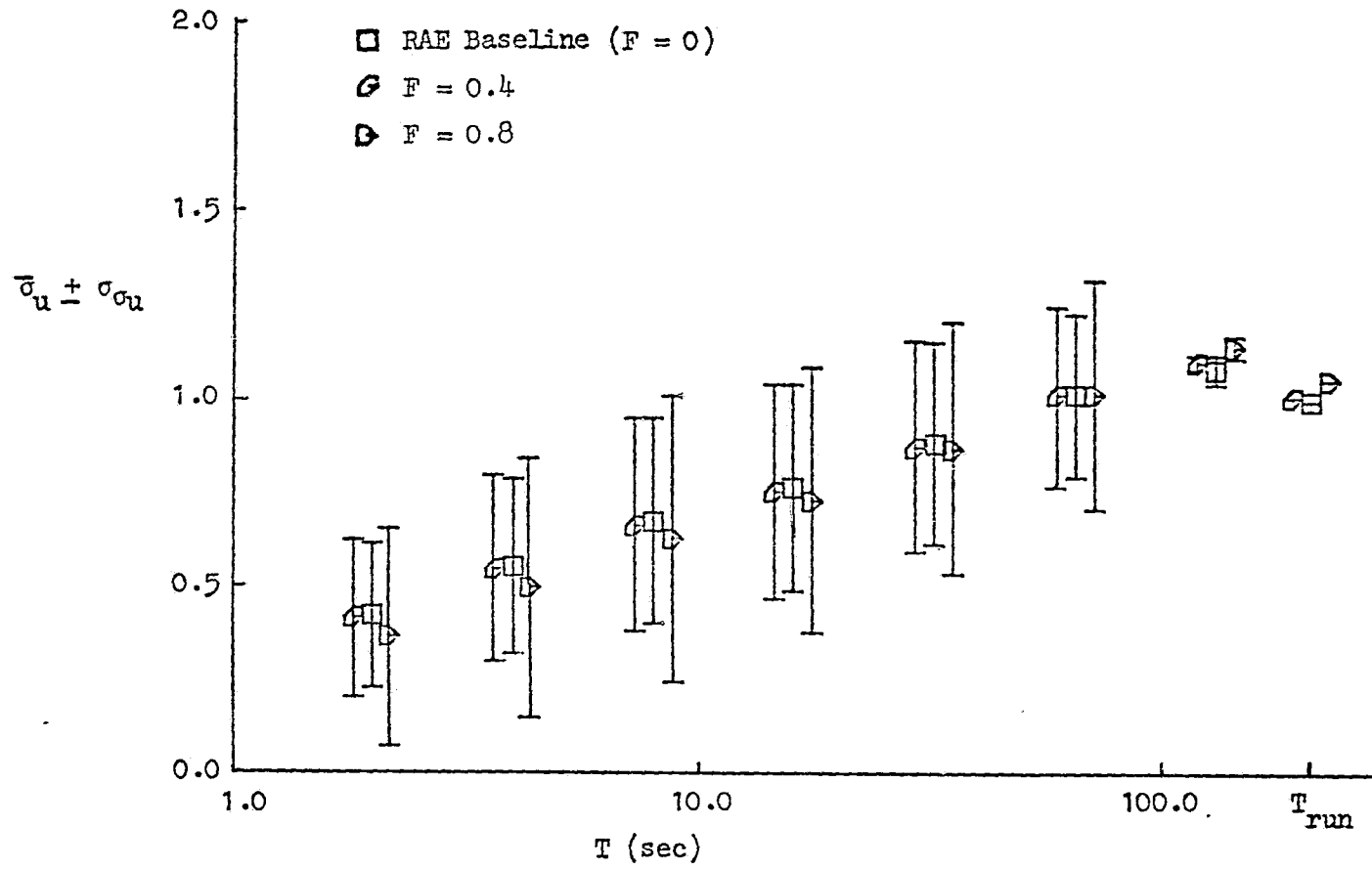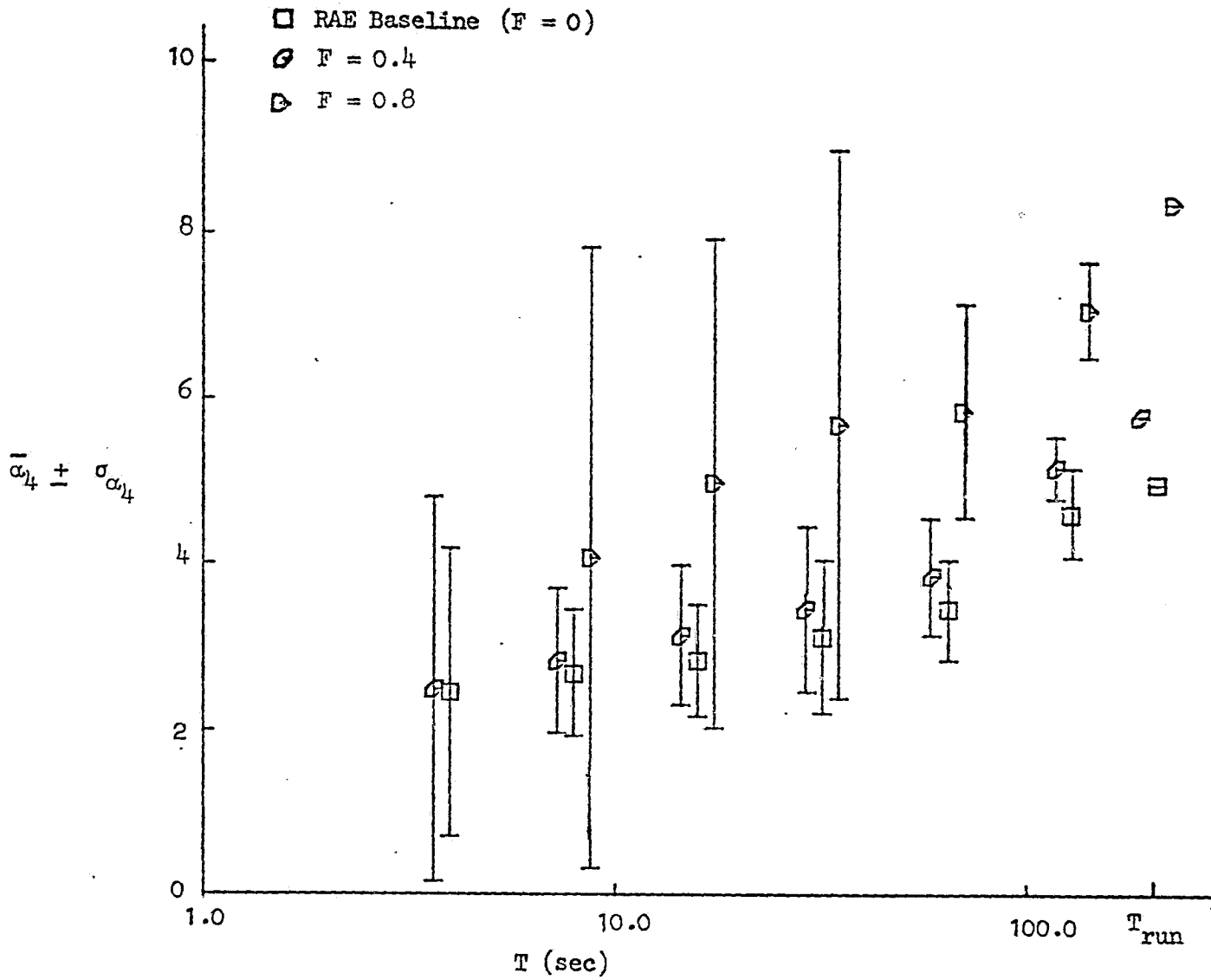
Figure 26. Effects of F on the u-Gust Kurtosis of the RAE Turbulence Model
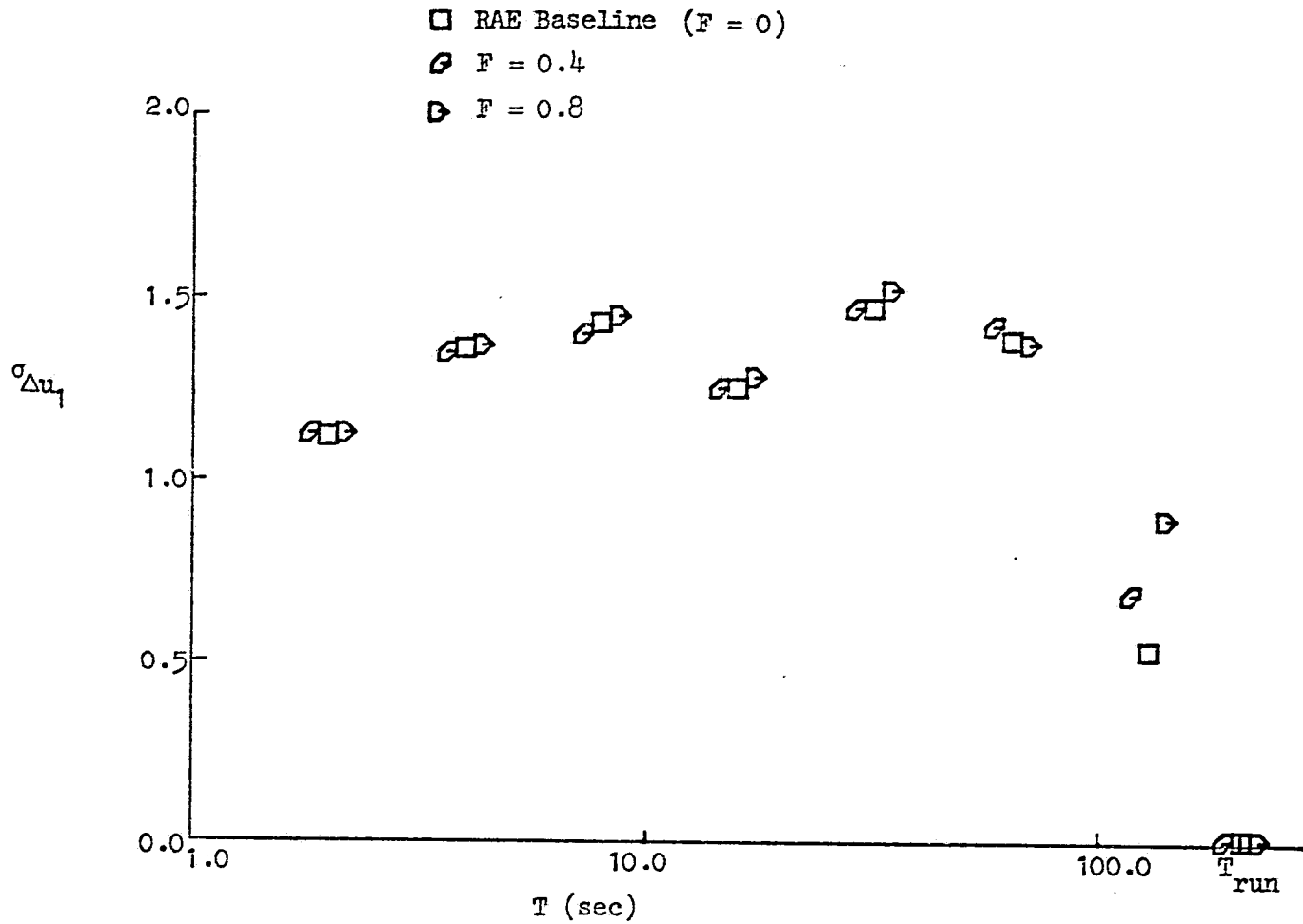
Figure 27. Effects of F on the u-Gust Effective Wind Shear Parameter
of the RAE Turbulence Model

Figure 28 contains time histories of u-gust and w-gust for three different values of R: 0.5, 0.7, and 0.9. We see that R has a significant effect on the magnitude of the turbulence; however, it is difficult to ascertain any changes in the spectral or statistical properties of the turbulence solely from time histories. The effects of R on the spectral characteristics of u-gust are presented in Figs. 29, 30, and 31. Note that increasing R has the effect of reducing the amount of high-frequency power. This is best demonstrated in the power fraction plots of Fig. 31. While the effect of R on the power fraction of the u variance appears to be non-linear with frequency, this is not the case. If, for example, the frequency at a power fraction of 0.90, $\omega(0.90)$, is plotted versus R using linear scales, it can be seen that $\omega(0.90)$ is directly proportional to R. The point is that frequency content, as reflected by the power fractions, can be nearly linearly controlled via the decay ratio R. However, as mentioned before, R will also affect the statistical properties of the turbulence.

The effects of R on the probability density function (PDF) are depicted in Fig. 32. Changing R from 0.7 to 0.5 does not have a very noticeable effect on the PDF, but going from 0.7 to 0.9 does have a definite effect on the low probability regions of the PDF (i.e., the "tails"). Thus we can expect R to have an effect on the higher order moments of the turbulence.

The effects of R on the limited window standard deviation, $\overline{\sigma}_u$, and the dispersion of the standard deviation, σ_{σ_u}, of u-gust are shown in Fig. 33. Both $\overline{\sigma}_u$ and σ_{σ_u} monotonically increase with increasing R, with the biggest increment in both parameters occurring for R = 0.7 to 0.9. The parameter $\overline{\sigma}_u$ can be linearly altered with the intensity control parameter, SIGMA (see Section III.F), which as no effect on σ_{σ_u}.

The effects of R on the mean limited window kurtosis, $\overline{\alpha}_4$, and the standard deviation of the limited window kurtosis, σ_{α_4}, of u-gust are shown in Fig. 34. $\overline{\alpha}_4$ is monotonically decreased with increasing R at low values of T ($\overline{\alpha}_4$ = 2.7 to 1.7 for R = 0.5 to 0.9, respectively at T = 4.0 sec), but is not discernibly affected by R at high values of T (e.g., $\overline{\alpha}_4$ = 3.5 to 3.4 at T = 64 sec). σ_{α_4} is not noticeably or consistently altered by R.
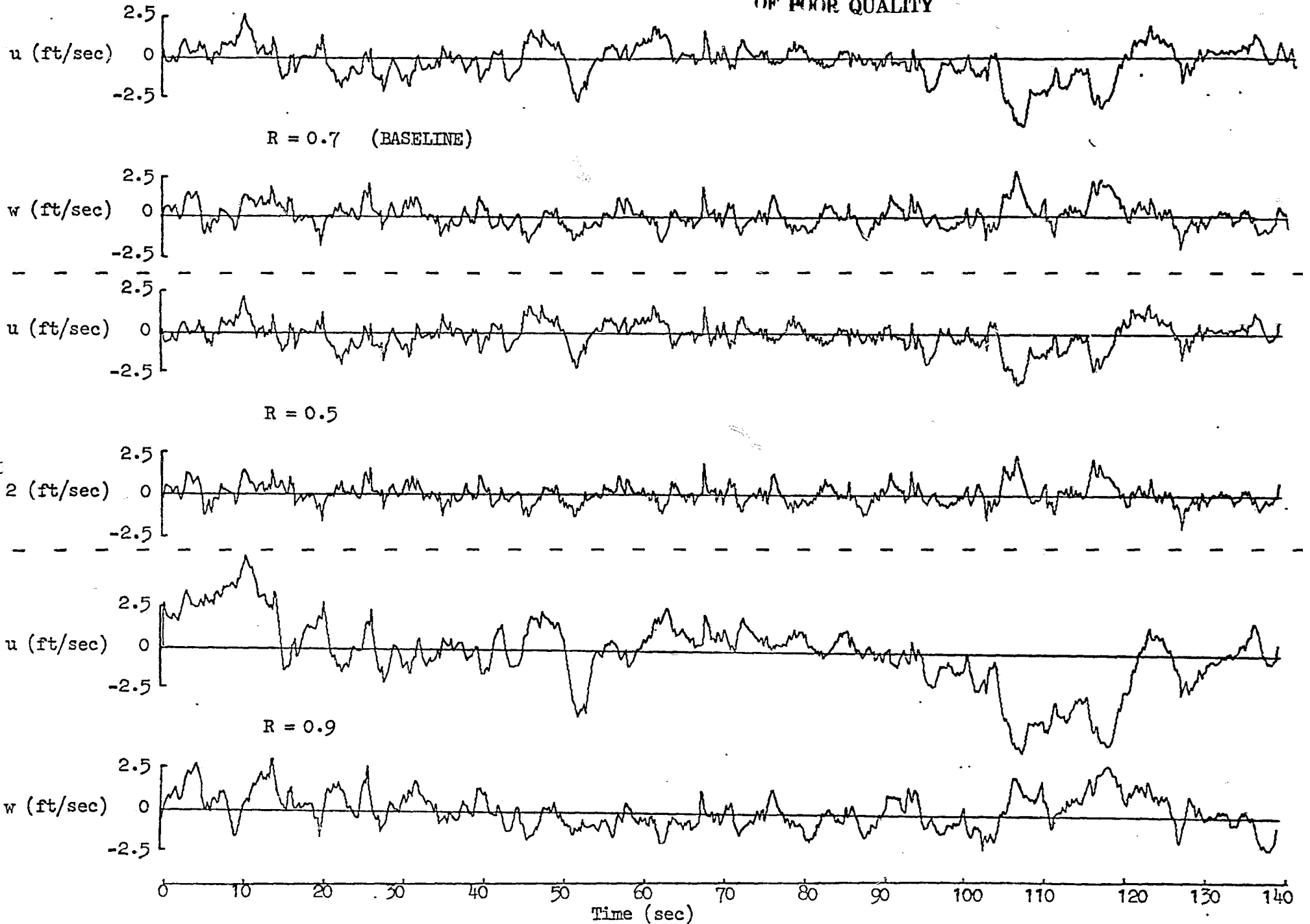
Figure 28. Effects of R on Temporal Characteristics of the RAE u- and w-Gust Turbulence
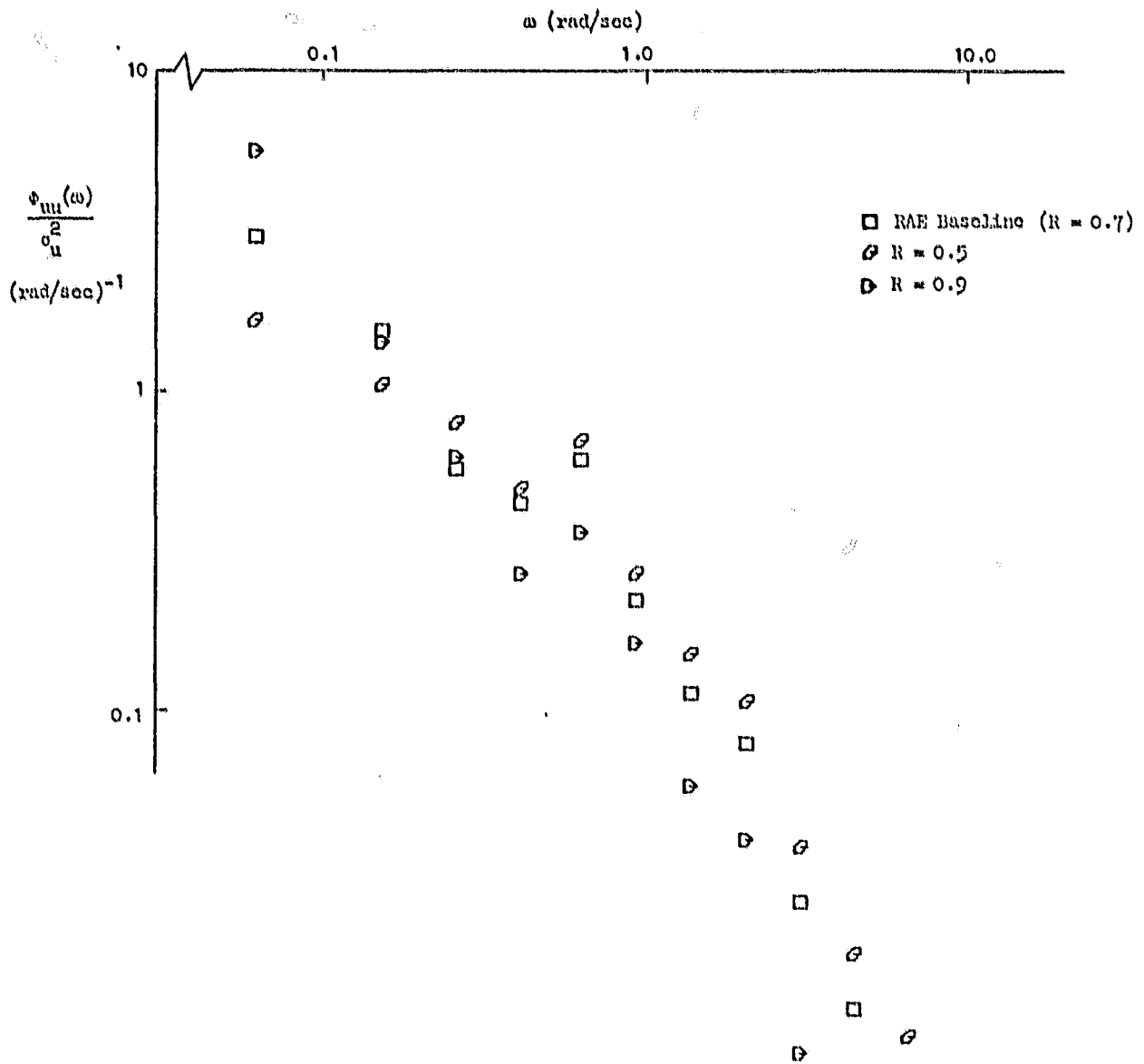
Figure 29. Effects of R on $\Phi_{uu}(\omega)$ of the RAE Turbulence Model
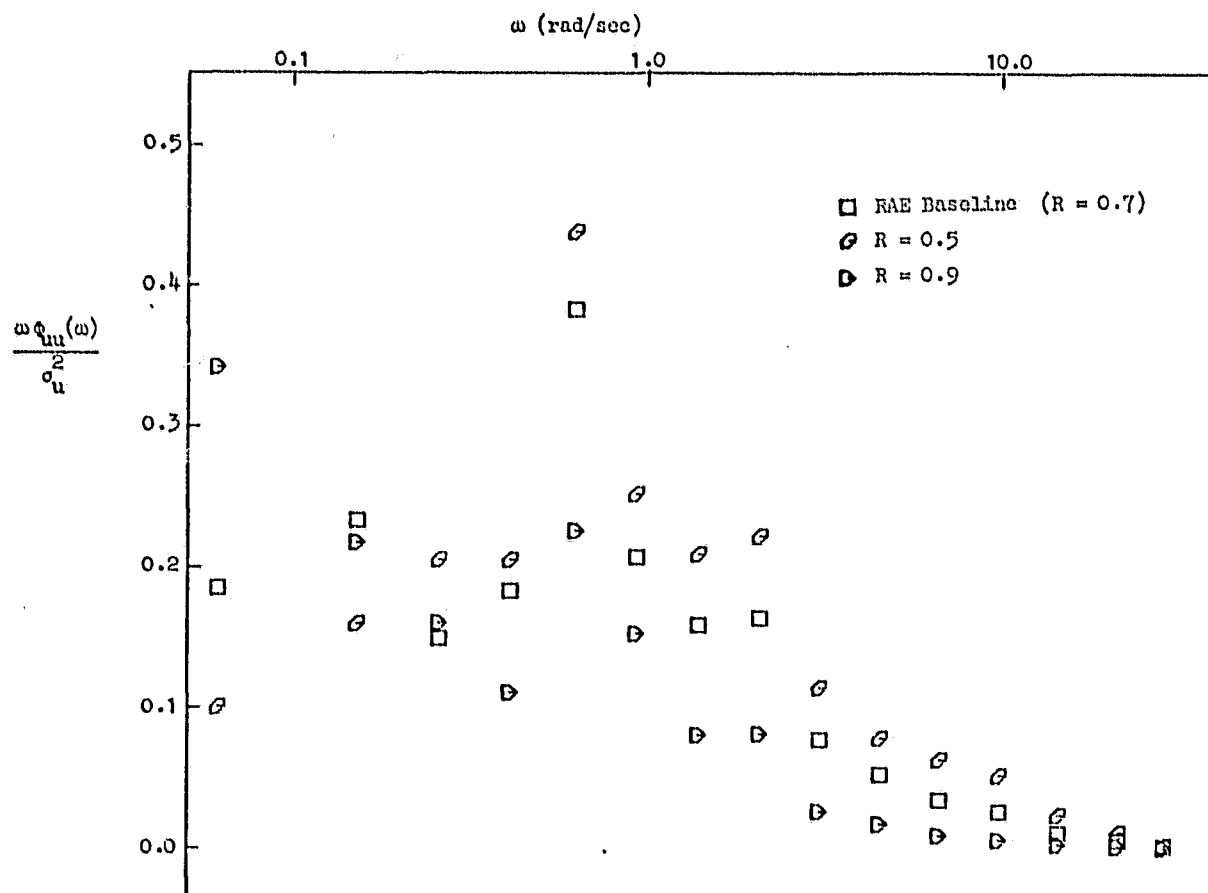
Figure 30. Effects of R on $\omega\Phi_{uu}(\omega)$ of the RAE Turbulence Model
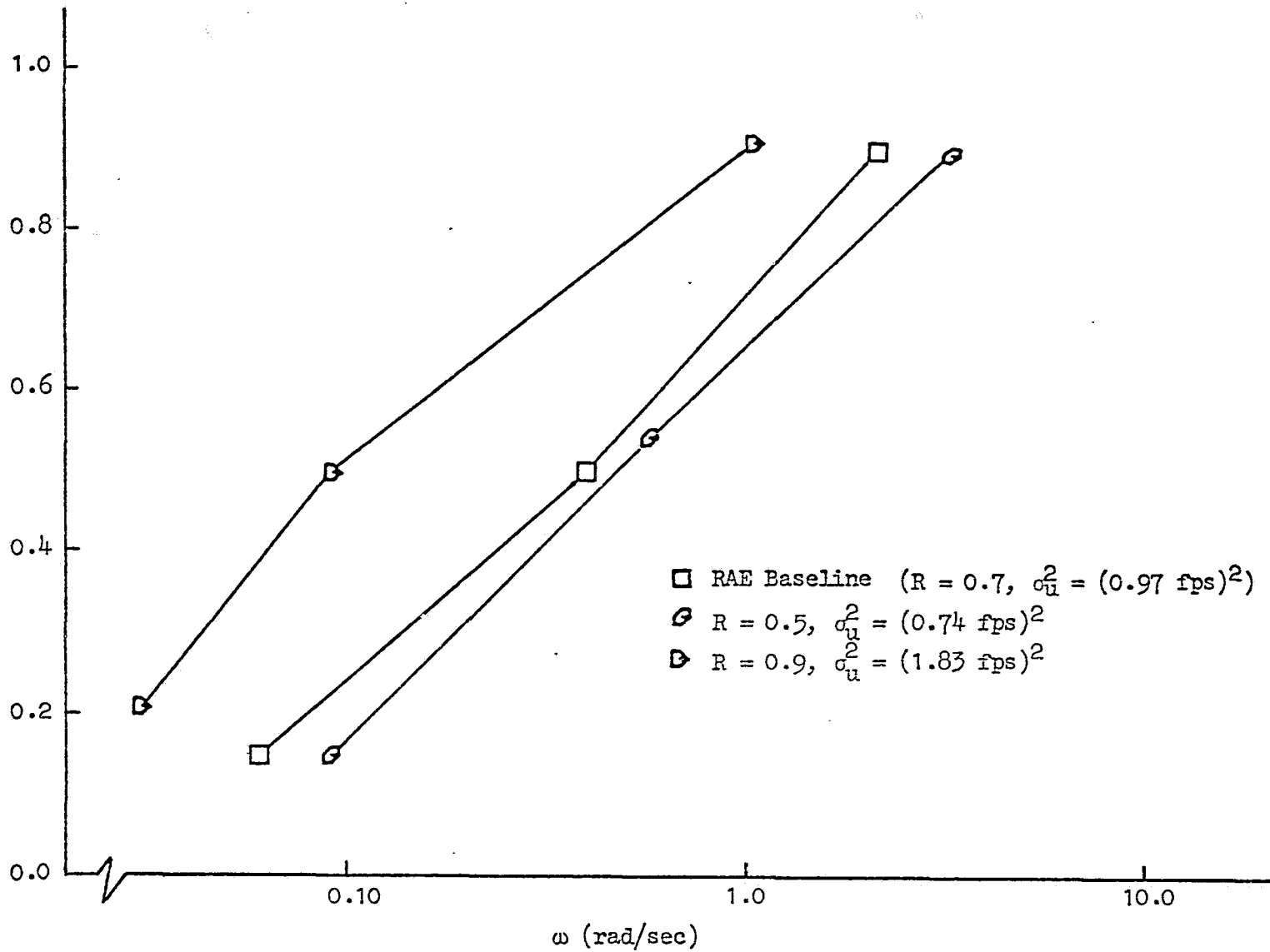
Figure 31. Effects of R on the Power Fraction of the u-Gust Variance
Versus Frequency of the RAE Turbulence Model

The chart plots Power Fraction of u Variance (y-axis, 0.0 to 1.0) versus ω (rad/sec) (x-axis, logarithmic from 0.10 to 10.0).

Legend:
- □ RAE Baseline $(R = 0.7, \; \sigma_u^2 = (0.97 \text{ fps})^2)$
- ⊖ $R = 0.5, \; \sigma_u^2 = (0.74 \text{ fps})^2$
- ▷ $R = 0.9, \; \sigma_u^2 = (1.83 \text{ fps})^2$

47

Figure 32.   Effects of R on the Probability Distribution Function
of u-Gust of the RAE Turbulence Model

Figure 33.   Effects of R on the rms u-Gust of the RAE Turbulence Model

Figure 34. Effects of R on the u-Gust Kurtosis of the RAE Turbulence Model

R has a large effect on the standard deviation of the effective wind shear, $\sigma_{\Delta u_1}$, as is demonstrated in Fig. 35. The effect is non-linear because the change in $\sigma_{\Delta u_1}$ at all values of T was much larger for changing R from 0.7 to 0.9 than it was for changing R from 0.7 to 0.5.
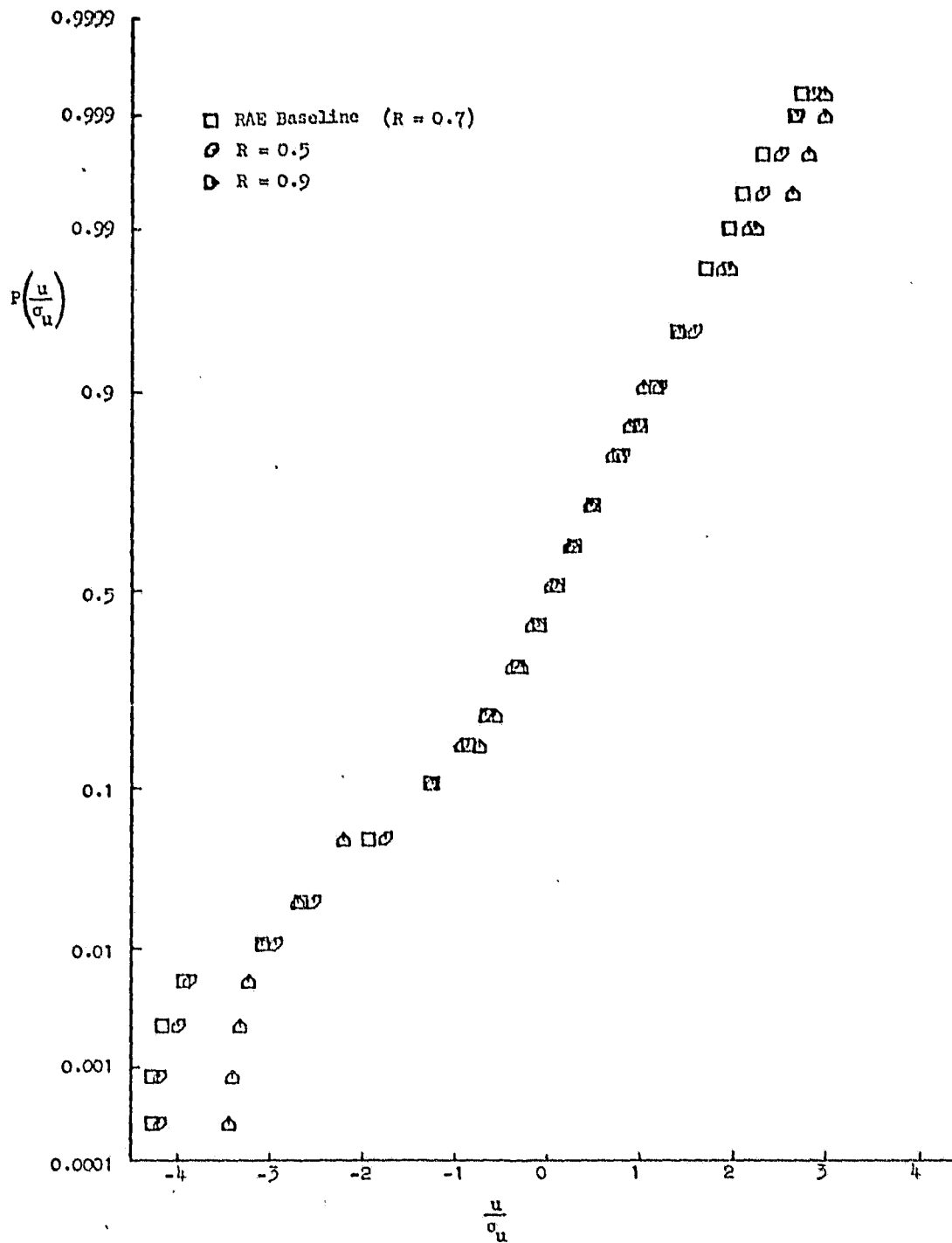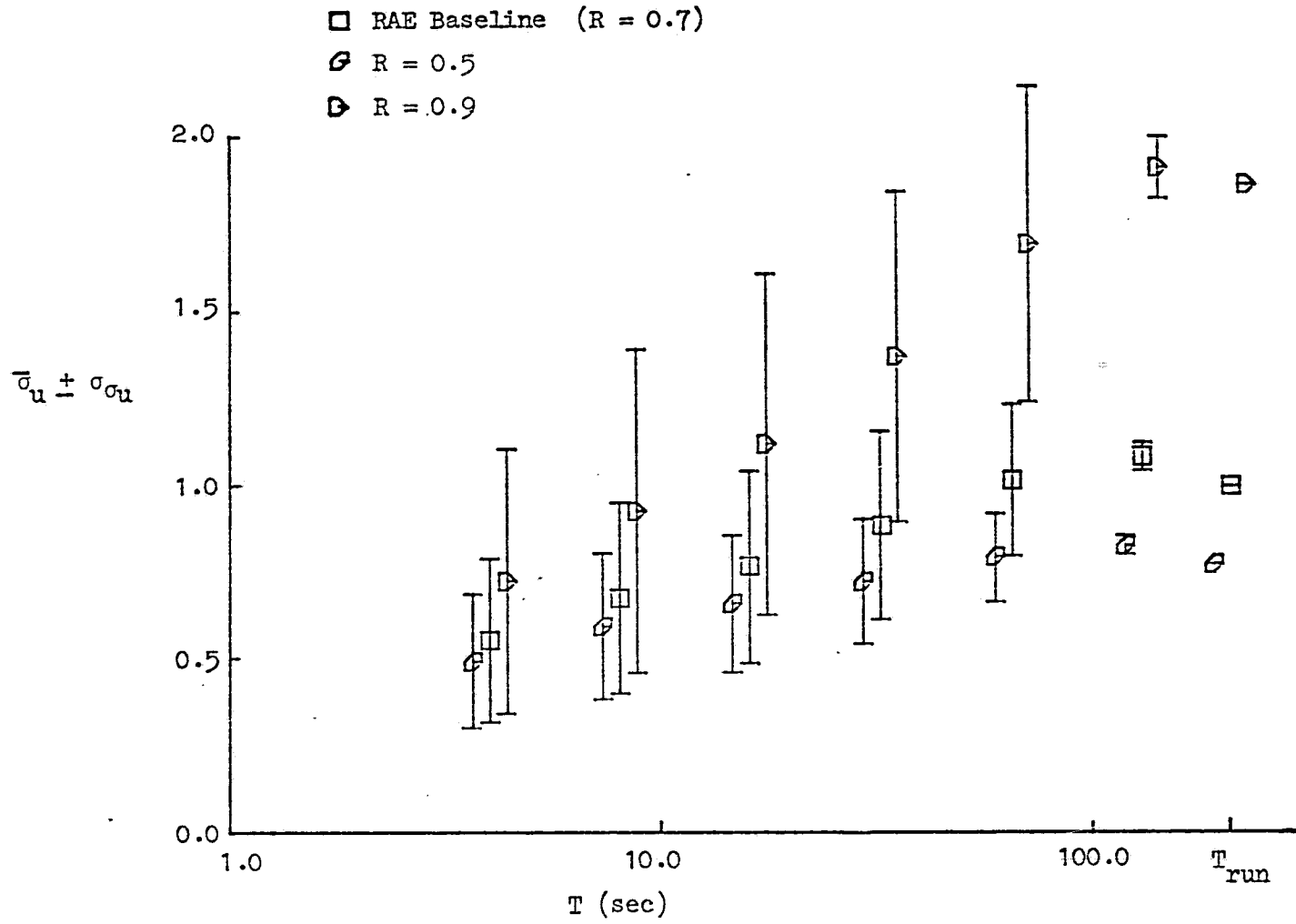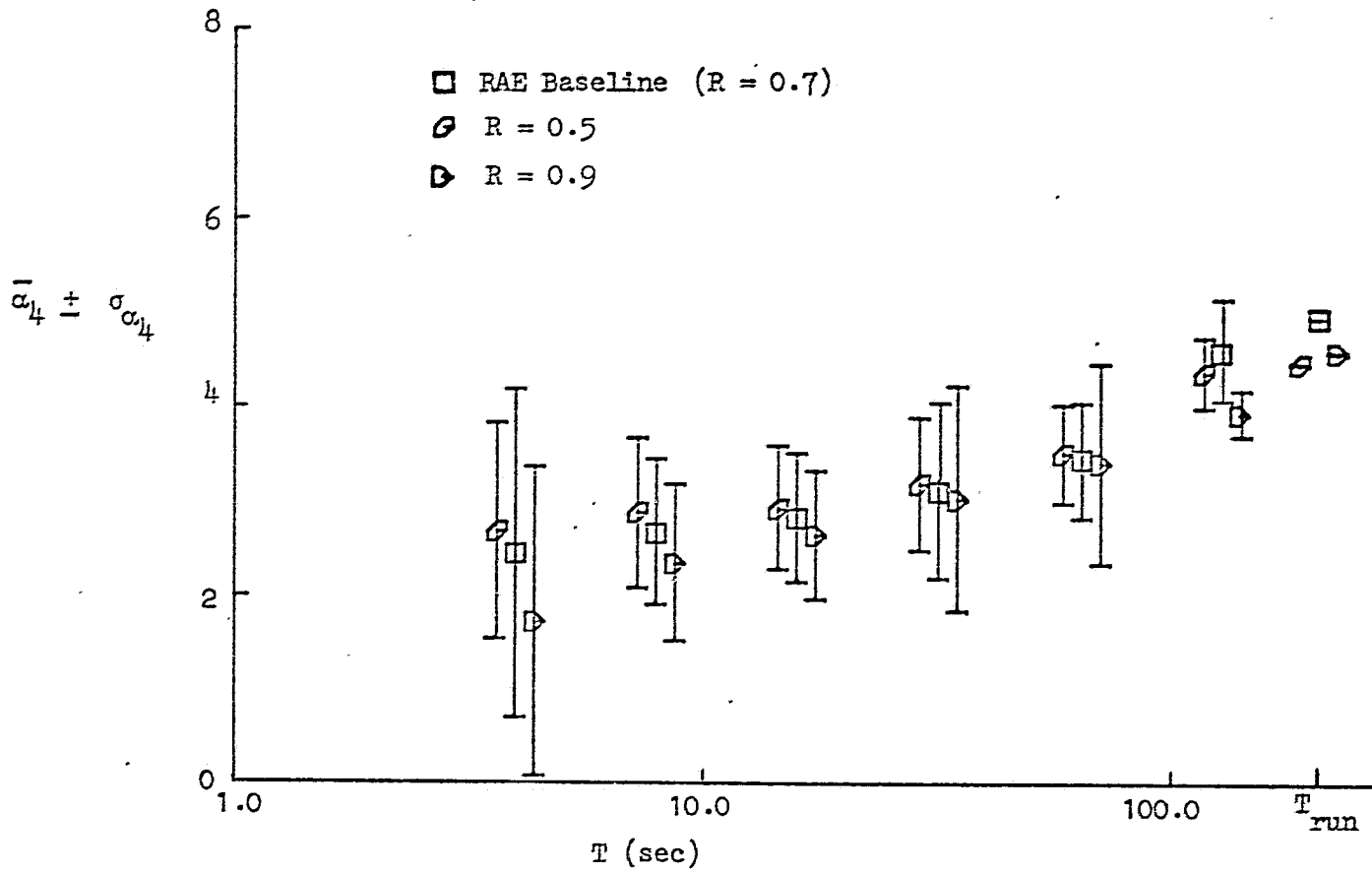
D. ALTITUDE CONTROL, HCG

The altitude parameter, HCG, affects only the w-gust component. The low-, mid-, and high-frequency components of w-gust are linearly decreased to zero as HCG goes from 2500 ft to 800 ft, from 800 ft to 200 ft, and from 200 ft to 50 ft above ground level, respectively. Thus w-gust is unaffected by HCG above 2500 ft, and is zero when HCG is below 50 ft. The temporal effects of HCG on w-gust are demonstrated in Fig. 36. The time history of u-gust is included in Fig. 36 for comparison with the w-gust time history for HCG above 2500 ft. More about the comparison between these two time histories will be said later.

From the time histories of Fig. 36, one can see that the main effect of decreasing HCG is to reduce the amount of low-frequency power contained in w-gust. This is confirmed by the power spectral density plots of Figs. 37 and 38 and the power fraction plots of w-gust versus frequency shown in Fig. 39.

Figure 40 shows that decreasing altitude tends to increase the normalized amplitude of low probability gusts. Thus w-gust will become less Gaussian with decreasing altitude (in contradistinction to Dryden model turbulence where w-gust is Gaussian at all altitudes).

Decreasing HCG also decreases the total amount of power in w-gust, which is demonstrated in the plot of the mean limited window standard deviation, $\bar{\sigma}_w$, and the dispersion of the limited window standard deviation, σ_{σ_w}, of w-gust shown in Fig. 41.

Figure 42 shows that the mean limited window kurtosis, $\bar{\alpha}_4$, and the standard deviation of the limited window kurtosis, σ_{α_4}, of w-gust generally increase with decreasing altitude. This is true only for T much less than the total run length.
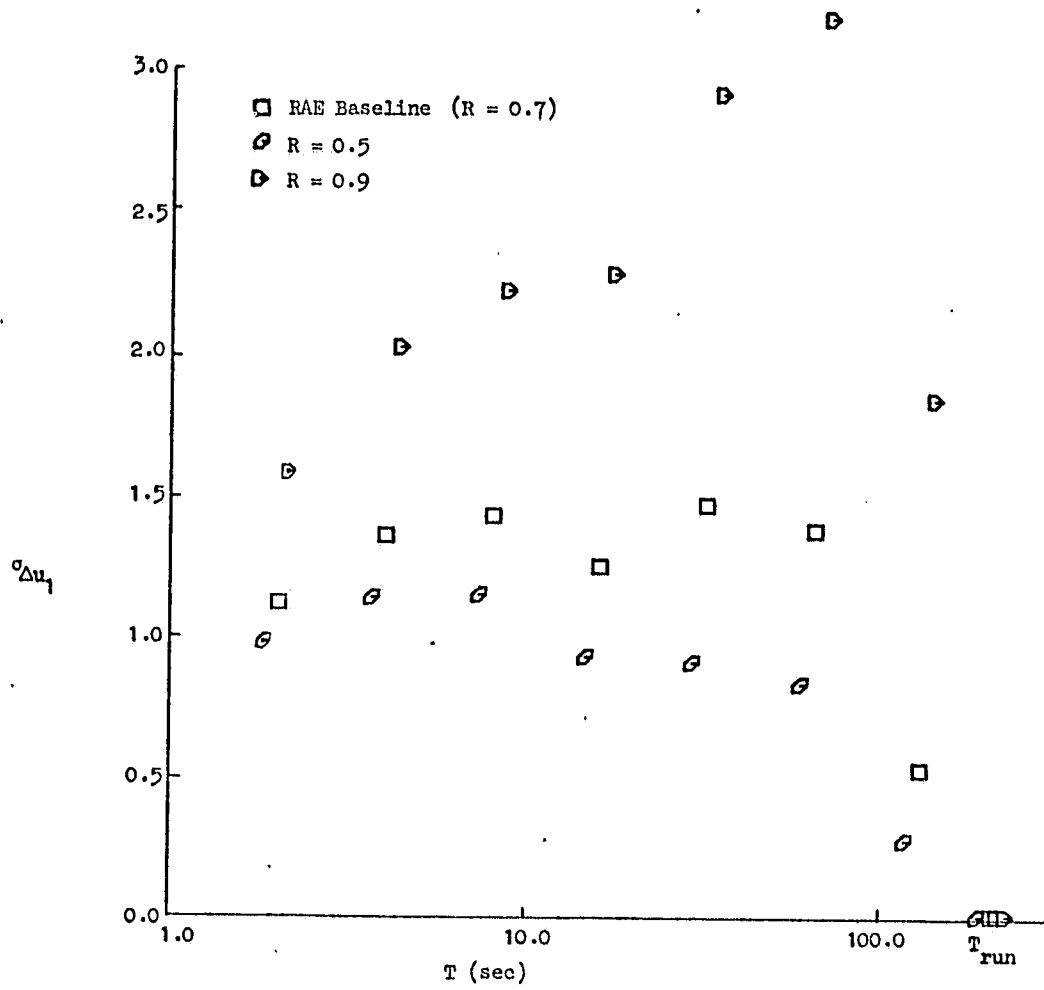
Figure 35. Effects of R on the u-Gust Effective Wind Shear Parameter of the RAE Turbulence Model

u-gust for all HCG

2.5

u (ft/sec) 0

-2.5

w-gust for HCG ≥ 2500 ft

2.5

w (ft/sec) 0

-2.5

w-gust for HCG = 800 ft

2.5

w (ft/sec) 0

-2.5

w-gust for HCG = 200 ft

2.5

w (ft/sec) 0

-2.5

0   10   20   30   40   50   60   70   80   90   100   110   120   130   140

Time (sec)
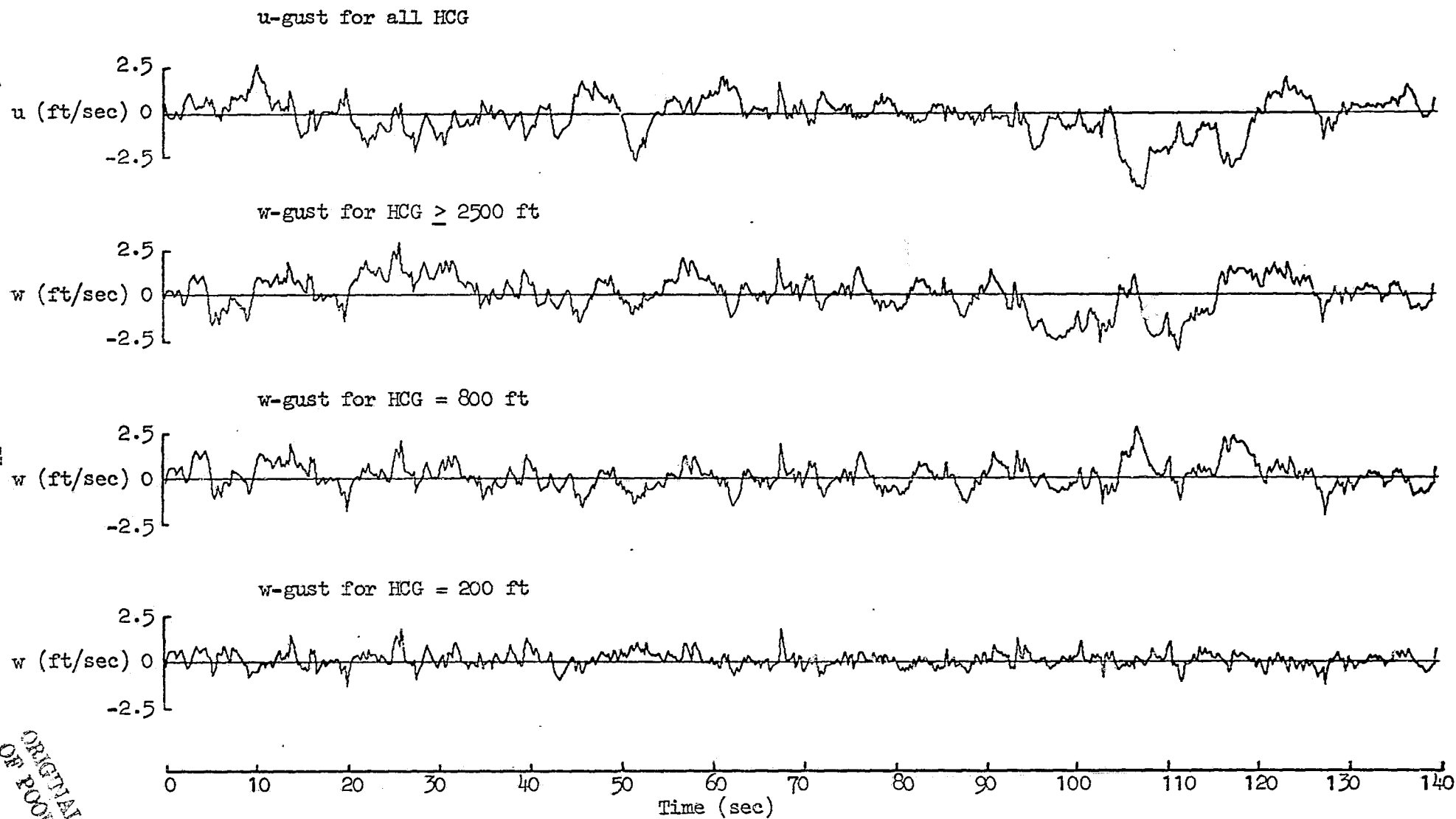
Figure 36.   Effect of Altitude on the Temporal Characteristics
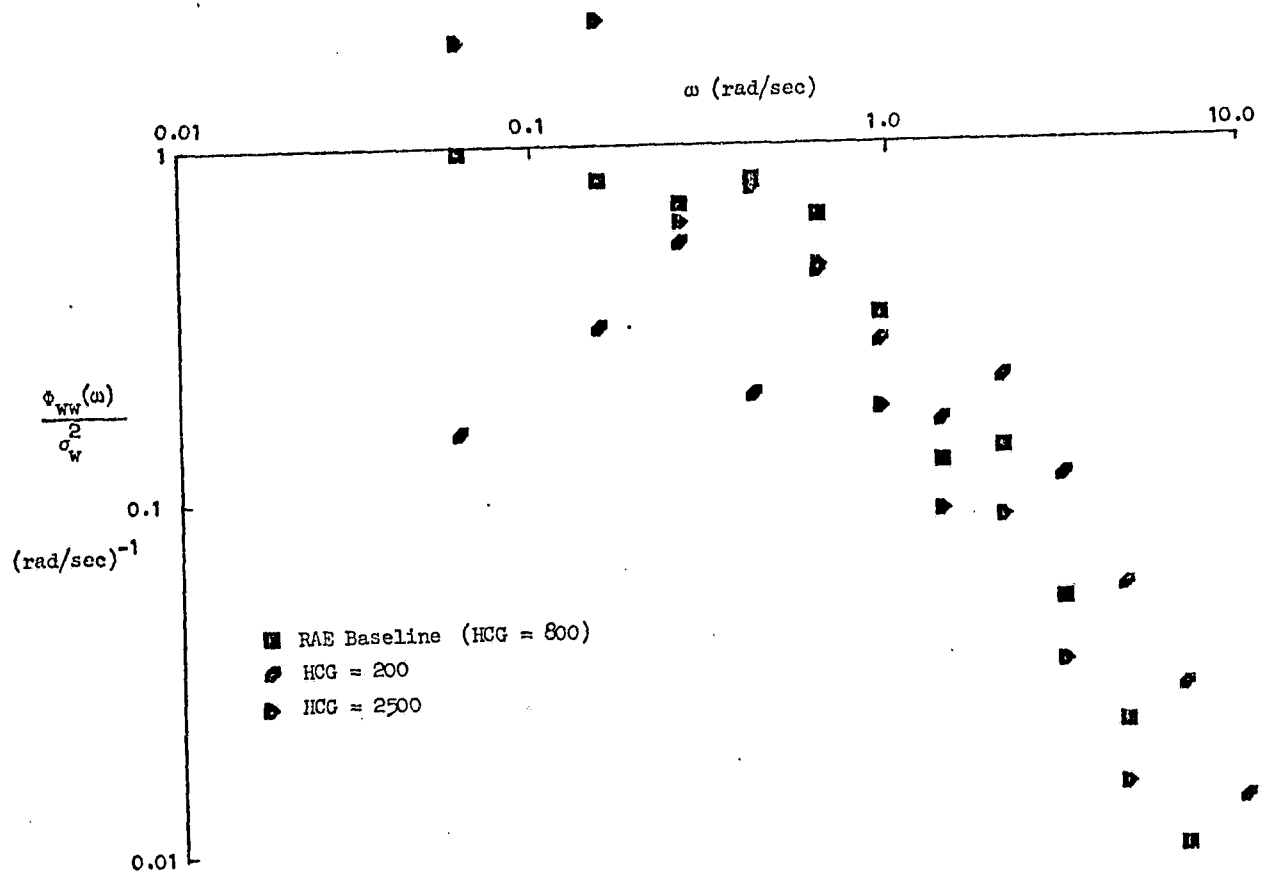
Figure 37. Effects of HCG on $\Phi_{WW}(\omega)$ of the RAE Turbulence Model
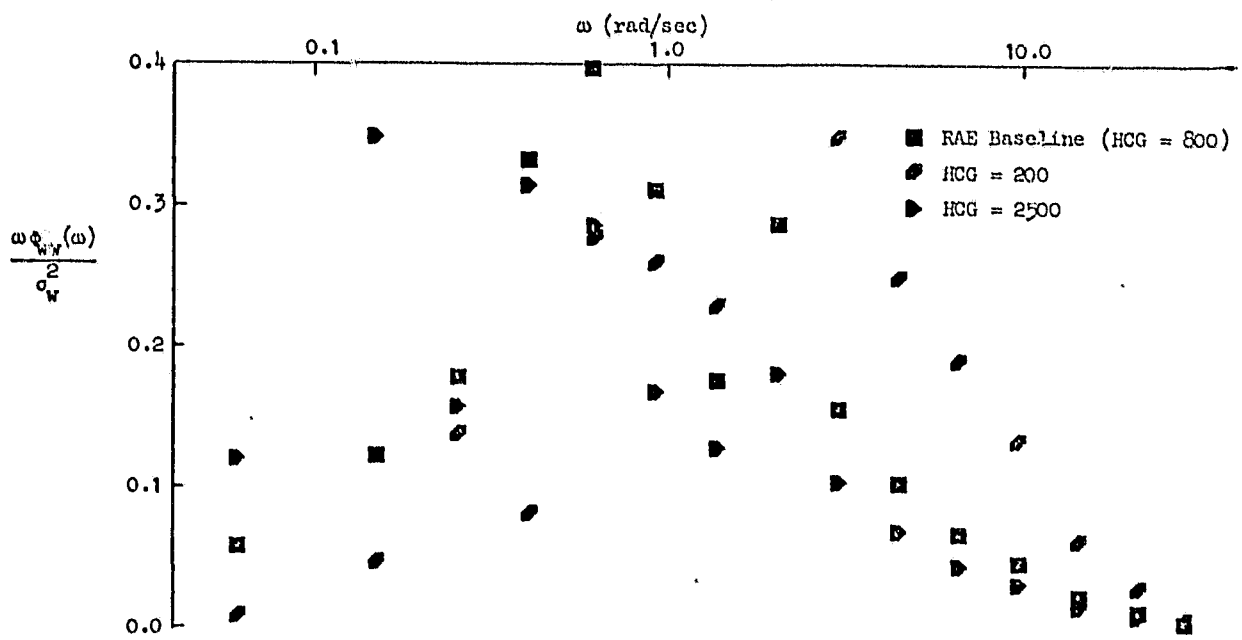
Figure 38. Effects of HCG on $\omega\phi_{ww}(\omega)$ of the RAE Turbulence Model
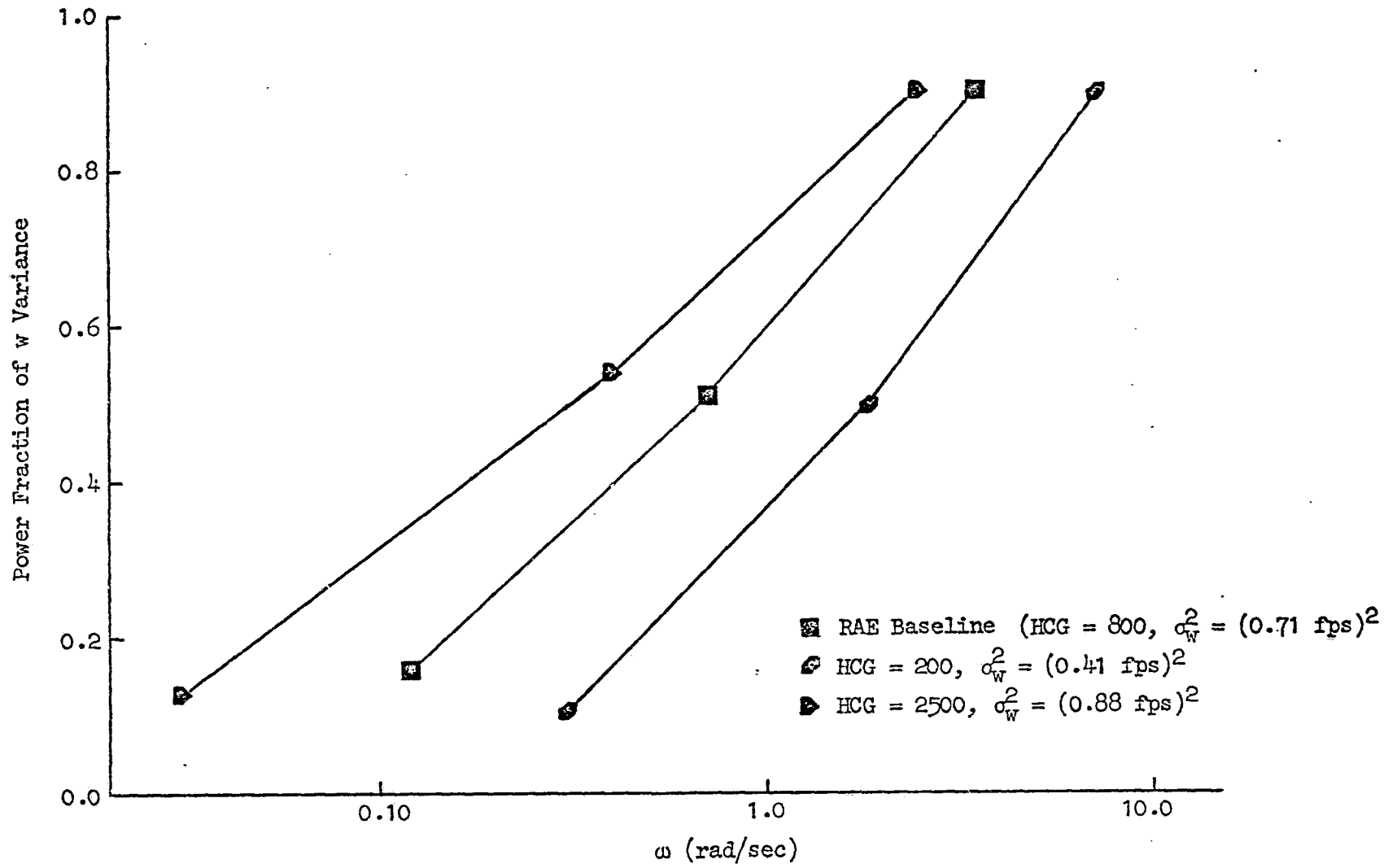
Figure 39. Effects of HCG on the Power Fraction of the w-Gust Variance
Versus Frequency of the RAE Turbulence Model
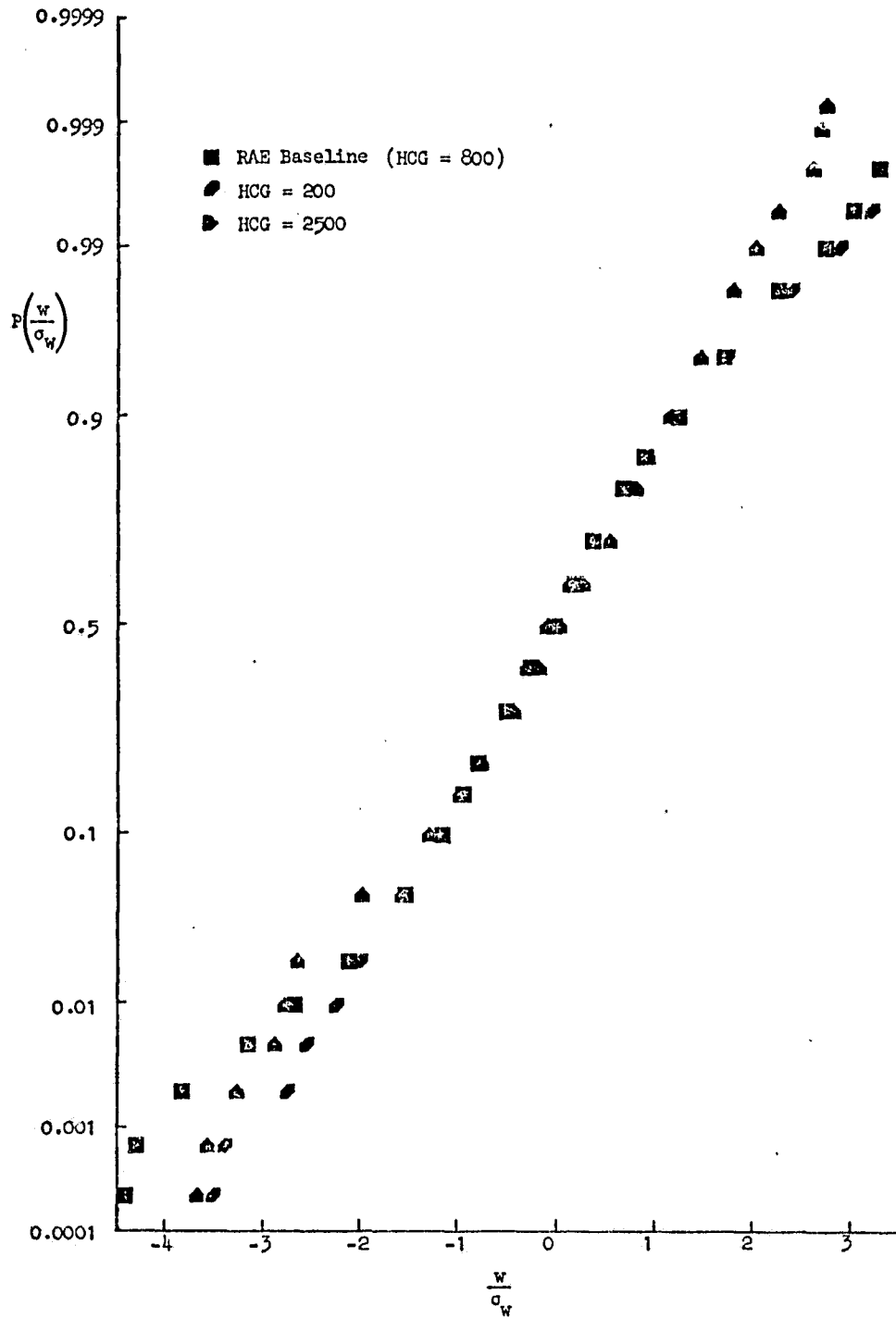
Figure 40.   Effects of HCG on the Probability Distribution Function
of w-Gust of the RAE Turbulence Model
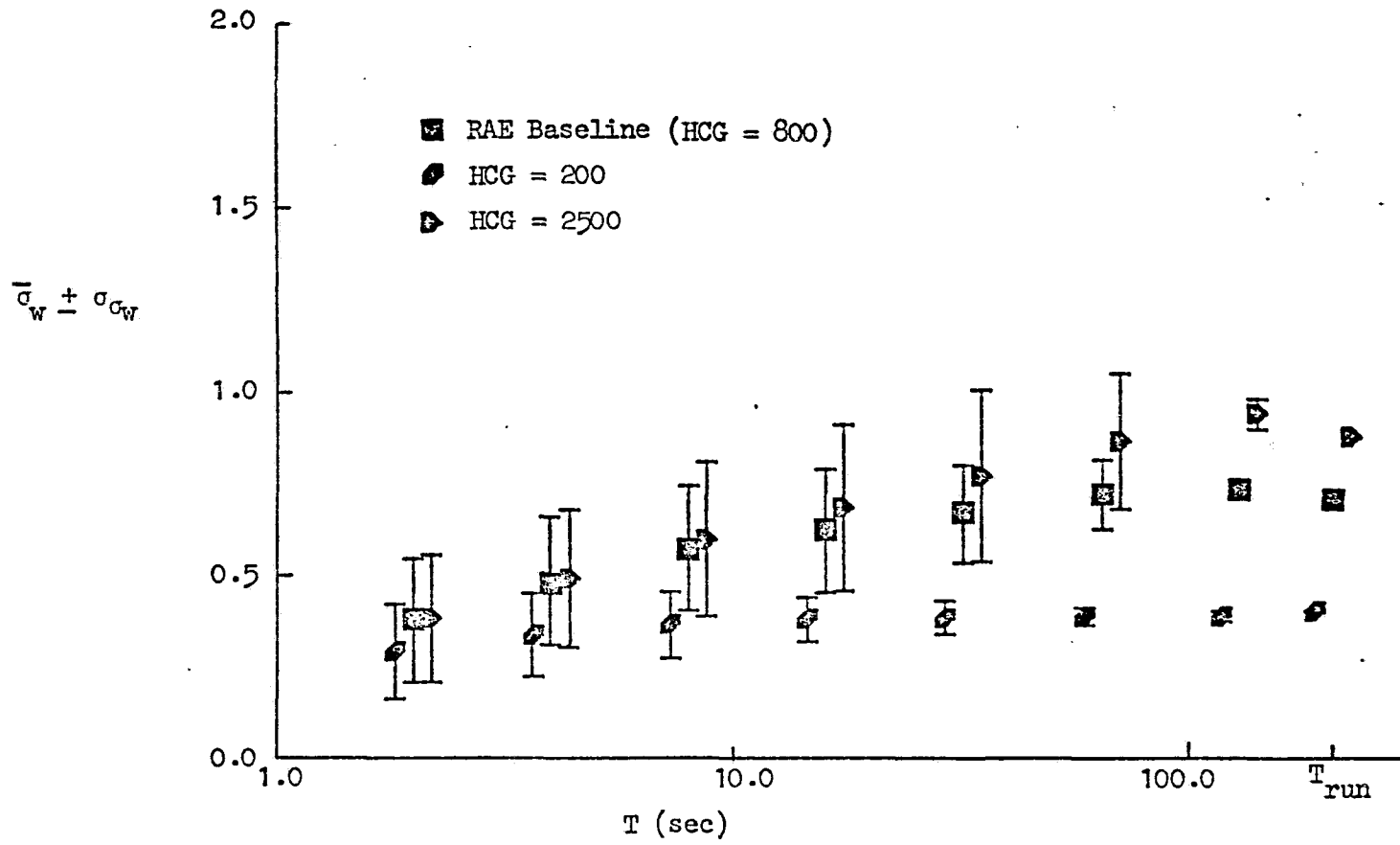
Figure 41. Effects of HCG on the rms w-Gust of the RAE Turbulence Model
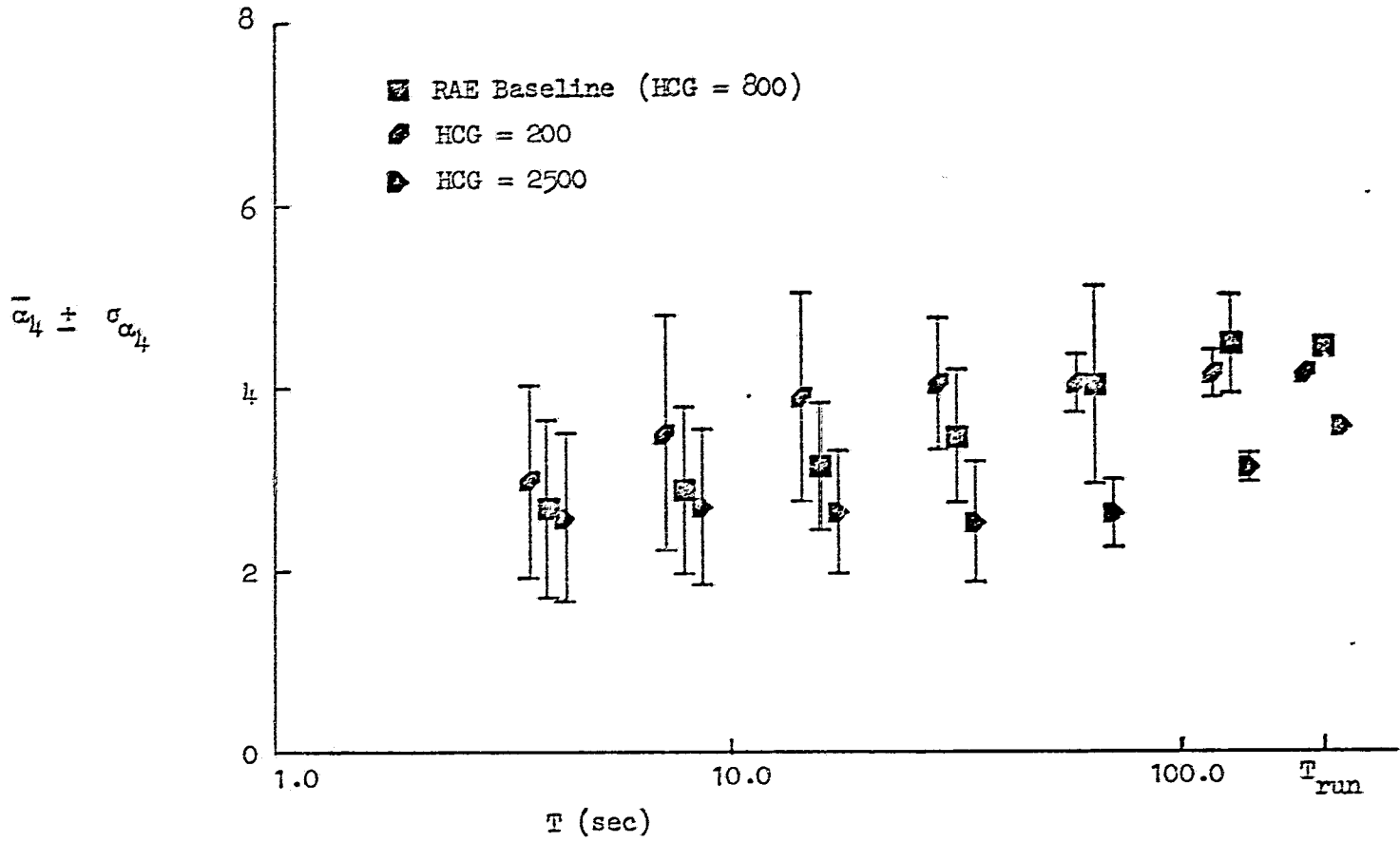
Figure 42. Effects of HCG on the w-Gust Kurtosis of the RAE Turbulence Model

Figure 43 shows that altitude has a large and consistent effect on the effective wind shear parameter of w-gust, $\sigma_{\Delta w}$. Note that $\sigma_{\Delta w}$ is monotonically decreased with decreasing altitude.

A close comparison of the u- and w-gust time histories shown in Fig. 36 reveals a strange feature of the RAE turbulence model. There appears to be very high correlation between u-gust and w-gust, especially for HCG $\geq$ 2500 ft. Notice that many of the large u- and w-gusts occur at the same point in time, have the same shape, but occasionally are of opposite polarity (i.e., simply 180 degrees out of phase). We say that this feature is strange because such high correlation between the turbulence components are very rare in the Dryden model where the components are intentionally designed to be independent.

In order to quantify the correlation described above the coherence function between u^2 and w^2 was calculated.*

$$\rho_{u^2 w^2}^2 (\omega) = \frac{\left| \Phi_{u^2 w^2}(j\omega) \right|^2}{\Phi_{u^2 u^2}(\omega) \; \Phi_{w^2 w^2}(\omega)}$$

$$\rho_A^2 = \int_0^\infty \rho_{u^2 w^2}^2 (\omega) \; dw$$

$$\equiv \quad \text{overall coherence}$$

The results for HCG = 2500, 800, and 200 ft are plotted in Fig. 44. The plots of $\rho_{u^2 w^2}^2 (\omega)$ versus ω contain a lot of scatter, but generally show an increase in the coherence as altitude is increased. The best measure of the u- and w-gust correlation is reflected by the overall coherence, ρ_A^2, which monotonically increases with increasing altitude.

As a basis for comparison the coherence for a high altitude Dryden model turbulence run was calculated (i.e., above 1750 ft so that the rms of u- and w-gust would be about equal). The results are presented and compared to the

---

* The coherence of u and w did not demonstrate the high correlation because of the occasional 180 degree phase shift between u and w noted above.

Figure 43. Effects of HCG on the w-Gust Effective Wind Shear Parameter
of the RAE Turbulence Model

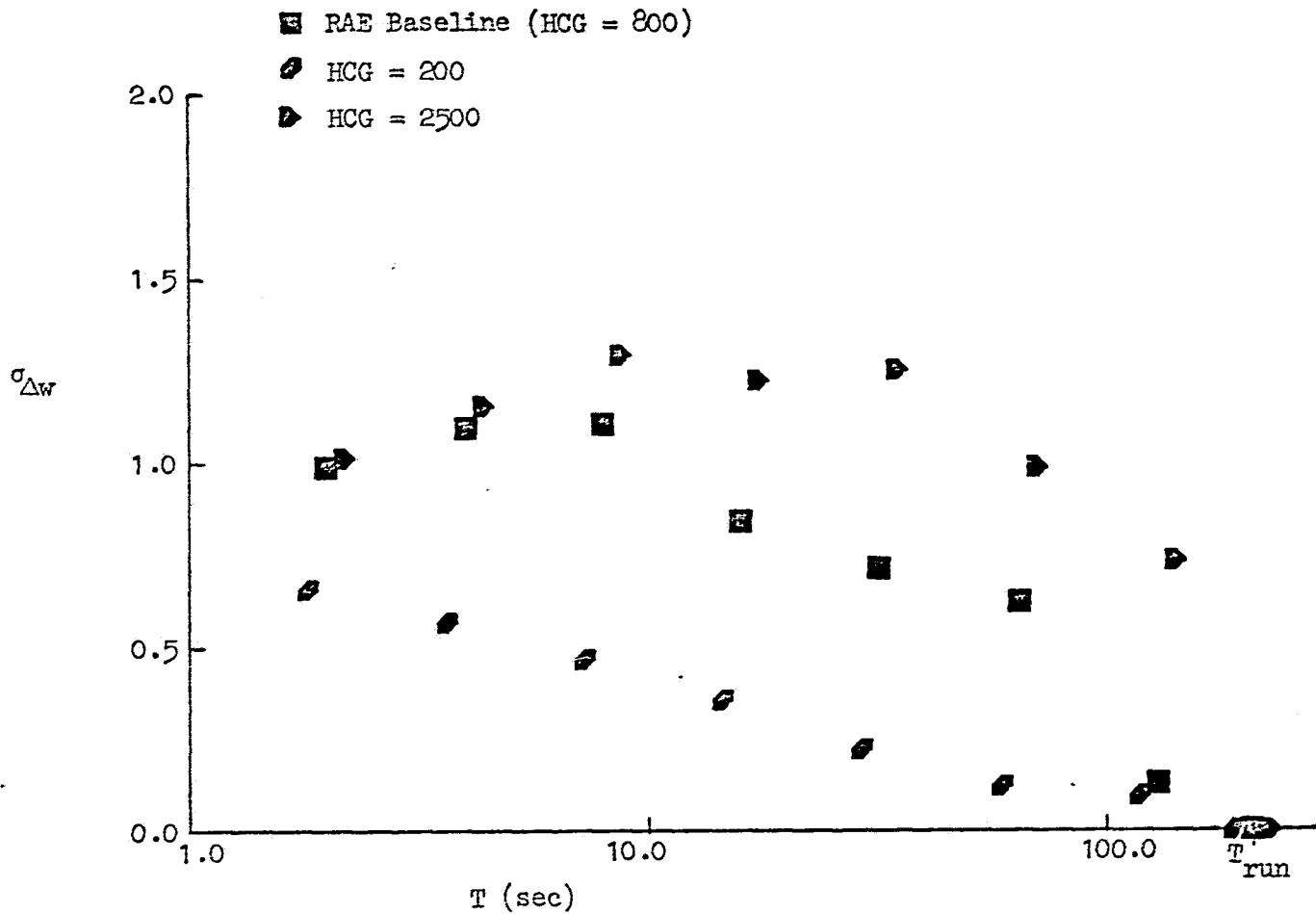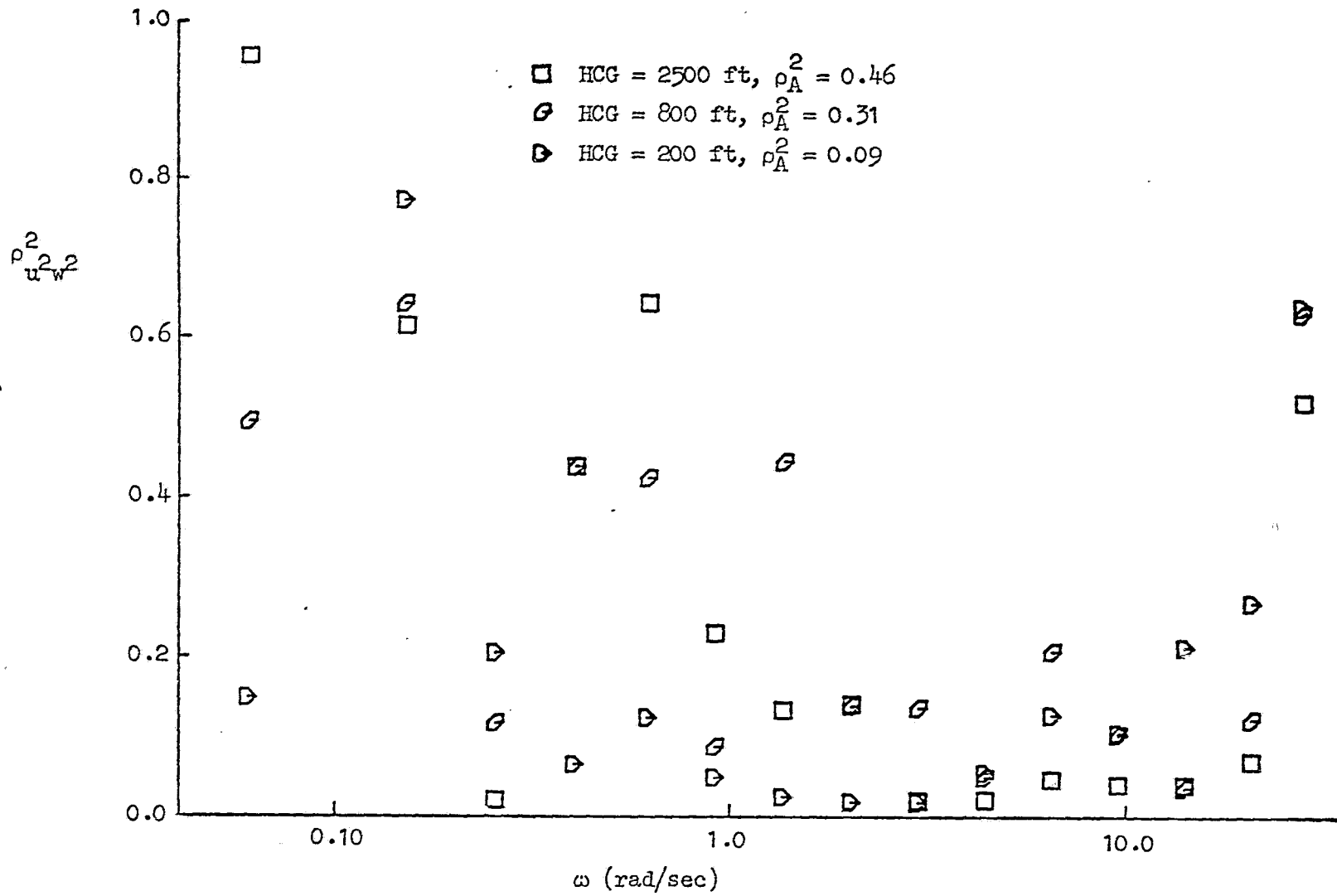Figure 44. Coherence Between u^2 and w^2 of the RAE Turbulence Model at Three Altitudes

RAE coherence in Fig. 45. Note that ρ_A^2 for the RAE model is much higher than for the Dryden model.

The reason that so much has been said about the coherence is because it is generally overlooked as a turbulence feature (as mentioned before, the coherence of the u- and w-gust of the Dryden model is theoretically zero), yet could be an important parameter when evaluating a computer-generated turbulence model or analyzing real-world turbulence. For example, the aircraft excursions resulting from highly coherent turbulence should be larger than those resulting from highly incoherent turbulence because the aircraft is being disturbed in all three axes at the same time.

E. FRAMETIME CONTROL, DT

The frametime, DT, has strange and totally unexpected effects on the temporal and spectral characteristics of the RAE turbulence. Unlike the Dryden turbulence model (where the frametime will not affect the turbulence characteristics until the break frequency of the shaping filters approaches the Nyquist frequency), the frametime in the RAE turbulence model will affect the characteristics of the gust characteristics if 1/DT is not an integer. This phenomenon is demonstrated in the time histories and power spectral plots shown in Fig. 46.

Visual inspection of Fig. 46 shows that the time histories for DT = 0.10, 0.20, and 0.05 seconds are virtually identical. But the time history for DT = 0.15 seconds appears to be shifted in time and there is more high-frequency content. This effect is difficult to see from the power spectral plots shown in Figs. 47 and 48, but is confirmed by the power fraction versus frequency plot shown in Fig. 49. Note that the frequency at a power fraction of 0.90 was increased by about 1.0 rad/sec for DT = 0.15 sec but was virtually unchanged for DT = 0.05 or 0.20 sec as compared with DT = 0.10 sec. The low-frequency end of the power fraction curve is about the same for all the frametimes. The frametime did not have a noticeable effect on any of the statistical properties of the turbulence.

The reason for the strange effect noted above is found in the way the RAE model is implemented. The "rise time" of the high-frequency gust component
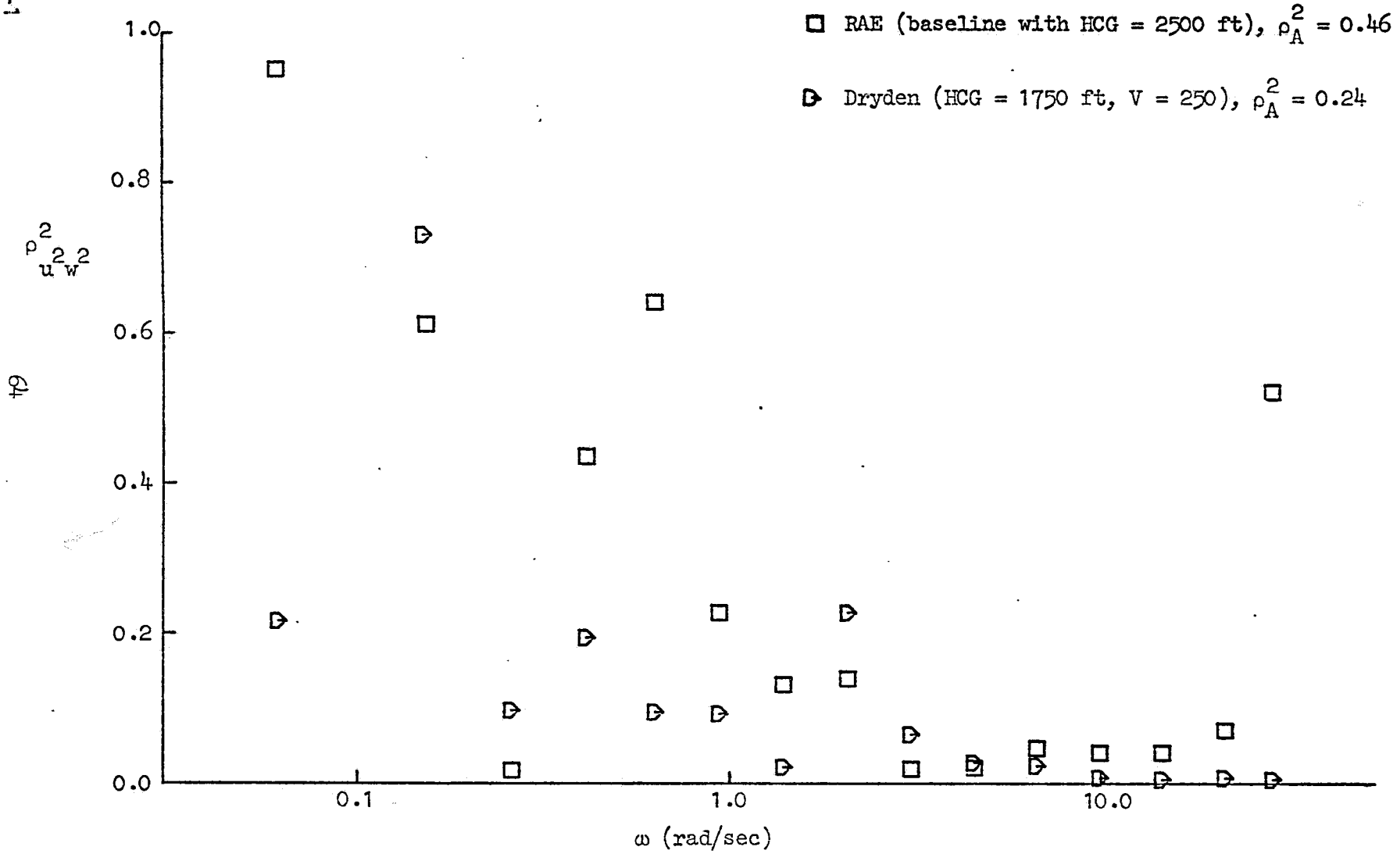
Figure 45. Comparison of the RAE and Dryden u^2 and w^2 Coherences
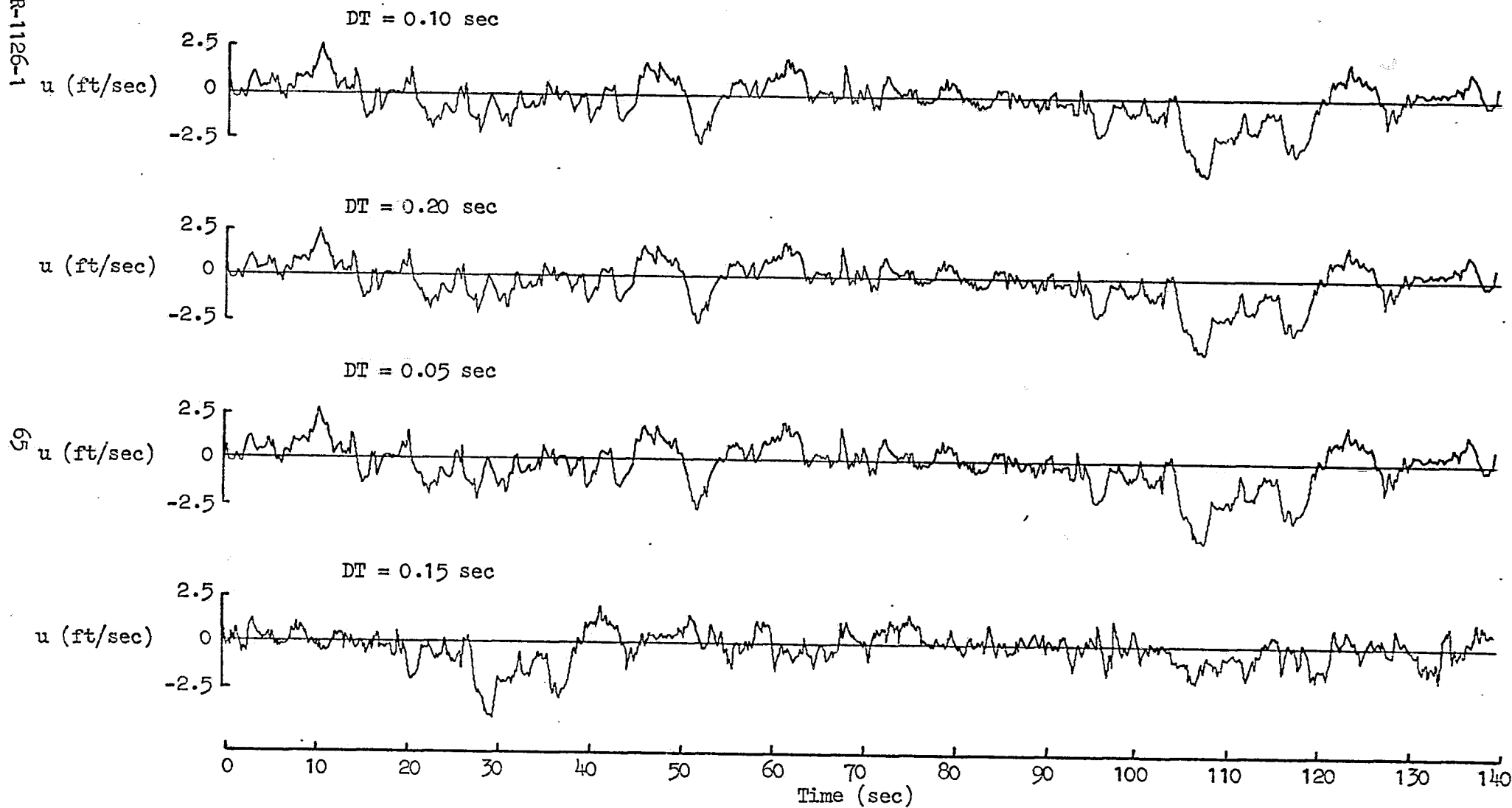
Figure 46. Effects of Frametime on the Temporal Characteristics

65
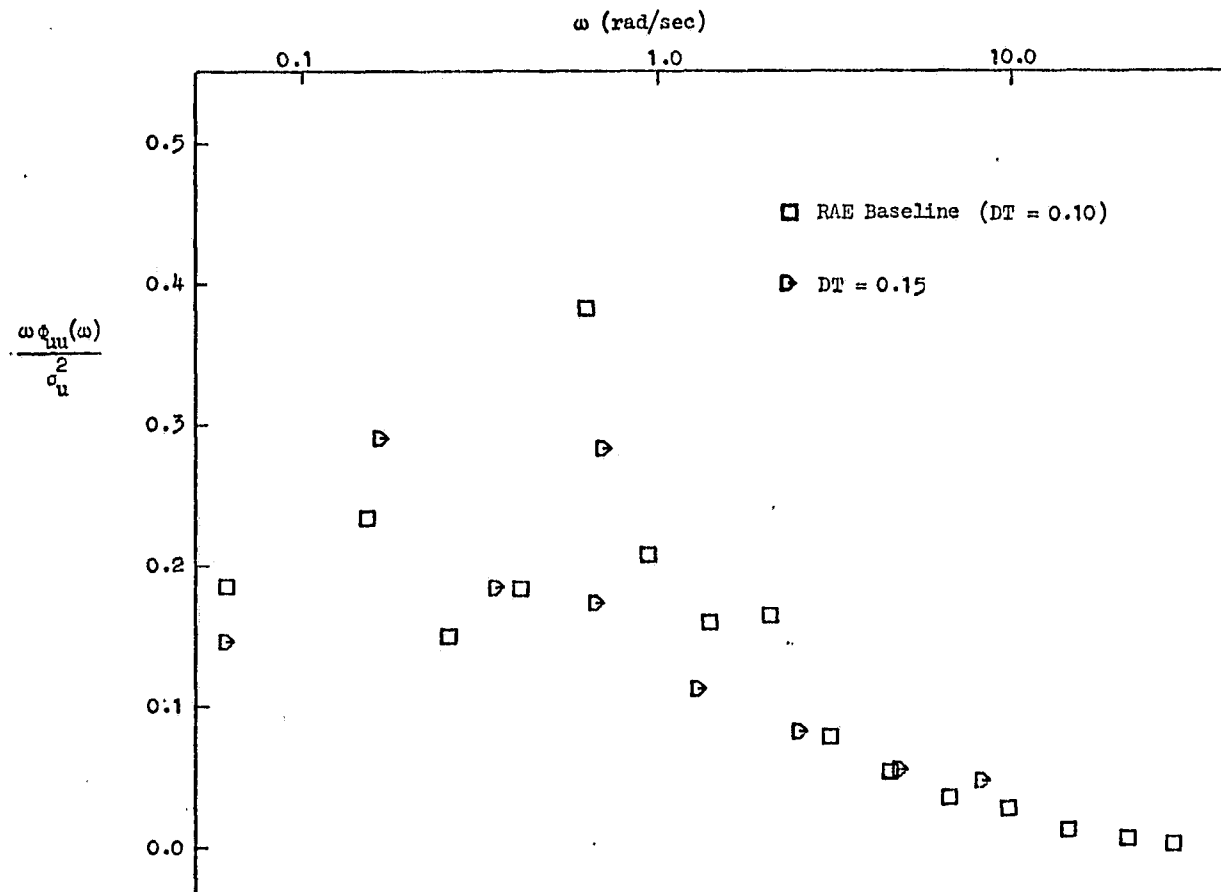
Figure 47. Effects of DT on $\Phi_{uu}(\omega)$ of the RAE Turbulence Model
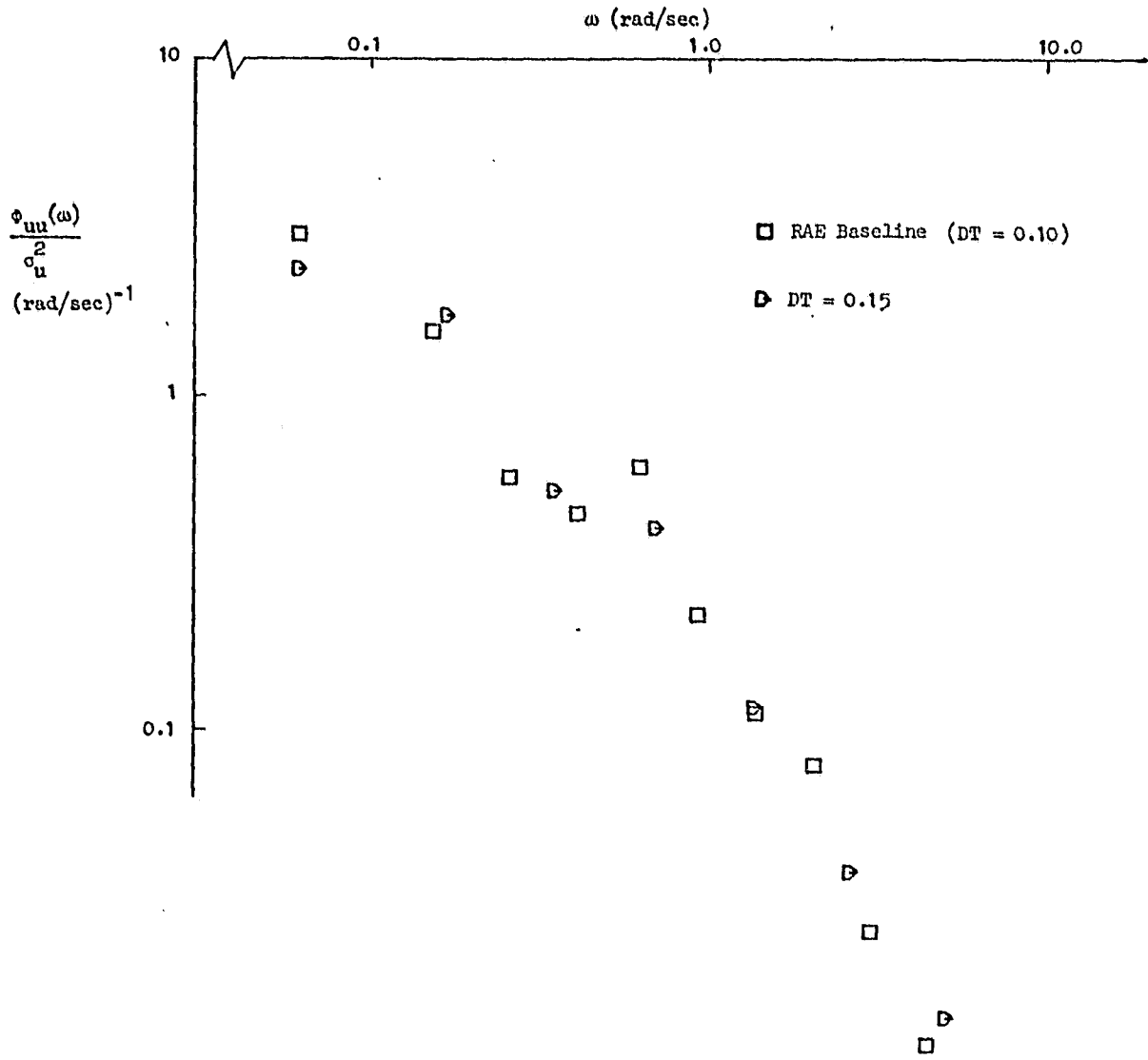
Figure 48. Effects of DT on $\omega\Phi_{uu}(\omega)$ of the RAE Turbulence Model
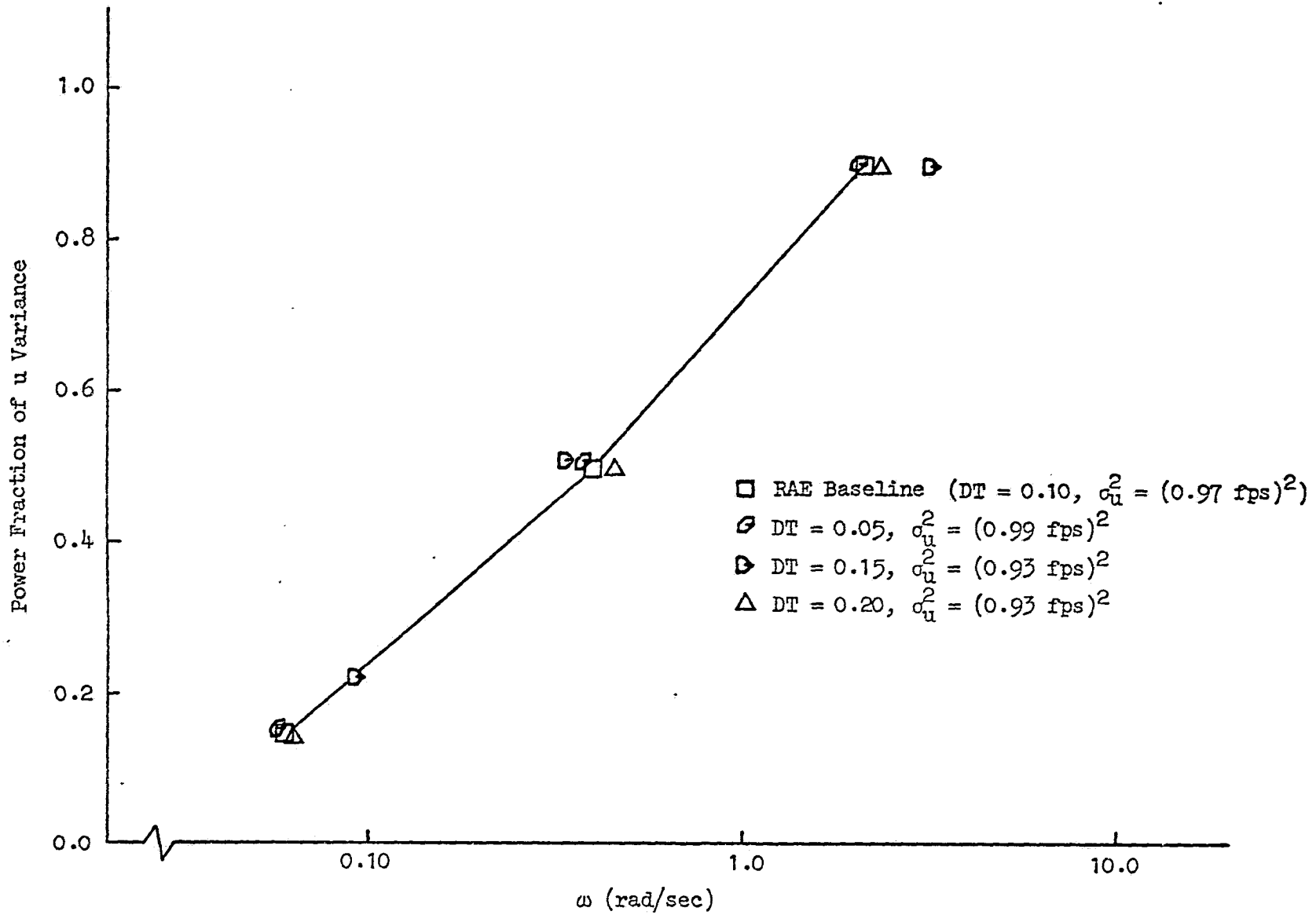
Figure 49. Effects of DT on the Power Fraction of the u-Gust Variance
Versus Frequency of the RAE Turbulence Model

is expressed as an integer number of samples of the frametime,

$$MRT3 = (5/NGUSTS)/DT$$

Because of truncation, the _true_ rise time, $TRT3 = MRT3 \cdot DT$, is incorrect for non-integer values of $1/DT$. For example, for $NGUSTS = 5$ and $DT = 0.10$, 0.20, and 0.15 sec T_{RT3} is:

$$TRT3 = \begin{cases} 1.0 \text{ sec for } DT = 0.10 \text{ sec} \\ 1.0 \text{ sec for } DT = 0.20 \text{ sec} \\ 0.90 \text{ sec for } DT = 0.15 \text{ sec} \end{cases}$$

F. INTENSITY CONTROL, SIGMA

The overall intensity is controlled by the parameter SIGMA. The variances of the three gusts components, u-gust, v-gust, and w-gust, all scale linearly with SIGMA, regardless of the values of NGUSTS, F, R, HCG, or DT. None of the other statistical, temporal, or spectral properties of the turbulence are affected by SIGMA. It should be emphasized that, unlike the Dryden model, the standard deviation of the RAE model turbulence is not equal but only proportional to SIGMA.

SECTION IV

SUMMARY AND RECOMMENDATIONS

The characteristics of the complex RAE atmospheric turbulence model have been analyzed and presented in the foregoing sections with two main objectives. The first was to compare the RAE model with a relatively well known form, the Dryden model. The second objective was then to vary systematically the RAE model parameters in order to observe their overall effect on temporal, spectral, and statistical properties. It is important to recognize, however, that although the numerical properties are analyzed in detail, we still do not have a clear definition of how they impact pilot opinion.

The results of comparing the Dryden and RAE models reveal that the spectral and statistical properties of the individual turbulence components can be made to appear similar if the input parameters of the RAE model are properly chosen. One striking difference between the two models is the high coherence among the turbulence components of the RAE model. The high coherence is visible by examining the time histories of u- and w-gust (or u- and v-gust) and is best quantified by computing the coherence between u^2 and w^2. This feature of the RAE turbulence is emphasized because the individual components of Dryden turbulence are intentionally designed to lack coherence. The high coherence among the components of the RAE model turbulence could be an important feature when using it in aircraft simulation investigations.

The qualitative effect of each of the six RAE model parameters on spectral and statistical characteristics are summarized in Table 4. Quantitative effects are given in Section III.

The four most influential RAE model parameters are SIGMA, NGUSTS, F, and R. SIGMA varies intensity directly but affects no other property of the turbulence. NGUSTS varies bandwidth directly and F varies the probability distribution directly. R is a parameter which has strong but diverse effects on a number of properties and should be adjusted with considerable caution.

TABLE 4

SUMMARY OF THE SPECTRAL AND STATISTICAL EFFECTS
OF THE RAE TURBULENCE MODEL PARAMETERS

Turbulence Property	RAE Model Parameter					
	Bandwidth Control NGUSTS	Probability Distribution Control F	Decay Ratio Control R	Intensity Control SIGMA	Altitude Control HCG	Frametime Control DT
Remarks:	Primary determinant of bandwidth but also has a noticeable effect on intensity.	Primary determinant of probability distribution but has an indirect effect on spectral properties.	Affects many properties simultaneously and should be varied with great caution.	Varies only the intensity but its numerical value does not necessarily correspond to actual rms.	Affects w-gust only but impacts many of its properties.	No effect on turbulence properties unless integer condition is not met (1).
Spectral:						
High Frequency Power	Increase(2)	No change	Decrease	No change	Decrease	Conditional
Low Frequency Power	No change	Decrease	Decrease	No change	Decrease	No change
Statistical:						
Variance	Increase	No change	Increase	Increase	Increase	No change
Kurtosis	No change	Increase	Decrease	No change	Decrease	No change
Stationarity(3)	No change	Decrease	Decrease	No change	Increase	No change

(1) The frametime should be set such that 1/DT is an integer, otherwise the high frequency spectral characteristics are affected.

(2) The word "increase" refers to the effects of increasing the magnitude of the indicated RAE model parameter on spectral and statistical properties. Numerical values for the amount of change can be obtained from Section III.

(3) Stationarity is reflected by the dispersion of the statistics in sampling over a limited window. Small dispersion implies high stationarity.

Parameters having effects of lesser importance are HCG and DT. HCG, the altitude parameter, mainly varies the intensity and frequency content of w-gust. DT sets the turbulence frametime and a number of parameters internal to the RAE model.

Practically speaking, we should point out that the values of RAE model parameters are, in reality, restricted. For example, HCG is determined by the particular aircraft altitude. Frametime, DT, must not only be compatible with the simulation computer frametime but must also be set such that $1/DT$ is an integer. From our study, the decay ratio, R, affects all turbulence properties; therefore, we recommend that it be set at a fixed value (about 0.7) and not be used as a "control." NGUSTS, the bandwidth control, should be set according to airspeed in order to provide a desired scale length. (As in the Dryden model, scale length, hence NGUSTS, could also be varied as a function of altitude.)

In view of the above parameter constraints, we are left with two primary controls for the RAE model, SIGMA and F. SIGMA, the intensity control, is perhaps the most fundamental determinant of turbulence effects. Certainly for the Dryden model its influence has been shown to be paramount (Ref. 5). The probability distribution control, F, adjusts the non-Gaussian qualities — the relative frequency of occurrence of large magnitude gusts. It too has been judged important (Ref. 8), but its desired numerical value is less well defined. Several research studies have shown that the non-Gaussian characteristics of turbulence can be quite important in a piloted simulation (Refs. 8, 9, 10, and 11).

With only two input variables to be concerned with, an experiment could be carried out to evaluate the RAE turbulence model in a piloted simulator. We recommend that such an experiment be designed to compare the RAE model with some of the other so-called non-Gaussian turbulence models (Refs. 3, 8, 9, 10, and 11) in addition to comparing it with the Dryden model. As an alternative to using a real-time piloted simulation, an experiment could be performed using a realistic pilot model in a non-real-time environment similar to that described in Ref. 12. This would be cheaper than a real-time piloted simulation, and it would permit a researcher to isolate better the effects

of the turbulence model without having to cope with unintentional changes in piloting techniques.

One additional recommendation is to decouple the effects of the RAE parameters on the turbulence characteristics, especially those of NGUSTS. Note from Table 4 that changing NGUSTS increases the high-frequency power and increases the variance of the turbulence. Using the results of Section III, the RAE model could be programmed in such a way that the variance would be unaffected by changes in NGUSTS. Also note from Table 4 that F affects the low frequency power as well as the kurtosis and stationarity of the turbulence. However, the magnitude of the low-frequency power changes due to changing F are fairly small (see Section III), and hence we do not recommend that any model changes be made in order to eliminate this effect. It is not known if it is possible (or indeed even desirable) to separate the simultaneous changes in kurtosis and stationarity, although further research of these characteristics of atmospheric turbulence should be performed. As mentioned before, the intensity control parameter, SIGMA, is indeed an independent control in that it affects only the turbulence component variances.

REFERENCES

1. Tomlinson, B. N., _Developments in the Simulation of Atmospheric Turbulence_, Royal Aircraft Establishment Technical Memorandum FS 46, September 1975.

2. Dull, T. C., J. F. Moynes, and J. T. Gallagher, "Active Control of Ride Quality for Advanced Fighter Aircraft Within Various Turbulence Environments," Presented at the Naval Postgraduate School Control Systems Criteria Symposium, Monterey, California, 11-13 July 1978.

3. Jansen, C. J., _A Digital Turbulence Model for the NLR Moving-Base Flight Simulator, Part I_, National Aerospace Laboratory NLR The Netherlands Memorandum VS-77-024 U, 29 August 1977.

4. Chalk, C. R., T. P. Neal, T. M. Harris, et al, _Background Information and User's Guide for MIL-F-8785B (ASG)_, "Military Specification — Flying Qualities of Piloted Airplanes," AFFDL-TR-69-72, August 1969.

5. Heffley, Robert K., Robert L. Stapleford, and Robert C. Rumold, _Airworthiness Criteria Development for Powered-Lift Aircraft_, NASA CR-2791 (also FAA-RD-76-195), February 1977.

6. McRuer, Duane, Irving Ashkenas, and Dunstan Graham, _Aircraft Dynamics and Automatic Control_, Princeton University Press, Princeton, New Jersey, 1973.

7. Hofmann, Lee Gregor, _Wind, Wind Shear, and Turbulence Models for the System Performance Analysis_, Systems Technology, Inc., Working Paper 1043-2R, December 1973, Revised October 1974.

8. Reeves, P. M., G. S. Campbell, V. M. Ganzer, and R. G. Joppa, _Development and Application of a Non-Gaussian Atmospheric Turbulence Model for Use in Flight Simulators_, NASA CR-2451, September 1974.

9. Van de Moesdijk, G. A. J., _Non-Gaussian Structure of the Simulated Turbulent Environment in Piloted Flight Simulation_, Delft University of Technology Memorandum M-304, April 1978.

10. Jacobson, I. D., and D. Joshi, "Investigation of the Influence of Simulated Turbulence on Handling Qualities," _J. of Aircraft_, Vol. 14, No. 3, March 1977, pp. 272-275.

11. Jacobson, I. D., and D. S. Joshi, "Handling Qualities of Aircraft in the Presence of Simulated Turbulence," _J. of Aircraft_, Vol. 15, No. 4, April 1978, pp. 254-256.

12. Lehman, John M., Robert K. Heffley, and Warren F. Clement, _Simulation and Analysis of Wind Shear Hazard_, FAA-RD-78-7, December 1977.